For Reference

NOT TO BE TAKEN FROM THIS ROOM

Ex libris
universitatis
albertaensis

UNIVERSITY OF ALBERTA
QUAECUMQUE VERA

THE UNIVERSITY OF ALBERTA

GAS-LIQUID FLOW IN VERTICAL PIPES

A DISSERTATION
SUBMITTED TO THE SCHOOL OF GRADUATE STUDIES
IN PARTIAL FULFILMENT OF THE REQUIREMENTS FOR THE
DEGREE OF MASTER OF SCIENCE

FACULTY OF ENGINEERING

by
JAMES S. C. DUNN

EDMONTON, ALBERTA
APRIL, 1952.

Digitized by the Internet Archive
in 2017 with funding from
University of Alberta Libraries

https://archive.org/details/gasliquidflowinv00jame

ACKNOWLEDGEMENTS

The author wishes to express appreciation to Dr. G. W. Govier, under whose supervision this project was carried out, and whose guidance, criticism and patience have contributed greatly to the investigation.

Appreciation is also expressed to Mr. N. Panasiuk who helped with the construction of equipment.

TABLE OF CONTENTS

Page

List of Tables ii

List of Figures iii

The Problem 1

Summary 2

Chapter

I. Introduction 4

II. Review of Literature 5

III. Experimental Equipment 21

IV. Experimental Procedures 37

V. Experimental Data 39

VI. Calculated Results 43

VII. Interpretation and Correlation of Results. 48

VIII. Conclusions. 102

Appendices 105

A. Calibrations 105
B. Experimental Data. 112
C. Calculated Results 126

Nomenclature 146

Bibliography 148

LIST OF TABLES

Table Page

I. Calibration of Water Orifice Plates 106

II. Calibration of Air Orifice Plates - Experimental Data . . 109

III. Calibration of Air Orifice Plates - Calculated Results . . 110

IV. Supplementary Data 113

V. Single-Phase Water Flow Experimental Data. 114

VI. Single-Phase Air Flow Experimental Data. 115

VII. Two-Phase Flow Experimental Data 116

VIII. Effect of Liquid Phase Surface Tension Experimental Data . 125

IX. Single-Phase Water Flow Calculated Results 127

X. Single-Phase Air Flow Calculated Results 128

XI. Two-Phase Flow Calculated Results. 129

XII. Variation of Maximum and Minimum Points with Water Rate. . 138

XIII. Effect of Liquid Phase Surface Tension Calculated Results. 139

XIV.. Hydrostatic Head and Irreversibility Components of Pressure Drop... 140

XV. Friction Factor - Reynolds Number Results. 141

XVI. Friction Factors at Certain Reynolds Numbers 145

LIST OF FIGURES

Figure Page

1. Flow Circuit. 22
2. Air-Water Mixing Section. 24
3. Upper Flow Section. 27
4. Top Half of Air-Water Separator 28
5. Bottom Half of Air-Water Separator. 29
6. Panel Board 31
7. Downstream Pressure Tap and Separator Assembly. 32
8. Mid-Point Pressure Tap and Separator Assembly 34
9. Mid-Point Pressure Controller 35
10. Mid-Point Pressure Control Valve. 36
11. Friction Factor - Reynolds Number Plot for Single-Phase Water Flow. 49
12. Friction Factor - Reynolds Number Plot for Single-Phase Air Flow. 50
13. Slug Flow 53
14. Transition from Slug to Froth Flow. 54
15. Froth Flow. 55
16. Transition from Froth to Annular Film Flow. 56
17. Annular Film Flow 57
18. Transition from Annular Film to Mist Flow 58
19. Variation of Pressure Drop with Discharge Air-Water Ratio (1/2 inch Tube, Water Rate - 4.17 lbs./ft^2 sec.). 60
20. Variation of Pressure Drop with Discharge Air-Water Ratio (1/2 in. Tube, Water Rate - 8.10 lbs./ft^2 sec.). 61

LIST OF FIGURES - (Continued)

21. Variation of Pressure Drop with Discharge Air-Water Ratio (1/2 inch Tube, Water Rate - 17.6 lbs./ft^2 sec.). 62

22. Variation of Pressure Drop with Discharge Air-Water Ratio (1/2 inch Tube, Water Rate - 51.0 lbs./ft^2 sec.). 63

23. Variation of Pressure Drop with Discharge Air-Water Ratio (1-inch Tube, Water Rate - 4.15 lbs./ft^2 sec.) 64

24. Variation of Pressure Drop with Discharge Air-Water Ratio (1-inch Tube, Water Rate - 8.00 lbs./ft^2 sec.) 65

25. Variation of Pressure Drop with Discharge Air-Water Ratio (1-inch Tube, Water Rate - 17.9 lbs./ft^2 sec.) 66

26. Variation of Pressure Drop with Discharge Air-Water Ratio (1-inch Tube, Water Rate - 51.9 lbs./ft^2 sec.) 67

27. Effect of Water Rate on the Maximum and Minimum Pressure Drops - 1/2-inch Tube 69

28. Effect of Water Rate on the Maximum and Minimum Pressure Drops - 1-inch Tube 70

29. Effect of Water Rate on the Discharge Air-Water Ratios Corresponding with the Maximum and Minimum Pressure Drops - 1/2-inch Tube 71

30. Effect of Water Rate on the Discharge Air-Water Ratios Corresponding with the Maximum and Minimum Pressure Drops - 1-inch Tube 72

31. Effect of Liquid Phase Surface Tension on the Pressure Drop-Discharge Air-Water Ratio Curve (1-inch Tube, Water Rate - 4.15 lbs./ft^2 sec.). 74

32. Variation of Air-Water Ratio in the Test Section with Discharge Air-Water Ratio (1/2-inch Tube, Water Rate - 4.17 lbs./ft^2 sec.) 76

33. Variation of Air-Water Ratio in the Test Section with Discharge Air-Water Ratio (1/2-inch Tube, Water Rate - 8.10 lbs./ft^2 sec.) 77

34. Variation of Air-Water Ratio in the Test Section with Discharge Air-Water Ratio (1/2-inch Tube, Water Rate - 17.6 lbs./ft^2 sec.) 78

LIST OF FIGURES - (Continued)

35. Variation of Air-Water Ratio in the Test Section with Discharge Air-Water Ratio (1/2-inch Tube, Water Rate - 51.0 lbs./ft^2 sec.) 79

36. Variation of Air-Water Ratio in the Test Section with Discharge Air-Water Ratio (1-inch Tube, Water Rate - 4.15 lbs./ft^2 sec.) 80

37. Variation of Air-Water Ratio in the Test Section with Discharge Air-Water Ratio (1-inch Tube, Water Rate - 8.00 lbs./ft^2 sec.) 81

38. Variation of Air-Water Ratio in the Test Section with Discharge Air-Water Ratio (1-inch Tube, Water Rate - 17.9 lbs./ft^2 sec.) 82

39. Variation of Air-Water Ratio in the Test Section with Discharge Air-Water Ratio (1-inch Tube, Water Rate - 51.9 lbs./ft^2 sec.) 83

40. Variation of Hydrostatic Head and Irreversibility Components of Pressure Drop with Discharge Air-Water Ratio (1-inch Tube, Water Rate - 4.15 lbs./ft^2 sec.). 88

41. Variation of Friction Factors with Reynolds Number - 1/2-inch Tube 90

42. Variation of Friction Factor with Reynolds Number - 1-inch Tube 91

43. Effect of Water Rate on Friction Factor - 1/2-inch Tube . . . 95

44. Effect of Water Rate on Friction Factor - 1-inch Tube 96

45. Effect of Gas Phase Density on Friction Factor 97

46. Effect of Tube Diameter on Friction Factor - Mid-Point Pressure 18 p.s.i.a. 99

47. Effect of Tube Diameter on Friction Factor - Mid-point Pressure 36 p.s.i.a. 100

48. Water Orifice Calibrations. 107

49. Water Orifice Calibrations. 108

50. Air Orifice Calibrations 111

THE PROBLEM

The problem undertaken is an investigation of the significance of certain variables on the pressure drop and the liquid hold-up in flowing two-phase mixtures of air and water in vertical tubes. The objective is to present the pressure drop data in the form of a friction factor - Reynolds number relationship with the necessary other parameters similar to that for single-phase flow.

SUMMARY

Pressure drops, gas-liquid discharge ratios and gas-liquid test section ratios are determined for air-water mixtures flowing upward in vertical butyrate plastic tubes having inside diameters of 0.640 inches and 1.049 inches, and test section lengths of 22.78 feet and 22.88 feet respectively. For four constant water rates varying from 4.15 lbs./ft^2 sec. to 51.9 lbs./ft^2 sec., the air rate varies from zero to 0.97 ft^3/sec. (at 14.4 PSIA and 60°F.) for test section mid-point pressures of 18 PSIA and 36 PSIA.

At each water rate the measured pressure drop is found to pass through a first minimum point, in which the flowing mixture is characterized by slug flow, a maximum point, in which the flow is a frothy mixture of the two phases, a second minimum, in which the air travels in a core through an annular film of water, and then to increase steadily in the mist flow region as the air-water discharge ratio is increased.
The pressure drops at these inflection points become greater as the water rate increases, and at high water rates the second minimum point disappears. Doubling the gas phase density results in the pressure drop discharge air-water ratio curve lagging the corresponding curve at the lower density. Tubing diameter shows only slight effects on the pressure drop.

The measured pressure drops are separated into two components, hydrostatic head and friction losses, by a method proposed by Radford. Superficial friction factors, based on the flowing gas phase and arbitrarily defined as

$$f_G = \frac{\beta}{2} \quad \frac{DA^2}{V_G^2 N} \quad \frac{\Sigma F_G}{G^2}$$

are calculated from the friction losses and are plotted against superficial Reynolds numbers also based on the flowing gas phase occupying the entire cross-section of the tube. These friction factors are found to be as much as 1000 times greater than friction factors for single-phase flow. With increasing Reynolds numbers the friction factors decrease sharply (at a negative slope of 2.1) over the range studied. A separate curve is found for each water rate, gas phase density and tube diameter. The effects of these variables on the friction factor appear to be inter-related and are complex.

Further studies are necessary before a complete correlation of the variables is possible.

CHAPTER I

INTRODUCTION

The problem of predicting the pressure drop attending the vertical upward flow of gas-liquid mixtures in tubes (e.g. gas or air lifting of oil or water) has never been solved in a satisfactory manner. The lack of usable data to apply to such a problem is probably due to the complexity of this type of flow. Whereas in single-phase flow the calculation of pressure drops in tubes can be made easily from a knowledge of the physical properties and the rate of flow of the fluid, and the length, diameter and roughness of the tube, in two-phase flow the calculation is more difficult since the friction factor is not a unique function of Reynolds number and tube roughness. Thus the influence of the physical properties of both the gas phase and the liquid phase, the rates of flow and the proportions of each phase entering or leaving the tube, the proportions of each phase in the tube, and the length, diameter and roughness of the tube may be important.

The present study is undertaken to obtain data on the effects of water rate, gas phase density, tube diameter and flow pattern on the pressure drop and the liquid hold-up of air-water mixtures flowing in vertical tubes, with a view to correlating the results in a manner analogous to that for single-phase fluids.

CHAPTER II

REVIEW OF LITERATURE

Prior to 1928 little or no research had been carried out on the simultaneous flow of liquids and gases in vertical pipes. The gas lift, the most common example of two-phase flow, had been successfully applied to the lifting of oil in wells and its use probably reached a peak in the oil fields of Oklahoma in the period 1927-1928. Yet an understanding of the mechanisms governing this type of flow had not been obtained.

The term "gas-lift" has been restricted to the process of flowing a well by means of, or with the aid of, artificially injected gas. However, the flow of gas-oil mixtures in vertical pipes is essentially the same irrespective of whether the flow is natural, using formation gas, or induced, using air or gas lift. Accordingly a solution to either of the two types of flow will be a solution to both.

Over the past twenty-five years several reports of experimental work on two-phase vertical flow have been published. Many articles on the air gas lift and its use in the oil field are also available. Versluys has published several papers discussing vertical flow of gas-liquid mixtures. In one of his earliest papers (20) published in the United States, the theory of flowing oil wells is developed in mathematical form. A theoretical discussion of the energy balance in a gas lift is given. Two cases are treated: (1) where the gas is insoluble in the liquid, and (2) where the gas is soluble in the liquid. For each of these cases the author derives an equation summing up the work performed on, and by, the gas-oil mixture in rising

through a vertical pipe. The constants in the mathematical formulae set forth in this paper would have to be ascertained from experiments.

In another paper (21) Versluys discusses irregular flow in detail. The causes and effects of intermittent flow are explained, and a method of selecting the proper length and diameter of tubing under these flow conditions is given. Graphs are presented to show the flow conditions at various gas-oil ratios and tubing sizes, and to estimate the quantity of gas that must be injected into an intermittent well in order to establish regular flow.

In two papers published in England Versluys discusses the principles of gas lift and the conditions under which gas and liquid mixtures rise. In the first paper (22) he explains the mechanism of lifting a liquid by means of a compressed gas. In the companion paper (23) he discusses the principles limiting the different conditions under which the flow of gas and liquid through a vertical pipe can take place. The author states that two stable conditions are possible in the mixture of liquid and gas. These are the foam condition and the mist condition, and are dependent upon the volumetric ratio of gas to liquid present in the pipe. Between the two an unstable condition exists and in actual flow the two arise alternately but immediately each converts itself into the other. The result is that gas and liquid tend to segregate and form slugs or to fill the tube with slugs of mist and foam. This causes fluctuations which may pass into real heading and surging.

Uren and his co-workers were among the first to conduct experiments on the flow of gas-oil mixtures in vertical pipes (18). They measured pressure losses for air-oil mixtures at many different flow velocities in a

vertical 2-inch pipe 41 feet high. In approaching the problem of evaluating and formulating the variables influencing pressure loss, they assumed that the Fanning and the Poiseuille equations would comprise all of the variables involved. These equations are used in computing the value of the friction factor and the absolute viscosity for various air-oil mixtures.

The authors present graphs showing the variation of specific gravity, viscosity and pressure drop with air-oil ratios up to 6000 cubic feet of air per barrel of oil, log log plots of velocity versus pressure drop and friction factor, and friction factor versus Reynolds number. The assumption that the Poiseuille equation holds true over the entire range of viscous and turbulent flow and can be used in solving for the viscosity of the air-oil mixture is an erroneous one, since the equation is applicable to laminar unidirectional flow only. In presenting these results, the authors do not explain how the velocity term in the Reynolds number has been calculated and whether it is the velocity of the gas or of the liquid, or the slip velocity (i.e. the difference in the velocity between the air and the liquid). It would appear that this slip velocity and the resulting lower air-oil ratio in the tube was not perceived by them.

This slippage is one of the most important factors affecting the efficiency of the flow of oil and gas mixtures. Recognizing this fact, Moore and Wilde developed a method of measuring slippage in short experimental gas lifts. As shown in a paper presented by them (11), slippage can be easily calculated in a vertical pipe carrying a mixture of gas and oil if the fractions of the pipe occupied by the liquid and gas respectively are known. They measured the fraction of the pipe occupied by the liquid under a wide variety

of conditions and determined the relationship between this fraction and other quantities which are easily measured in ordinary work.

The authors correlate their data by means of an equation relating the ratio of fraction of pipe occupied by liquid to that occupied by gas (designated by the symbol X) to the pipe diameter, specific gravity of the liquid, relative volume velocity and surface tension of the liquid. The equation is not dimensionless. The solution of the equation must be made by successive approximations since the relative volume velocity is the function of this ratio X, as well as the rate of liquid flow, the rate of gas flow through the pipe and the average pressure in the pipe. A value of X is assumed and used to obtain the relative volume velocity. This value of the velocity is used in the solution of the equation for X. The calculation is repeated until the calculated value of X checks the assumed value. Having estimated X correctly, the corresponding value for the fraction of pipe occupied by liquid (Y) is easily found. The product of this fraction Y, the liquid density and the height of the gas-lift is taken to be the hydrostatic head of the liquid.

Friction loss is determined by subtracting the hydrostatic head and the velocity head from the total pressure drop in the flow pipe. Velocity head in most cases is negligible. The friction loss is subject to a fairly large error, since it is the difference of two large quantities, either of which may be subject to some inaccuracy in measurement. The authors maintain, however, that it is accurate enough to demonstrate that the Fanning equation can not be applied to the calculation of friction losses in the flow of heterogeneous fluids. The best correlation gives the friction

loss as a function of the linear velocity of the liquid, specific gravity and viscosity of the liquid, and the pipe diameter. However, attempts to calculate the pressure drops in flowing or gas-lifted oil wells usually give results which are too high. At the time that this paper was presented the authors were unable to explain the discrepancy between the experimental results and oil well data.

In a subsequent paper presented two years later (12), Moore and Schilthius bring forth a new hypothesis which presupposes certain conditions affecting the flow of oil and gas in wells. When the equations proposed by Moore and Wilde are corrected to allow for these conditions, an agreement between the observed and calculated performance of an actual well is obtained, which in most cases is quite satisfactory, although subject to certain limitations.

The authors are of the opinion that each variable in the equation for the pressure drop derived in the previous paper of Moore and Wilde influences the pressure drop in the proper manner, even though the results are in error. In all cases, it is observed that the calculated pressure drop is greater than the value observed, (i.e. the actual performance is more efficient than the equation would indicate). An analysis of actual well performance shows wells having flowing efficiencies of practically one hundred per cent, implying that the losses due to friction and slippage are negligible. Further investigation reveals that all such wells are producing with very little gas in excess of that dissolved in the oil at the pressure existing at the bottom of the well, and that in practically every case of a well flowing under these conditions, the efficiency is nearly

one hundred per cent. The authors give the following explanation for this apparently abnormal behavior:

> The gas coming out of solution from the oil as the pressure decreases, becomes dispersed throughout the oil in very fine bubbles forming a stable foam in which gas bubbles can not move except at very low velocities and consequently slippage is negligible. Under such conditions and at velocities sufficiently low to permit the neglect of friction, the pressure drop may be calculated with very little error by assuming that there are no friction or slip losses.

For wells producing a quantity of gas in excess of that dissolved in the oil at the pressure existing at the bottom of the well, the authors formulate the following hypothesis:

> It is assumed that the gas in solution evolves as the pressure decreases but that this gas forms a stable foam, and that little of the dissolved gas escapes from the foam phase. Thus the gas which comes out of solution is prevented from slipping past the oil. The free gas, however, does slip past the oil, or rather, the foam, and the amount of slippage depends upon the properties of the foam rather than the properties of the liquid. The lift may be considered as one in which a foam, comprising the liquid and the gas which has come out of solution, is lifted by the gas which is undissolved at the point of entrance.

The authors assume that the equations previously developed should hold, provided the physical properties and velocities used are considered to be those of the foam instead of the pure liquid, A corrected formula is given for calculating the free gas volume.

To check the hypothesis, the pressure drop in a number of wells is calculated and compared to the actual pressure drop observed. A table is presented showing the results of such calculations for a number of wells in several different fields. The calculated pressure drops agree reasonably well with the observed values, usually to within five per cent.

It is stated that the equations developed are subject to certain limitations, however. At low pressures or at low rates of flow the equations fail because of the instability of the foam. No account is taken of the properties of the gas. The friction equation is only a rough approximation.

The authors have prepared a series of curves showing pressure drop under various sets of conditions. These curves can be used in solving problems in tubing design. Two illustrations showing the use of these curves are presented.

Nowels (13) has developed a method for computing pressure drop in the flow string of an oil well somewhat similar to that of Uren. He is of the opinion that an adaptation of the Fanning equation would include all of the variables involved and that the friction factor in this equation would be some function of the Reynolds number just as in the case of the flow of single-phase fluids in pipes.

Using gas-lift data on 28 wells flowing through tubings varying from 2 1/4 to 6 1/4 inches in diameter, he determines Reynolds numbers and the friction factor in the Fanning equation and compares the two graphically. In determining the Reynolds number, the calculation of the average value of the weight of one cubic foot of the flowing mixture and the velocity of this mixture is based on the average pressure in the flow string.

Nowels later has found that Reynolds numbers derived in this manner are almost the same as those derived from using surface velocities and weights of one cubic foot of mixture at the well head pressures.

The determination of viscosity is more complicated. Nowels takes the plot of viscosity versus air-oil ratio of Uren (18) and transfers it to logarithmic paper. The resulting plot is found to be a straight line; (units of viscosity are changed to English units and the air-oil ratio is changed to percentage oil). Since this relation between viscosity and percentage oil in the mixture is a straight line with viscosity decreasing as the percentage oil becomes smaller, the curve extended downward will ultimately reach an imaginary point which will represent zero per cent oil and one hundred per cent air. He then finds an average viscosity for natural gas of the composition he is using, and plots this viscosity on the same value of the abscissa as the intersection of the Uren line with the viscosity of air. This point is then used as a point of origin for all the straight lines connecting it and values of the viscosities of crude oils of various gravities, (i.e. one hundred per cent oil).. A portion of this plot is enlarged and the abscissa logarithmic scale changed to read gas-oil ratios in cu. ft./barrel. Correction charts for temperature variations and per cent water in the crude are also made.

Nowels is then able to determine Reynolds numbers for any mixture of gas and oil flowing in a production tube. From the observed pressure drops in the gas-lifted wells, the friction factor in the Fanning equation is calculated. A plot of friction factor versus Reynolds number is made on logarithmic paper. The best-fit "curve" for each pipe size is found to be

at a 45° angle similar to the plot of Uren.

Nowels observes that the results show certain discrepancies. For a given Reynolds number, the friction factor increases in value as the pipe size increases, whereas the reverse of this relationship exists in horizontal pipes where the flow is turbulent. The 45° alignment of the straight-line curves representing values of friction factor indicates that vertical flow, in the pipe sizes dealt with, is of a viscous or streamline nature, in which case the Poiseuille formula would express the true relationship. This formula does not hold true in vertical flow, however, as impossible values for pressure drop are obtained. As Nowels says, "It is hardly conceivable that the flow of oil and gas in a flowing well would follow the viscous or streamline condition of flow due to the expansion of the gas and its rapid increase in velocity; yet the 45° angle slope to the curves on logarithmic paper indicates this viscous flow. At the entrance of the casing or tubing, viscous flow may exist but probably soon changes over into turbulent flow."

Although the friction factor increases in value as the diameter of pipe increases, the net result of a survey of the 28 wells shows that the pressure drop per unit length of pipe is greatest for pipes of small diameter. In other words, the friction is greater in small pipes than large ones even though the equations used for determining friction factor show it to be greater in value with pipes of large diameter. Nowels concludes that additional research and study of gas-lift data are necessary in order to correct the correlations that he has obtained.

Gosline (5) has also performed experimental work on a small gas-lift using air and three different liquids. He is most interested in annular

or wall film flow such as occurs in wells having small tubing, high gas-oil ratios and/or low submergences (bottom hole pressures). For this type of flow, he investigates the effect of air velocity on the drag coefficient at the air-liquid interface by measuring the air "core" velocity, the liquid annulus velocity and the liquid annulus thickness. The air velocities are sufficiently high to be in turbulent flow and the liquid velocities of such magnitude as to be in viscous flow.

Using these data the drag coefficient is calculated (using an equation developed in the paper) and plotted versus the air "core" velocity. Gosline finds that the coefficient of drag diminishes rapidly with the absolute velocity of the gas and that at any air velocity the drag is greater with liquids of greater viscosity.

Although not presenting any solution to two-phase flow, this paper provides a clearer understanding of the variables affecting the tractive forces at the air-liquid interface in wall film flow.

Cromer and Huntington (3) carried out a visual study of flowing air-water mixtures in a 98-foot length of vertical pipe set up in a derrick. Glass observation sections 2 feet long were placed at 14-foot intervals in the column and the flowing mixture photographed at these sections.

The four points which Shaw (15) has shown to be significant in the operation of an air-lift pump, (i.e. 1) the point of no flow due to deficiency of air; 2) the point of maximum efficiency; 3) the point of maximum yield, and 4) the point of no flow due to an excess of air,) are discussed by the authors with the aid of photographs taken at four of the observation sections along the pipe. Their paper is helpful in obtaining a better under-

standing of flow conditions of two-phase mixtures under varying air rates.

During the past six years several papers have been published covering research work on two-phase flow conducted at the University of California under the direction of R. C. Martinelli (7, 8, 9). Lockhart and Martinelli (7) have developed a generalized correlation for two-phase horizontal flow based on this previous work.

It has been demonstrated (8) that four types of flow mechanisms can exist during the simultaneous flow of a liquid and a gas or vapor. These flow mechanisms are:

(1) Flow of both the liquid and the gas may be turbulent.

(2) Flow of the liquid may be viscous and flow of gas may be turbulent.

(3) Flow of the liquid may be turbulent and flow of the gas viscous.

(4) Flow of both the liquid and the gas may be viscous.

Lockhart and Martinelli show that the pressure drop resulting from these various flow mechanisms can be correlated by means of two parameters ϕ and X. ϕ is equal to the square root of the ratio of the pressure drop per unit length during two-phase flow to the pressure drop per unit length for either the gas or liquid flowing alone. X is equal to the square root of the ratio of the pressure drop per unit length if the liquid flowed alone to the pressure drop per unit length if the gas flowed alone. The authors have plotted ϕ versus X, for ϕ based on both the gas pressure drop and the liquid pressure drop and for each of the four possible flow mechanisms (i.e. eight curves in all). On the same graph, curves of the fraction of tube filled with liquid and the fraction filled with gas are plotted against the parameter X.

It would appear that more data are needed to establish definitely the validity of these correlations. The effect of varying the liquid rate and the resulting change in flow pattern with varying liquid rate were not investigated.

However, van Wingen (19) compares pressure drops recorded in field lines between the well heads and the separators, with those computed by the method of Lockhart and Martinelli. He finds that at low rates of gas flow, the observed pressure drops are higher than those computed but that the difference is less than 1 p.s.i./1000 ft., and hence insignificant. At higher rates of gas flow, the divergence is higher but is in the direction of conservatism. Thus it would appear that for estimating the pressure drop for two-phase flow in horizontal pipes, this method could be of use.

McElwee (10) investigated viscous annular flow of air-kerosene mixtures in a vertical 5 m.m. pyrex tube in order to provide a further check on the analysis of two-phase flow using the flow parameters ϕ and X as developed by Martinelli and Lockhart.

The relation between flow parameters, presented in this previous work, is generally substantiated by McElwee. However, comparison of the results of this investigation and those obtained by Lockhart for the same flow conditions in capillary tubes shows a lack of correlation. This discrepancy renders questionable the neglect of surface and body forces in small tubes, in this and previous investigations. Since Lockhart's experiments were performed in capillary tubes, the possibility is indicated that the justification for neglecting capillary forces may depend upon tube size. McElwee presents an excellent photographic study of the several flow patterns

investigated with pictures taken at high speed (1/30,000th of a second).

Stuart F. Shaw is probably the leading authority in America, if not in the whole world, on the gas lifting of oil wells. Over the past 25 years he has published many papers discussing the gas lift, its use in various fields under many different conditions and the design of such installations (15, 16, 17).

In conducting his experimental work he has been more interested in the practical applications than in the fundamental understanding of two-phase flow patterns. In a booklet published in 1949 by The Agricultural and Mechanical College of Texas (17), a complete summary of Dr. Shaw's extensive investigations during the past ten years is given. Primarily, he has determined the productive capacities (i.e. the amount of liquid produced by a gas lift at any gas rate) of four diameters of pipe of various lengths when lifting oil and water by means of air lift.

Shaw previously showed (15) that there are four standard rates of flow which are significant in gas lift operations. As mentioned earlier, these are: 1) rate of no flow due to deficiency of gas; 2) rate of maximum efficiency; 3) rate of maximum yield, and 4) rate of no flow due to an excess of gas. Rates 1 and 4 have no practical application in lifting liquids. Shaw is principally concerned with rates 2 and 3. At these two rates he has varied the submergence (i.e. the static pressure at the fluid inlet), and has measured the gas and liquid rates. For each run he computes the percentage lifting efficiency (i.e. the foot-pounds of work performed in lifting a barrel of the liquid from the operating fluid level to the point of discharge divided by the number of foot-pounds given out by the gas employed in carrying on the lifting operation).

The results of this work are discussed by Shaw under three headings:

(1) Influence of submergence (upstream static pressure) on the capacity of a given flow pipe.

(2) Influence of length of pipe on the unit area capacity of the pipe.

(3) Influence of diameter of flow pipe on its unit area capacity.

(1) Increasing submergence increases the capacity of a pipe producing on air lift; also, as the percentage of submergence is increased, the lifting efficiency is increased up to some maximum point, but these tests do not definitely determine whether or not the lifting efficiency reaches some maximum point and then begins gradually to decline.

(2) At maximum capacity rate, unit area capacity at any given submergence increases with increased pipe length except for oil flowing in the small diameter tubes (1 inch and 1 1/2 inches). Similar results are obtained when producing at maximum efficiency rate. Shaw noted, however, that the graphs presented cannot be extrapolated to lengths of several thousand feet inasmuch as rates of flow indicated for such extrapolations would be far in excess of any production that has been obtained in oil wells for similar submergence conditions.

(3) With water, it would appear that capacities per square inch for all diameters of pipe tested remain fairly constant at a given submergence percentage. On the other hand, when lifting oil, there appears to be a marked tendency toward an increase in unit area capacity of the pipe as the diameter increases. Shaw again makes clear the fact that the data cannot be extrapolated to great depths.

In his conclusions to this report, Shaw formulates a very ambitions program for testing gas lifts. Such a plan, if carried out, would probably go a long way toward solving the difficulties of two-phase flow.

Carpenter (2), Gazley (4) and Jenkins (6) present pressure drop data for air-water mixtures in horizontal and vertical tubes, using "superficial" friction factors and Reynolds numbers calculated for the gas phase as though it is flowing alone in the tubes. They find that at any given gas flow, the addition of small amounts of liquid phase may increase the pressure drop from 2 to 50 times.

For horizontal tubes the friction factors increase with increased water rate at any Reynolds number and the flow pattern greatly influences the friction factor causing sharp rises in it during the transition regions between different flow patterns. These flow patterns are somewhat different from those in vertical tubes.

The data taken in the vertical tube are for downward annular flow. The results show friction factors near those for single-phase flow in the low turbulent region. At higher gas Reynolds numbers the friction factors pass through a maximum. The curves are extrapolated beyond this maximum with a negative slope in such a manner that they become roughly parallel to the curve for single-phase flow, implying that the water layer imparts "wavy roughness" characteristics to the gas flow. It is concluded that the orientation of the tubes is not important at high gas velocities.

A preliminary investigation of gas-liquid flow in vertical pipes was carried out by Radford (14) in 1949. The purpose of this work was to obtain a better fundamental understanding of the mechanism of two-phase

vertical flow, as in the case of an oil well producing a mixture of gas and oil. The equipment consisted of a vertical 23-foot section of clear, 1-inch plastic tubing with the necessary fittings for measuring the pressure drop and the rates of flow of the air and water used in the tests. Visual observations of the flow pattern were also made.

The results show that at any given water rate, as the air rate is increased from zero, the measured pressure drop passes through a first minimum point, a maximum point, a second minimum point, and then increases smoothly. Closely related to the change in pressure is a transition in the flow pattern from "slug" flow at the lowest rates, through "froth" flow and "film" flow to "mist" flow at the highest rates. This indicates that the flow pattern depends mainly on the air rate. Radford suggests that a modified Reynolds number based on the air rate might be used for further interpretive work.

The present project has been undertaken as a continuation of the work started by Radford. The equipment constructed by him is enlarged and improved such that the effects of tubing diameter and gas phase density can also be obtained. The equation developed in the earlier work is used to compute friction losses for pressure drops over a wide range of air rated at four different water rates. These losses, in turn, are used to compute friction factors (based on the flowing gas phase alone) by means of a Fanning-type equation, and are compared to Reynolds numbers (also based on the flowing gas phase alone), as suggested by Radford.

CHAPTER III

EXPERIMENTAL EQUIPMENT

The experimental equipment consists of a flow circuit through which air and water pass, and auxiliary equipment for measuring and controlling the flow variables. The details of each part are described separately.

1. Flow Circuit.

A schematic drawing of the flow circuit is shown in Fig. 1. It can be best explained under the following headings:

a. Air supply system.
b. Water supply system .
c. Mixing sections.
d. Test sections.
e. Air-water separation sections.

a. Air Supply System. Air supplied at 90 to 110 p.s.i. from a compressor is passed through a reducing valve which maintains the downstream pressure at 75 p.s.i., and then to the test equipment. A 1-inch "plug disc" globe valve controls the volume of air. For finer control a 1/4-inch by-pass line with a 1/4-inch needle valve is provided. Air flow is measured by an air flow manometer, connected to pressure taps located up and downstream from the orifice plate. In order to eliminate the necessity of frequently changing the orifice plates, two orifice unions are installed in parallel lines. The air flow manometer is connected to both sets of pressure taps. From the orifice unions the air supply line proceeds to the mixing section at the foot of the test sections. All lines between the air supply and the mixing section are one inch unless otherwise noted.

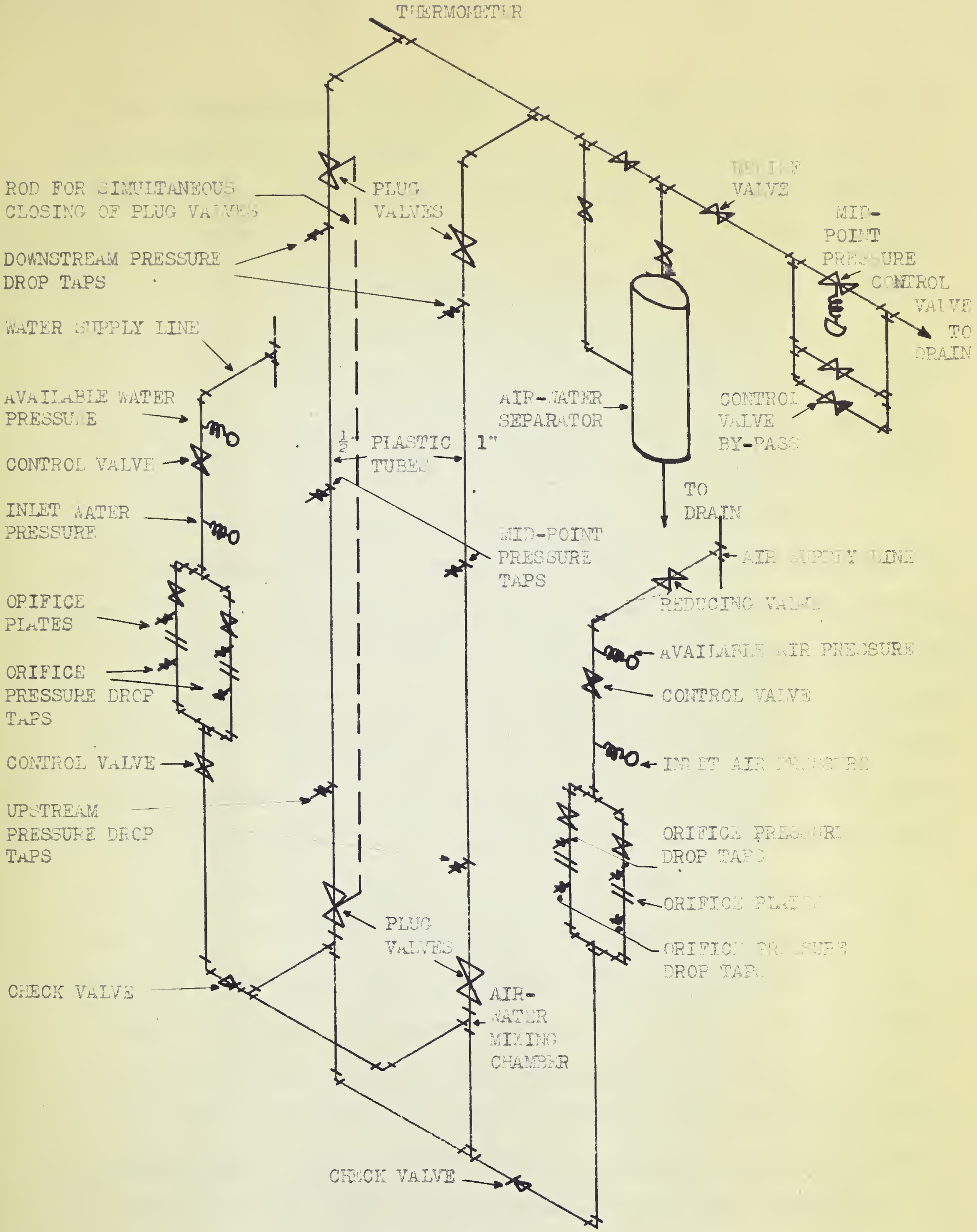

FIG. 1.— [illegible] O. CIRCUIT.

b. Water Supply System. Water is supplied at 23 p.s.i. from a constant level overhead tank. When the equipment is operated at the higher test section pressure (36 p.s.i.) the water is by-passed through a centrifugal pump having a capacity of 70 gallons per minute at 110 p.s.i. A 1-inch "plug disc" globe control valve and a water flow manometer connected to two sets of pressure taps on orifice lines are used to control and measure the water flow. A second control valve downstream from the orifice lines can be closed in order to prevent a negative pressure in the manometer, due to the water supply line to the mixing section being below the manometer. All lines between the water supply and the mixing section are one inch unless otherwise noted.

c. Mixing Section. The mixing section shown in Fig. 2 is merely a vertically placed 2" x 2" x 1" galvanized iron tee. Air enters the bottom 2-inch branch, water the 1-inch side branch, and the resulting air-water mixture flows through the top 2-inch branch. A 2" x 1" reducer and the female half of a 1-inch union at the top of the tee connect to the male half of a 1-inch union at the bottom of each test section. In the smaller test section there is a 1" x 1/2" reducer above this union connecting it to the plastic tube. Below the mixing section there is a two-inch union containing ten 2-inch diameter circular discs of 40-mesh screen which serve to disperse the air prior to mixing. A 2" x 1" reducer and a 1-inch union connect this union and the mixing section to the air supply line. Water from the water header enters the side branch of the mixing section through a 1-inch union. Check valves are located in both air and water lines upstream from the unions connecting them to the mixing section.

d. Test Section. There are two vertical test sections, sizes 1" and 1/2", each extending 35 feet above the mixing section. The actual transparent plastic tubes are each 30 feet long and lie between approximately 2 1/2-foot

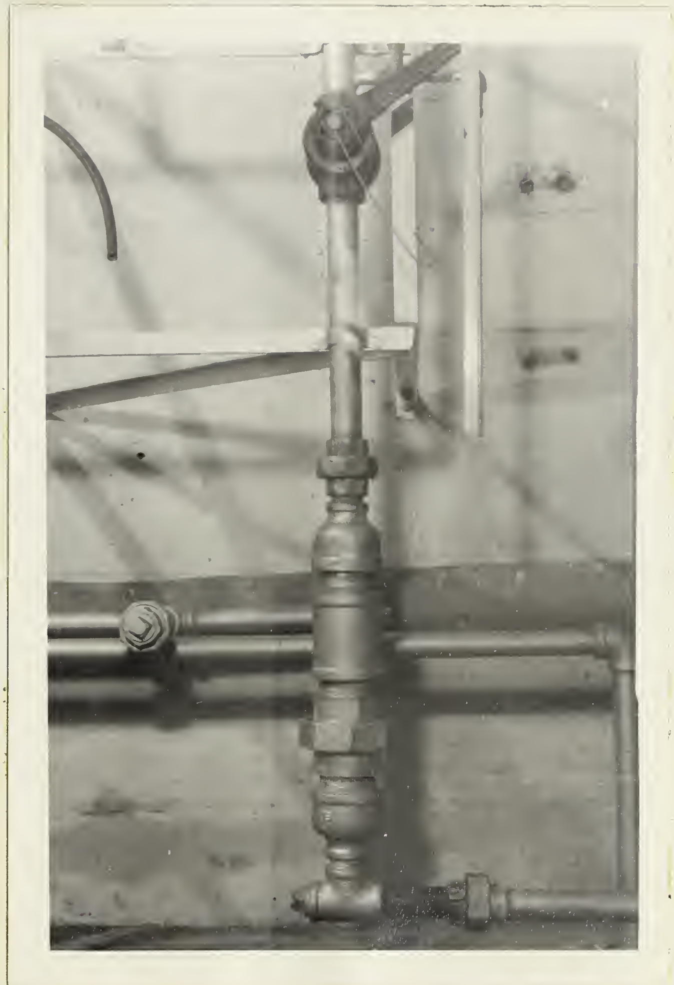

Fig. 2. Air-Water Mixing Station.

sections of galvanized iron pipe (1/2" for the smaller tube and 1" for the larger tube). Appropriately-sized lubricated plug valves are located in both the top and bottom sections of the galvanized pipe. The top and bottom plug valves of the test section being used are interconnected by a 3/4-inch angle aluminum rod. Immediately above the bottom valves there are 1/8-inch needle valves for draining the test sections. By moving the rod up or down , the top and bottom plug valves of the section being used can be opened or closed simultaneously. The actual inside diameters of the plastic in the two test sections are 1.049-inch and 0.640-inch. Each plastic test section contains two 15-foot lengths of clear butyrate tubing. In joining the sections of plastic tubing, a close fitting plastic sleeve is slipped over the butted ends and then sealed to the tubes, using chloroform.

In joining plastic tubing to a similar-sized section of galvanized iron pipe, a reducer is used. The small end of the reducer is screwed in the end of the galvanized pipe (see Fig. 7). The inside of the reducer is then machined so that the end of the plastic tube can be butted against the iron pipe inside the reducer. A split brass collar is fitted in a machined groove on the outer surface of the plastic tubing about 1/2-inch from the butted end. Above this is a snug-fitting bushing. Screwing the bushing in the reducer forces down on the collar, thus ensuring a snug fit between the butted ends of the plastic tubing and iron pipe.

The plastic test sections are fitted flush in the "V"s of 30-foot vertical sections of angle iron. Each angle iron section is spot welded to the grating of the floor levels and braced at the top and bottom to the wall.

In the larger tube the pressure drop is measured over a 22.88-foot section of plastic tube and in the smaller tube over a 22.78-foot section. The bottom pressure taps are about 8 feet above the mixing chamber.

The pressure taps in the flow sections are blocks of lucite machined to fit each tube. Each block has a hole bored and tapped for 1/8-inch fittings. A 3/16-inch hole is carefully drilled in the plastic tubing where the pressure station is desired. The plastic block is then placed on the tubing so that the 1/8-inch and 3/16-inch holes coincide. It is then sealed to the tube, using chloroform.

e. Air-Water Separation Section. The two vertical test sections can be connected separately to the 1-inch discharge header. In Fig. 3 the smaller tube is shown connected. The temperature of the air-water mixture is obtained from a thermometer in this header. The header connects to an air-water separator consisting of a 30-gallon hot water tank supported at the middle by flanges on the floor grating. The top half of the separator is shown in Fig. 4 and the bottom half in Fig. 5. A sight glass is fitted on the lower half of the tank to indicate the amount of water in the tank. The air-water mixture enters at the middle of the tank, the water falls to the bottom and the air passes out of the top. The separator can be by-passed if necessary. When the test equipment is running, about a foot of water, indicated by the sight glass, is kept in the separator to maintain the required pressure in the test section. A 1-inch "plug disc" globe valve at the bottom of the tank is used to control this water level. The water passes out through a 1-inch line to the drain. The air leaving the separator passes into the discharge line, through a 1-inch relief valve set to open at 30 p.s.i., and a 1/2-inch control valve, and into an open-ended vertical 6-inch drain pipe. The air separates to the atmosphere and any moisture in the air drops into the drain.

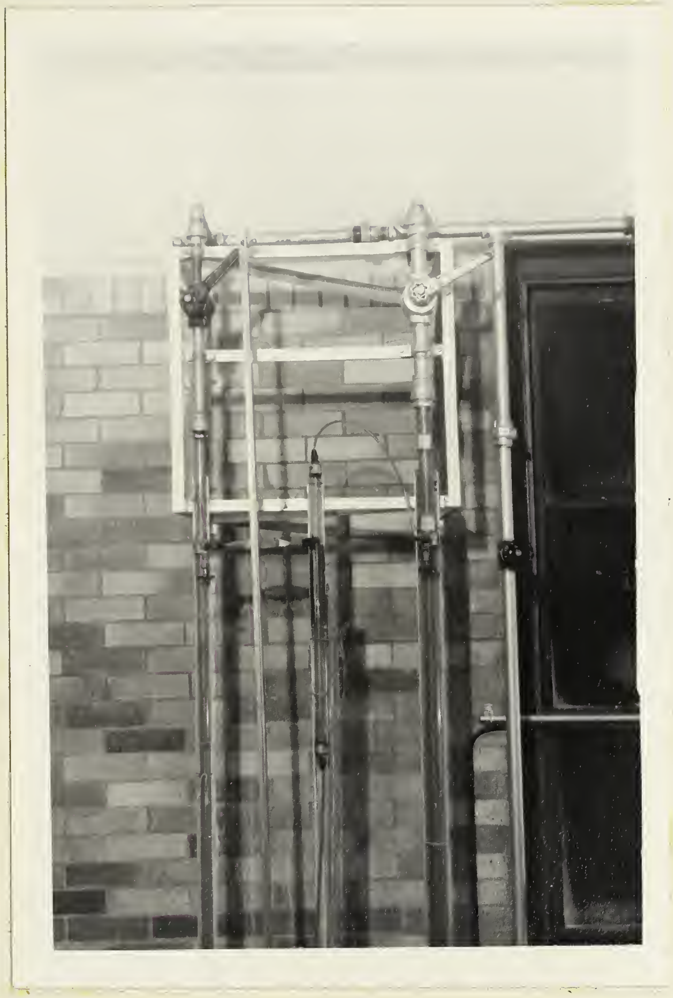

Fig. 3. Upper Flow Section.

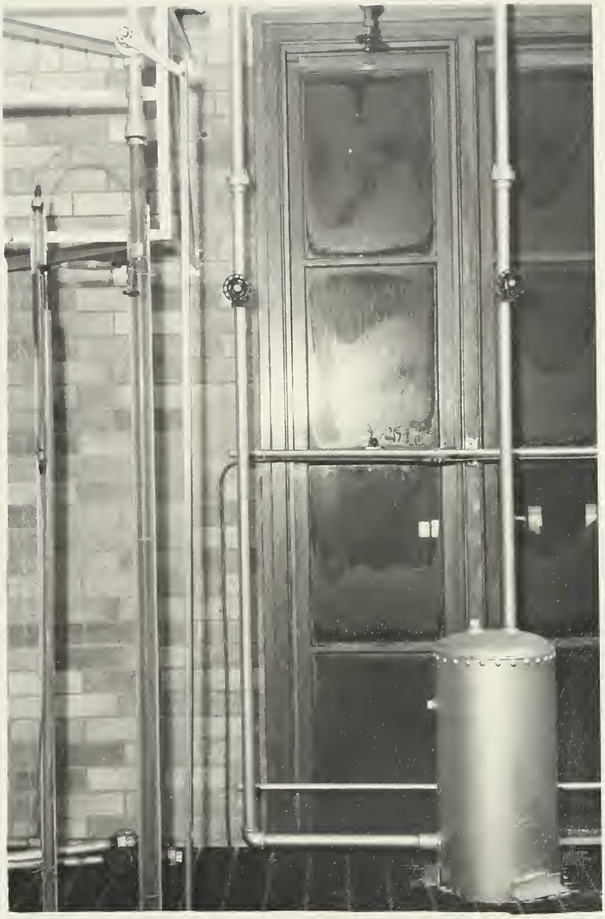

Fig. 4. Top Half of Air-Water Separator.

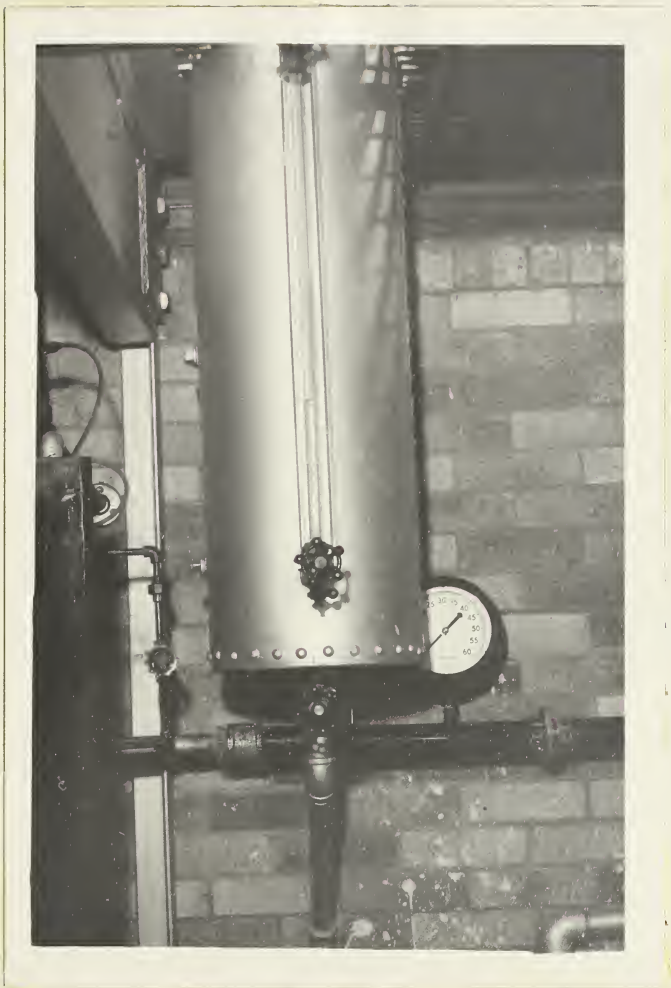

Fig. 5. Bottom Half of Air-Water Separator.

2. Auxiliary Equipment.

The panel board shown in Fig. 6 is situated on the same level as the air and the water control valves. The two test sections pass flush in front of the panel board. A third test section (3/4-inch size), not as yet in use, is also shown. On the extreme left of the panel board are four pressure gauges measuring the water and the air pressures above and below the globe control valves. Next is a 5-foot Meriam manometer for measuring the water orifice differential pressure. Two manometers are used, one containing mercury under water and the other, carbon tetrachloride under water. To the right of the water differential manometer is another 5-foot Meriam manometer (partially obscured in Fig. 6 by the 3/4-inch angle aluminum rod) containing mercury under air. This manometer has one leg open to the atmosphere and the other leg has two needle valves on it such that either the mid-point pressure in the test section or the static air pressure upstream from the air orifice can be measured. The next two 76-cm. Meriam manometers, containing mercury under air and water under air, measure the differential pressure drop of the flowing mixture over the test section. The 76-cm. Meriam manometer on the extreme left of the panel board measures the air orifice differential pressure. Two manometers are used, one containing water under air for low air rates and the other, mercury under air. All manometers have traps on both legs to prevent their fluids from being blown into the system.

On the upstream and downstream pressure taps and the test section mid-point pressure tap there are separators to prevent water from entering the manometer leads. Fig. 7 shows the downstream tap and separator. These are constructed of two-foot lengths of 1/2-inch butyrate tubing capped at

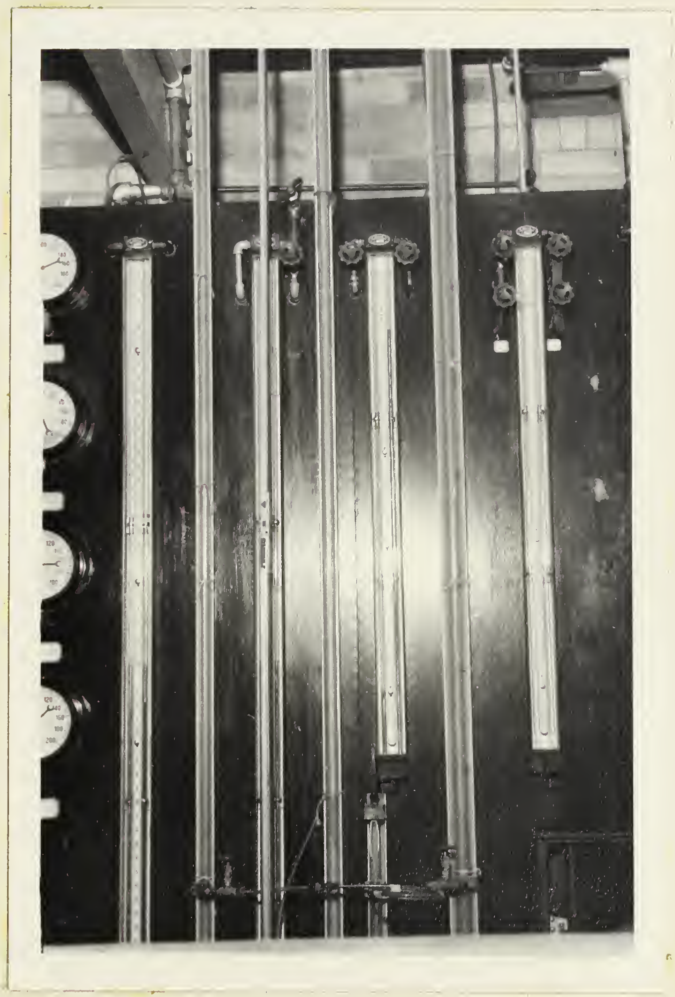

Fig. 6. Panel Board.

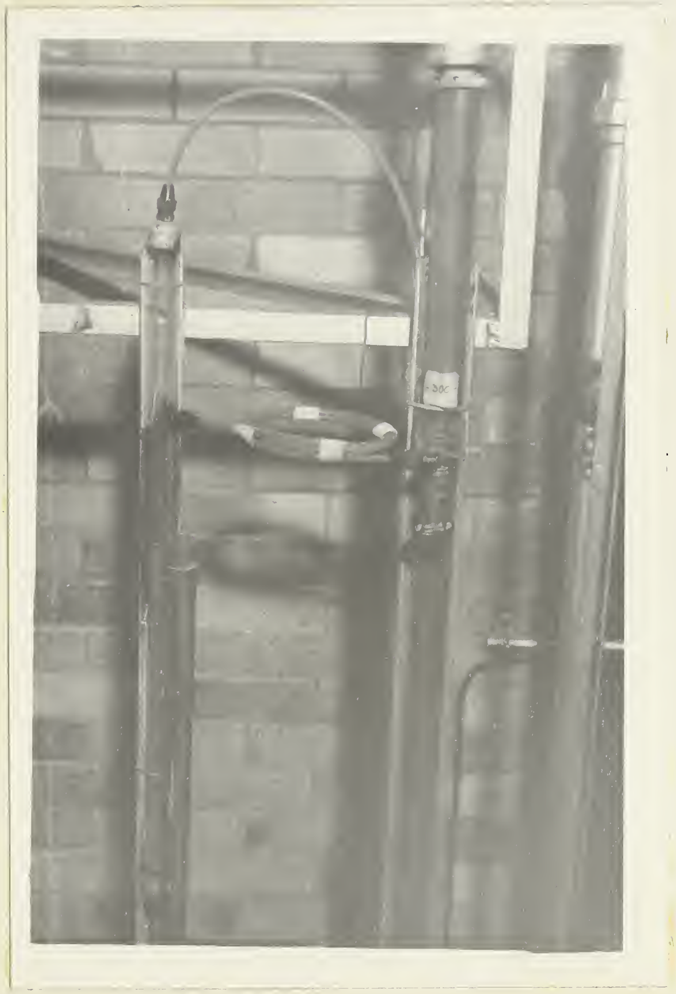

Fig. 7. Downstream Pressure Tap
and Separator Assembly.

either end with 1/2-inch galvanized iron caps that are drilled and tapped for 1/8-inch pipe. About eight inches from the top the butyrate tube is drilled and tapped and fitted with an 1/8-inch Saran fitting. This connects to the 1/8-inch needle valve on the Lucite pressure tap through a three foot length of Saran tubing that is coiled to a five-inch circle. The pressure tap and the Saran fitting are in the same plane. The function of the Saran coil is to prevent water from passing into the separator. Since the pressure in the test section tends to oscillate, any air-water mixture in the coil moves back and forth with these pressure variations and only a slight amount of water is lost in the separator. The manometer leads run to the tops of the separators. Any water in the bottom of the separator can be drained through 1/8-inch needle valves controlled on a panel board.

The separator at the mid-point pressure tap (Fig. 8) is slightly smaller than the other two, and has Lucite caps. The Saran tubing from the top of this separator divides, and one line goes to the 5-foot static manometer and the other to a Brown Air-O-Line pneumatic controller. This controller, by actuating a Belfield 1/2-inch motor valve in the air discharge line, maintains constant midpoint pressure in the test section. The instrument has a proportional plus reset type of control action and both the proportional band and the reset rate can be varied. Air from the air supply header, filtered and reduced to 17 p.s.i., operates the controller. The motor valve has a bypass consisting of a 1/2-inch hand control valve and a 1-inch gate valve in parallel. The controller is shown in Fig. 9, and the motor valve in the air discharge line is shown in Fig. 10.

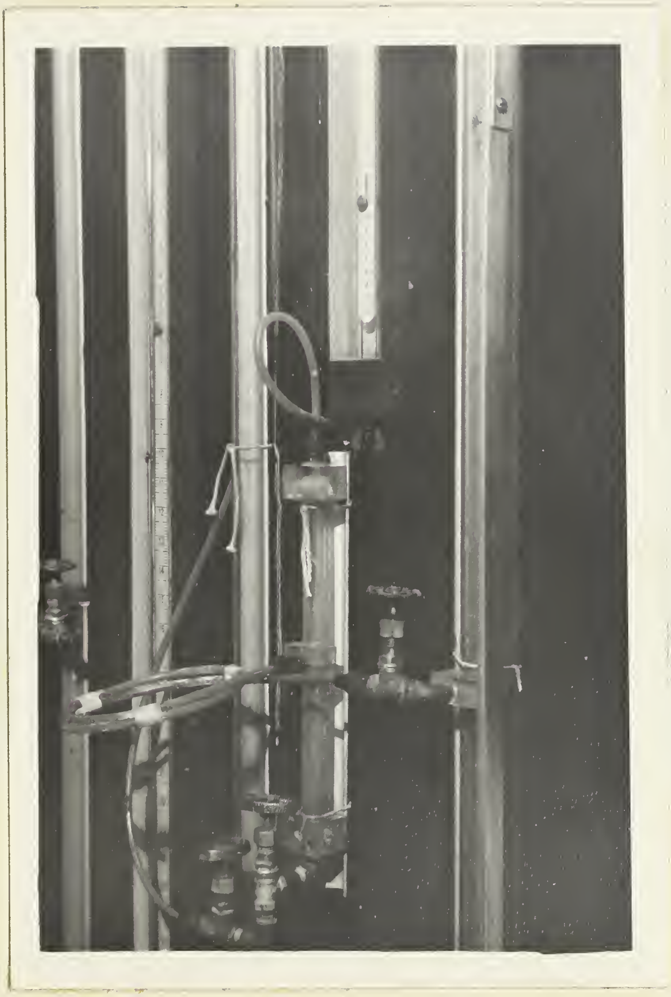

Fig. 8. Mid-Point Pressure Tap and Separator Assembly.

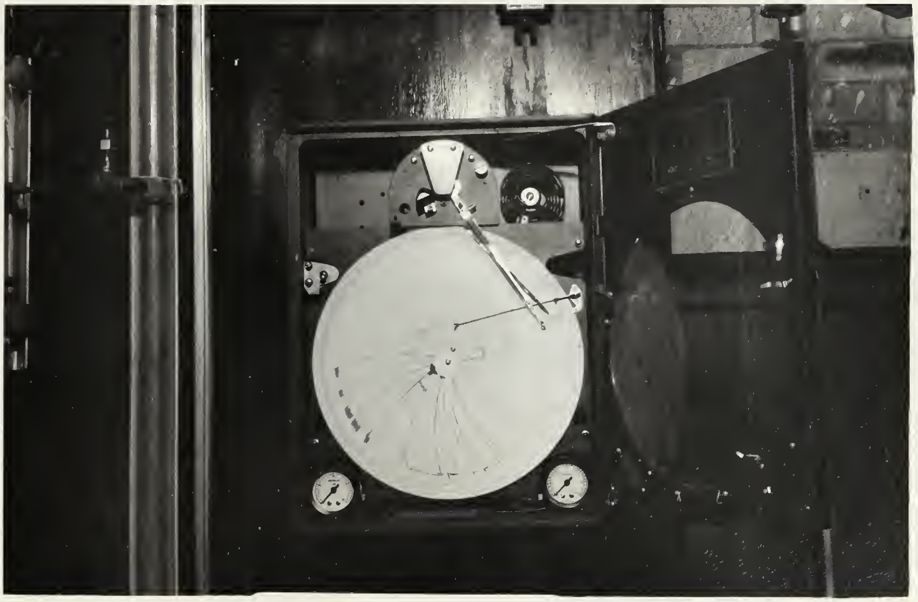

Fig. 9. Mid-Point Pressure Controller.

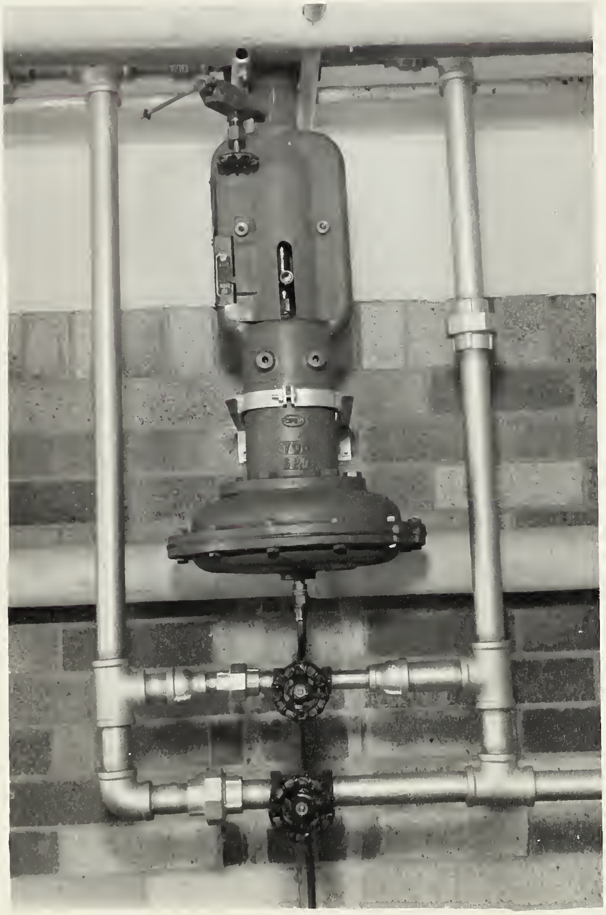

Fig. 10. Mid-Point Pressure Control Valve.

CHAPTER IV

EXPERIMENTAL PROCEDURES

In each tube, four series of constant water rate tests were made at test section mid-point pressures of 18 and 36 p.s.i.a. In all, 16 series of tests were made and for each series the air rate was varied from zero to the maximum rate attainable, the limit being reached when the mid-point pressure control valve and the control valve by-pass valves were wide open. (Any higher air rate resulted in the mid-point pressure increasing above the desired value.) In addition, an exploratory run was made at a water rate of 4.15 lbs/ft^2 sec. and a mid-point pressure of 18 p.s.i.a. in the 1-inch tube, in which a liquid detergent (Tergitol) was added to the water in such an amount that its concentration was one part in ten thousand parts water. The same operating procedure was followed in each test.

Operating Procedure.

With both plug valves open and all pressure taps on the test section and the water orifice lines closed, the water control valves above and below the orifice lines are opened to admit water to the test section., Water is flowed through the test section until no air bubbles are observed in the water in the plastic tube. The lower water control valve is then closed and the orifice line pressure taps (both lines) are opened. Valves on the traps on the water flow manometer are then opened to permit "de-airing" of the manometer. When "de-airing" is completed, the valve above the orifice not being used is closed, along with the pressure taps in the same line. Using both water control valves, a water rate slightly higher than desired is set. The air control valve is then opened carefully until approximately the desired

rate is reached. The mid-point pressure tap is then opened and the controller is turned on by admitting compressed air to it. The desired value of the mid-point pressure is set on the controller with the control index. Generally, a proportional band of 40% and a reset rate of 3 are found to give best control. The water and air rates are then adjusted to the desired values and conditions are kept constant for ten or fifteen minutes. During this period, the air-water mixture temperature and the air temperature are noted and the barometer is read. The pressure drop taps are then opened and readings are taken of the water flow manometer, the air flow manometer, the static air and the mid-point pressure manometer, the gauge static air pressure and the pressure drop manometer. The pressure drop taps are then closed and the rod connecting the top and bottom plug valves is briskly pulled down. The controller is then turned off and the air and water control valves are closed. After allowing the water five minutes to settle, the level of the water in the tubes is recorded. The exact volume between the plug valves has been determined and marks corresponding to 100 c.c. intervals are found on the plastic tubes. With the completion of the test, the rod connecting the top and bottom plug valves is raised and a new test is carried out in a similar manner.

CHAPTER V

EXPERIMENTAL DATA

The experimental data are presented in Tables I - III of Appendix A and in Tables IV - VIII of Appendix B. The data in Appendix A deal with calibrations and the data in Appendix B deal with the actual experimental tests.

Appendix A.

Table I contains data for the calibration of the water orifice plates. The test number is listed in column 1. Column 2 gives the amount of water collected in one-and two-litre flasks over the time interval listed in column 3. The calculated water rate, in ml/sec. and ft^3/sec. is shown in column 4. The differential across the water flow manometer is reported in column 5 as inches of mercury under water, or as inches of carbon tetrachloride under water. Plots of water rate versus manometer differential for the two orifice plates used are shown in Figs. 48 and 49 following Table I.

Table II presents data for the calibration of the air orifice plate constants using a critical flow prover. The number of the air orifice plate being calibrated is listed in column 1. The pressure, in p.s.i.a., upstream of the air orifice plate and the pressure differential, in inches of mercury under air, across the air orifice plates, are reported in columns 2 and 3 respectively. The temperatures, degrees absolute, and the pressure, in p.s.i.a. upstream of the critical flow prover are listed in columns 4 and 5 respectively. Column 6 gives the size of the critical flow prover and column 7 the critical flow coefficient of the prover.

The results calculated from the data in Table II are listed in Table III. The air orifice plate number is reported in column 1. The actual

flow rates, in 1000 ft^3/day are presented in column 2. These were calculated using the equation

$$Q_c = \frac{C\ P_c}{\sqrt{ST}}$$

where Q_c = rate of flow, 1000 ft^3/24 hrs. at 14.4 p.s.i.a. and 60°F.

C = critical flow coefficient.

P_c = pressure upstream of critical flow orifice, p.s.i.a..

S = specific gravity of the gas (= 1 for air).

T = upstream temperature of flowing gas, °R.

The air rate converted to ft^3/sec. is reported in column 3, the term $\sqrt{\frac{h_f\ P_f}{T}}$ calculated from columns 2, 3 and 4 of Table II, is given in column 4, and the air orifice plate constant, K, is listed in column 5. These constants were calculated from the equation in the booklet, "The Orifice Meter" published by the Pittsburgh Equitable Meter Company. The equation states that

$$Q_c = K \sqrt{\frac{h_f\ P_f}{T}}$$

where Q_c = air rate, ft^3/sec. at 14.4 p.s.i.a. and 60°F,

K = air orifice plate constant,

h_f = manometer difference, inches mercury under air,

P_f = pressure upstream of air orifice plates, p.s.i.a.,

T = air temperature, °R.

The average values of the constant for each plate, shown in column 5, are plotted versus their respective orifice diameters in Fig. 50 following Table III. The value of K for No. 2 Orifice Plate appears to be high. Since the value, 0.157, is above the curve which intersects the other three points,

is also higher than the value obtained by Radford (0.135), it is felt that the value of K at the point where the diameter of the plate intersects the line (0.147) will be more accurate, and hence is used.

Appendix B.

Table IV contains supplementary data giving the lengths and diameters of the test sections and the volumes of the test sections between plug valves.

Table V contains the single-phase water flow experimental date for the 1/2-inch tube. The test number is indicated in column 1 and the water temperature, in °F., in column 2. Column 3 gives the water rate, in ft^3/sec., flowing through the tube, and column 4 shows the pressure drop over the test section in cm. of carbon tetrachloride under water and in cm. of mercury under water.

Table VI contains the single-phase air flow experimental date. The test number is indicated in column 1, the test section in column 2 and the test section mid-point pressure in column 3. The flowing air rate, in ft^3/sec. at 14.4 p.s.i.a. and 60°F., is given in column 4 and the air temperature in °R., in column 5. In column 6 the measured pressure drop over the test section, in cm. of water under air and in cm. of mercury under air, is shown.

The two-phase flow experimental data are shown in Table VII. Column 1 gives the test number and column 2 the test section. The water rates in both ft^3/sec. and lbs,/ft^2 sec., are shown in column 3. The test section mid-point pressure is indicated in column 4 and the flowing air rate, in ft^3/sec., at 14.4 p.s.i.a. and 60°F., in column 5. In column 6 the measured pressure drop over the test section, in cm. of Hg under air, is shown.

Column 7 gives the volume of air in the test section for each run and column 8 the volume of water, in the test section. The sum of these two is equal to the total volume of the test section between the plug valves.

The results of the exploratory runs with one part in ten thousand of detergent added to the liquid phase, are shown in Table VIII. The test number is given in column 1, the flowing air rate in ft^3/sec. at 14.4 p.s.i.a. and 60°F, in column 2, and the measured pressure drop over the test section, in cm. of mercury under air, in column 3.

CHAPTER VI

CALCULATED RESULTS

The important results calculated from the original data are presented in Tables IX - XVI of Appendix C.

In Table IX the single-phase water flow calculated results for the 1/2-inch tube are shown. The test number is given in column 1. The water velocity, in ft./sec., is listed in column 2 and the measured pressure drop, calculated as ft. of water, in column 3. The Reynolds number, $\frac{\rho DV}{\mu}$, is shown in column 4. In column 5, the friction factor, defined as $f = \frac{gFD}{2V^2N}$, is given.

In Table X the single-phase air flow calculated results are presented. The test number is listed in column 1, the test section in column 2 and the mid-point pressure in p.s.i.a., in column 3. In column 4 the flowing air rate, in ft^3/sec. at flowing pressure and temperature, is shown and in column 5 the air velocity in ft./sec., calculated from the air rates of column 4 is shown. The measured pressure drop, in feet of air at flowing pressure and temperature, is given in column 6. The Reynolds number is shown in column 7 and the friction factor in column 8. These are calculated in the same manner as for the water flow results.

Plots of friction factor versus Reynolds number for the water flow and the air flow are shown in Figs. 11 and 12.

The calculated results of the two-phase data are shown in Table XI. The test number is shown in column 1 and the test section in column 2. The water rate, calculated in ft^3/sec, and in lbs/ft^2 sec. is shown in column 3 & 4. In column 5 the test section mid-point pressure in p.s.i.a. is given, and in column 6, the discharge air water ratio obtained by dividing the water rate

into the air rate (at 14.4 p.s.i.a. and 60°F.) is listed. The measured pressure drop , calculated in p.s.i./100 ft., is given in column 7. The test section air-water ratio, obtained by dividing the volume of water between the plug valves into the volume of air (columns 7 & 8, Table VII) is shown in column 8.

The measured pressure drops are plotted versus the discharge air-water ratios for each water rate at both mid-point pressures in both tubes in Figs. 19 - 26. The test section air-water ratios are plotted versus the discharge air-water ratios in Figs. 32 - 39.

The values of the pressure drops and the discharge air-water ratios corresponding to each maximum and minimum point in Figs. 19 to 26 are shown in Table XII. The test section is listed in column 1, the mid-point pressure in p.s.i.a. in column 2, and the water rate in lbs/ft^2 sec. in column 3. In columns 4 and 5 the pressure drop and the discharge air-water ratio at the first minimum are listed; in columns 6 and 7 the pressure drop and the discharge air-water ratio at the maximum are listed, and in columns 8 and 9 the pressure drop and discharge air-water ratio at the second minimum are listed.

In Figs. 27 and 28 the pressure drops at these inflection points are plotted versus water rate, and in Figs. 29 and 30 the discharge air-water ratios are plotted versus the water rate.

The calculated results of the exploratory runs with detergent added to the water are shown in Table XIII. The test number is given in column 1, the discharge air-water ratio in column 2, and the measured pressure drop in column 3. The measured pressure drops are plotted versus the discharge air-water ratio in Fig. 31. The curve for the two-phase flow without any deter-

gent (Fig. 23) is also shown in Fig. 31 for comparison.

In Table XIV the two components of the pressure drop, the hydrostatic head and the irreversibilities are calculated for various discharge air-water ratios in the 1-inch tube at 18 p.s.i.a. for a water rate of 4.15 lbs/ft^2 sec. In column 1 the discharge air-water ratios are listed and in column 2 the measured pressure drops at these discharge ratios (taken from the 18 p.s.i.a. curve in Fig. 23) are listed. The equation for the pressure drop is

$$\frac{\Delta P}{\Delta X} = \frac{g}{\beta} \frac{(\frac{G}{L}) + 1}{(\frac{G}{L} v_G) + v_L} + \frac{\Sigma F_L}{\Delta X \left[(\frac{G}{L} v_G) + v_L \right]}$$

The term $\frac{g}{\beta} \frac{(\frac{G}{L}) + 1}{(\frac{G}{L} v_G) + v_L}$ represents the hydrostatic head component of the pressure drop. In column 3 the values of this component are multiplied by the ratio $\frac{144}{100}$ to give the units of p.s.i./100 ft. The term $\frac{\Sigma F_L}{\Delta X \left[(\frac{G}{L} v_G) + v_L \right]}$ represents the irreversibility component of the pressure drop and is obtained by subtracting the hydrostatic head component from the measured pressure drop (column 3 from column 2). The units are p.s.i./100 ft. In Fig. 40 the two components of the pressure drop and the pressure drop itself are plotted versus the discharge air-water ratio.

The calculated results of the superficial friction factors and Reynolds numbers are presented in Table XV. In column 1 the test section is shown; in column 2 the water rate in lbs/ft^2 sec. is shown, and in column 3 the mid-point pressure in p.s.i.a. is shown. In column 4 the pressure drop, in p.s.i./100 ft. is given and in column 5 the corresponding discharge air-water ratio in ft^3 s.c./ft. is given These two columns are obtained from

the curves of Figs. 19 to 26 and the values have been chosen to include the entire curves. The mass rate of flow of air, in lbs/sec. is shown in column 6. The air is assumed to be saturated with water vapor. In column 7 the friction loss term, ΣF_L, of the irreversibility component of the pressure drop is given. The units of this term are ft.lbs_f/lb_m of water. To obtain ΣF_G, the friction loss in terms of the flowing gas, the values of ΣF_L are multiplied by $\frac{L}{G}$, the ratio of the mass rate of flow of water to the mass rate of flow of the air. These are listed in column 8. The superficial friction factors based on the flowing gas phase are given in column 9. These are calculated from the equation defining the friction factor as

$$f_G = \frac{\beta}{2} \left(\frac{DA^2}{v_G^2 N}\right) \frac{\Sigma F_G}{G^2}$$

Superficial Reynolds numbers based on the flowing gas phase are shown in column 10. These are obtained from the equation

$$Re_G = \frac{DV_G \rho_G}{u_G} .$$

The friction factors for each water rate and each mid-point pressure in the 1/2-inch tube are plotted versus Reynolds numbers in Fig. 41. The corresponding curve for the 1-inch tube is shown in Fig. 42.

In Table XVI friction factors at Reynolds numbers of 2000, 6000, 10,000 and 20,000 for each curve in Figs. 41 and 42 are presented. The test section is shown in column 1, the mid-point pressure, in p.s.i.a., in column 2 and the water rate, in lbs/ft^2 sec., in column 3. In column 4 the ratio of the gas phase specific weight to the liquid phase specific weight is shown. In columns 5, 6, 7 and 8 the friction factors at Reynolds numbers of 2000,

6000, 10,000 and 20,000 are listed.

In Figs. 43 and 44 the friction factors at these Reynolds numbers are plotted versus (W + 0.1), where W is the water rate in lbs/ft^2 sec. In Fig. 45 the same friction factors are plotted versus $\frac{\rho_G}{\rho_L}$, the ratio of the gas phase specific weight to the liquid phase specific weight. In Figs. 46 and 47, the friction factors are plotted versus the tube diameters for each mid-point pressure.

CHAPTER VII

INTERPRETATION AND CORRELATION OF RESULTS

A. Single-Phase Flow.

In Fig. 11 the plot of friction factor versus Reynolds number for water in the 0.640-inch tube is shown. For comparison, the friction factor curve obtained by Radford for the 1.049-inch tube and the curve for smooth pipes are also plotted. It will be noted that the curves for the 0.640-inch and the 1.049-inch tubes are above the curve for smooth pipes. The data in the smaller tube were taken immediately following the pure air runs. The air carried with it a slight oil mist from the compressors and this oil may have been deposited on the walls of the tube to give the effect of roughness since the tube should be smooth or nearly so.

In Fig. 12 the plot of friction factor versus Reynolds number for air in both tubes at both pressures is shown. Only the data in which the measured pressure drops corresponding with manometer readings greater than 8 c.m. of water are plotted, in order to reduce possible error. Even after eliminating the low pressure drop results, the data show random scattering and lie mostly below the curve for smooth pipes. The data taken at 36 p.s.i.a. in the 0.640-inch tube are the exception and are close to, or on, the smooth pipe curve. Results from previous work in the 1.049-inch tube are also plotted. They lie even farther below the smooth pipe curve.

A comparison of the water and air data shows contradictory results. It seems hardly possible that mis-alignment of the pressure tap openings into the tubes or burrs or other roughnesses would cause the discrepancies in the air data, since their effect would also be noticed in the water data. Leaks in the manometer lines and pressure taps can hardly be considered a source of

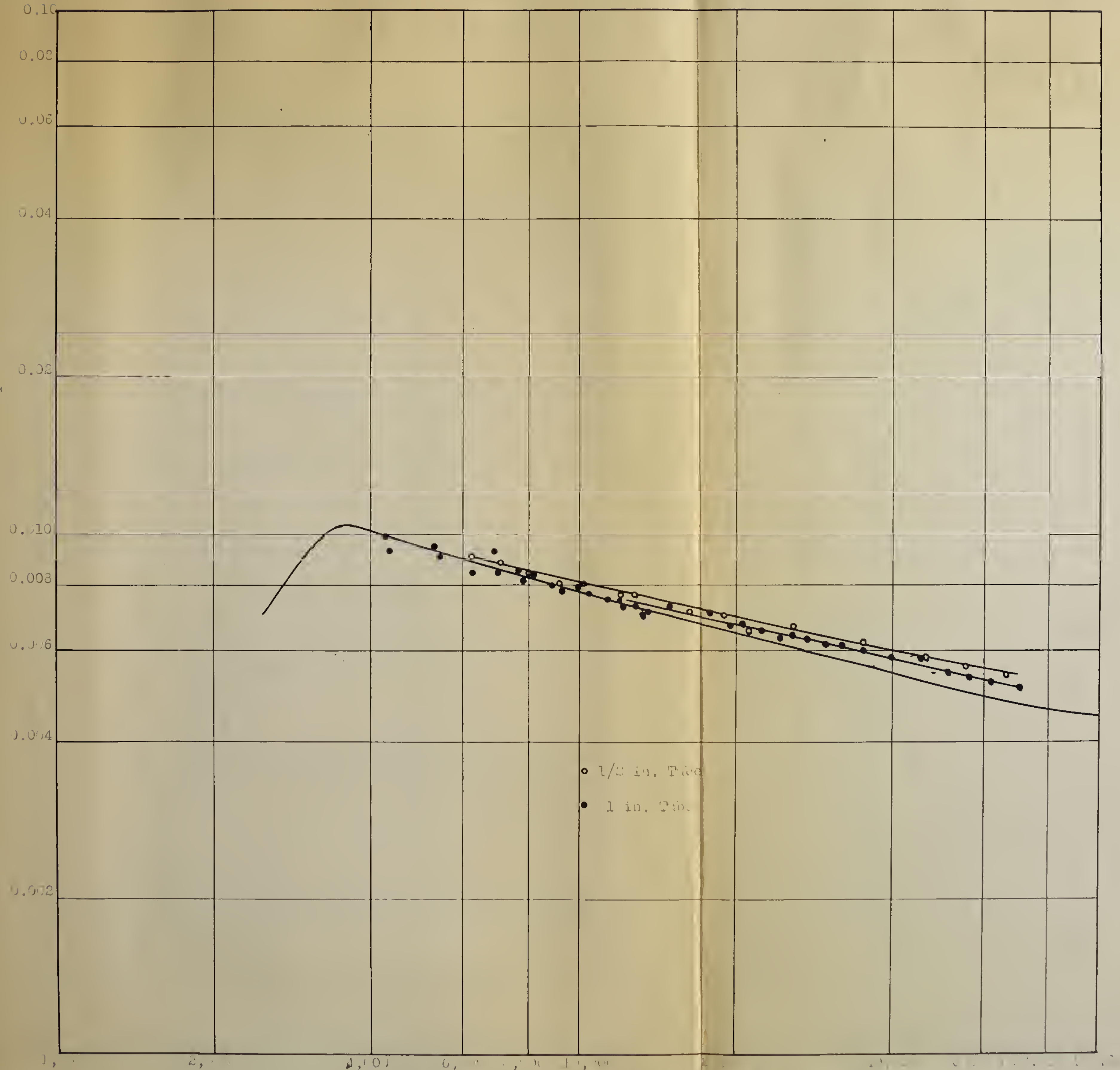

Fig. 11. Reynolds Number Plot for Single-Phase Water Flow.- Friction Factor.

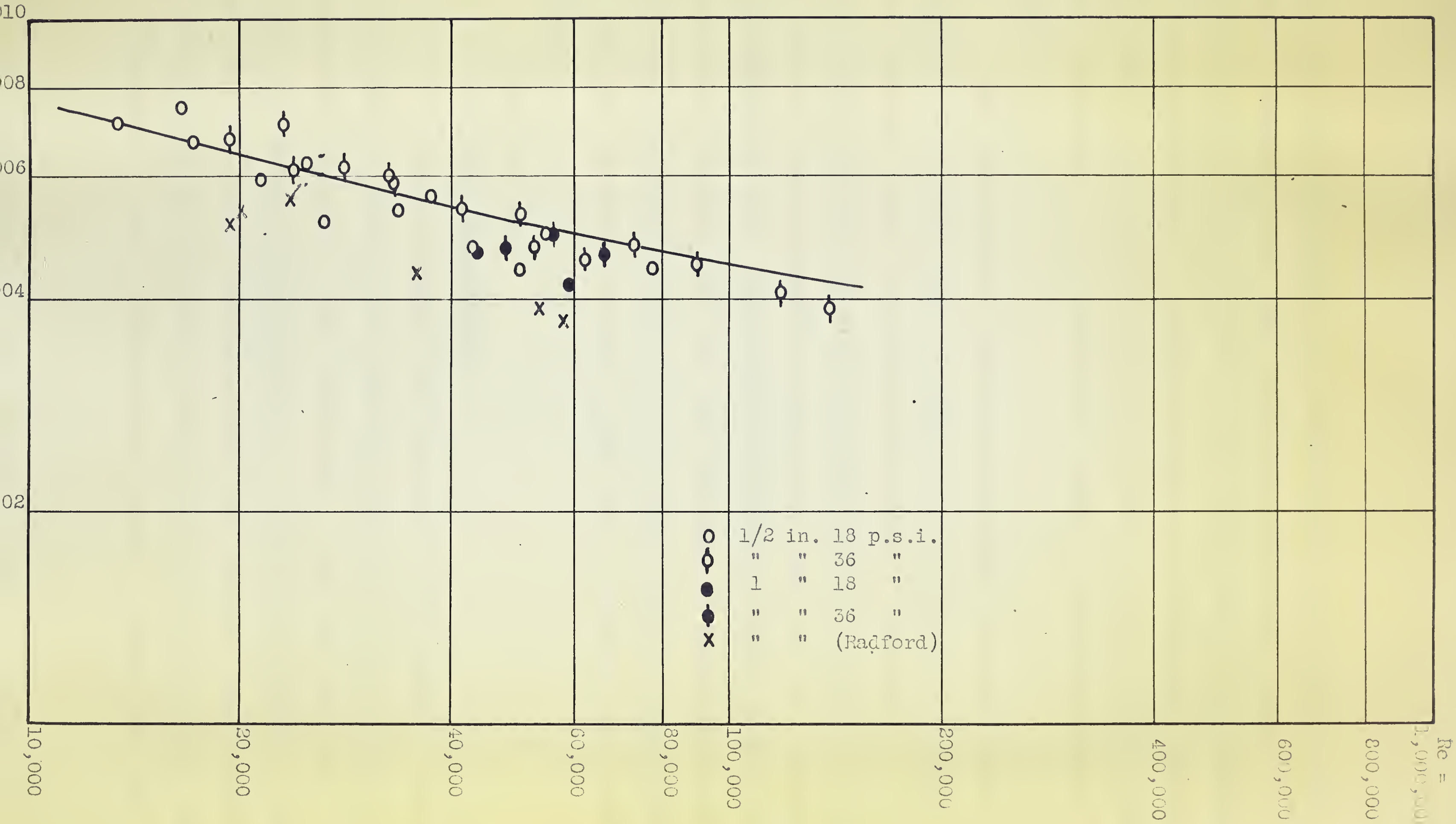

Fig. 12. Friction Factor - Reynolds Number Plot for Single-Phase Air Flow.

error since they were prevented by frequent testing with a soap solution. Errors in measuring the air flow would not be great enough to account for the errors either. The calibrations of the orifice plates used to measure the air were checked until consistent results were obtained. The effect of water vapor or fine oil mist in the air, on the viscosity of the air would not be great enough to affect either the viscosity or the density significantly.

Thus, no completely satisfactory explanation has been found to account for the scattered data. It might be well to note that, as Binder (1) says, "One cannot expect a high degree of accuracy in determining f. For smooth tubing actual data may show a variation or scatter of ±5 per cent in f. For commercial steel or wrought iron pipe, actual data may show a variation within ±10 per cent in f." The average of the water and the air data is within 5 per cent of the smooth pipe curve. The conformity of these data to within 5 per cent of the accepted values of f for a smooth pipe is an indication that the tubes are smooth or nearly so, and that the pressure drop data are reliable.

B. Two-Phase Flow.

1. Visual Observations.

Pressure drops for the flowing air - water mixtures in the two test sections were measured for various air rates over as wide a range as possible at each of the four different water rates. These data were taken at two constant test section mid-point pressures. For both test sections, at any water rate and at either mid-point pressure, the flowing two-phase mixture was observed to follow the same flow pattern with increasing air rate. Thus the introduction of air into flowing water results in bullet-shaped slugs of

air travelling up through the water separated by pistons of water. This is the slug flow region and is shown in Fig. 13. Increasing the air rate causes the slugs to become longer and bubbles of air to form in the water pistons. Such is the case in Fig. 14 where the top half of the photograph shows part of an elongated slug of air and the bottom half a piston of water mixed with bubbles of air. Gradually the pistons of water become frothy and merge together into "froth" flow characterized by a more nearly uniform mixture of air and water occupying the whole cross-section of the tube. The motion of the water appears to be random. This flow pattern is shown in Fig. 15. Further increasing the air rate results in part of the water moving up the walls of the tube, as in Fig. 16. Gradually less and less water mixes with the air until all the water moves up the tube walls and the air passes up the center in a core. Thus the annular film flow region is reached as shown in Fig. 17. With still higher air rates, the air core picks up the water as a mist, as in Fig. 18. Eventually, all of the water is flowing as a mist in the air at higher air rates. This is the mist flow region.

2. Pressure Drop Results.

a. Pressure Drop vs. Discharge Air Water Ratio Curves.

Pressure drops, calculated as p.s.i./loo ft. of tube are plotted against air-water discharge ratios for both test sections and for both pressures for each of the four water rates in Figs. 19 to 25. The observed flow patterns at each air rate were used to show the range of each type of flow pattern, viz., slug, froth, annular film and mist, on these curves. These ranges are similar to those obtained in earlier work (14).

It will be noted that the curves all show the same general shape. With only water flowing in the test sections (zero air-water discharge), the

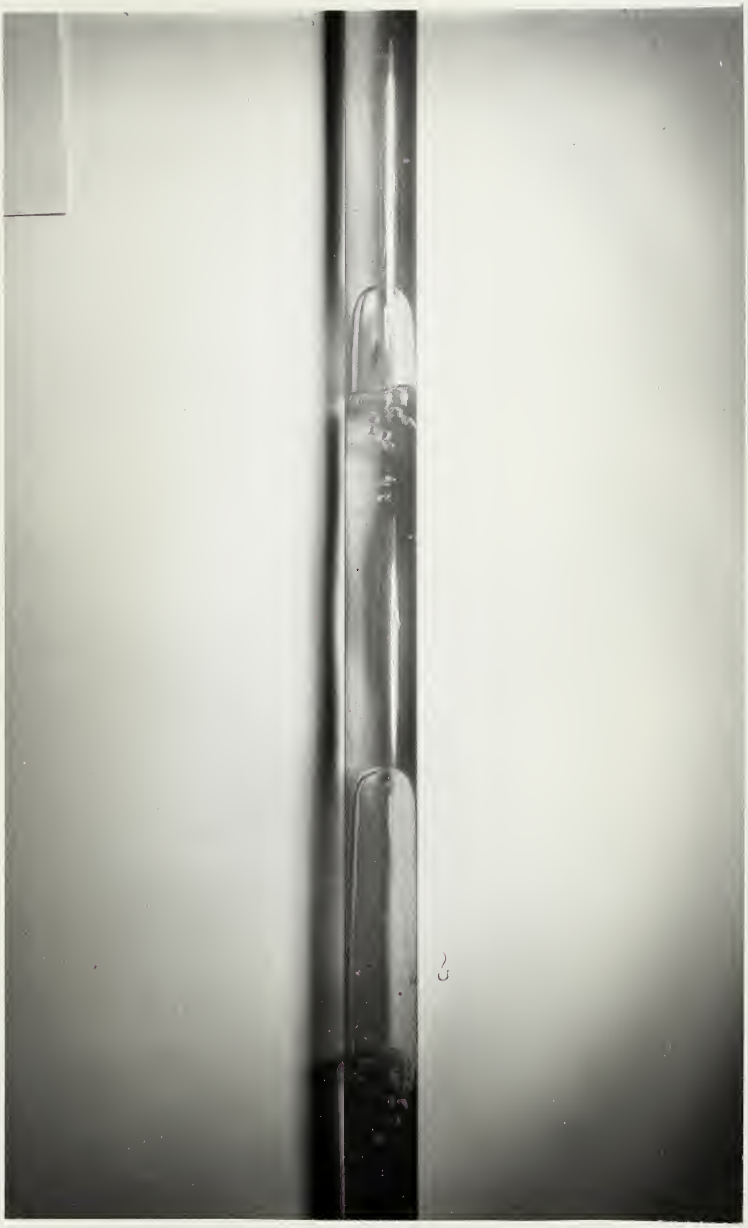

Fig. 13. Slug Flow.

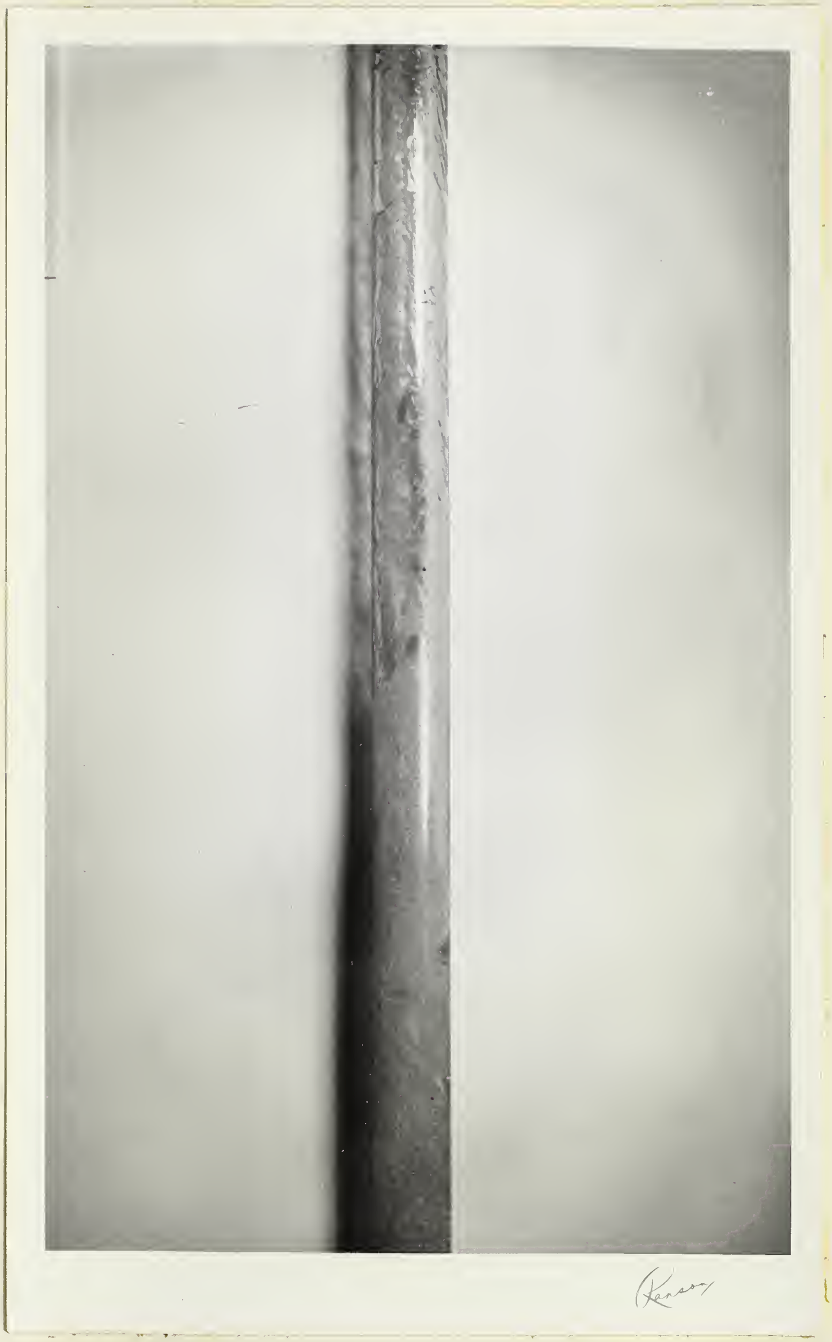

Fig. 14. Transition from Slug to Froth Flow.

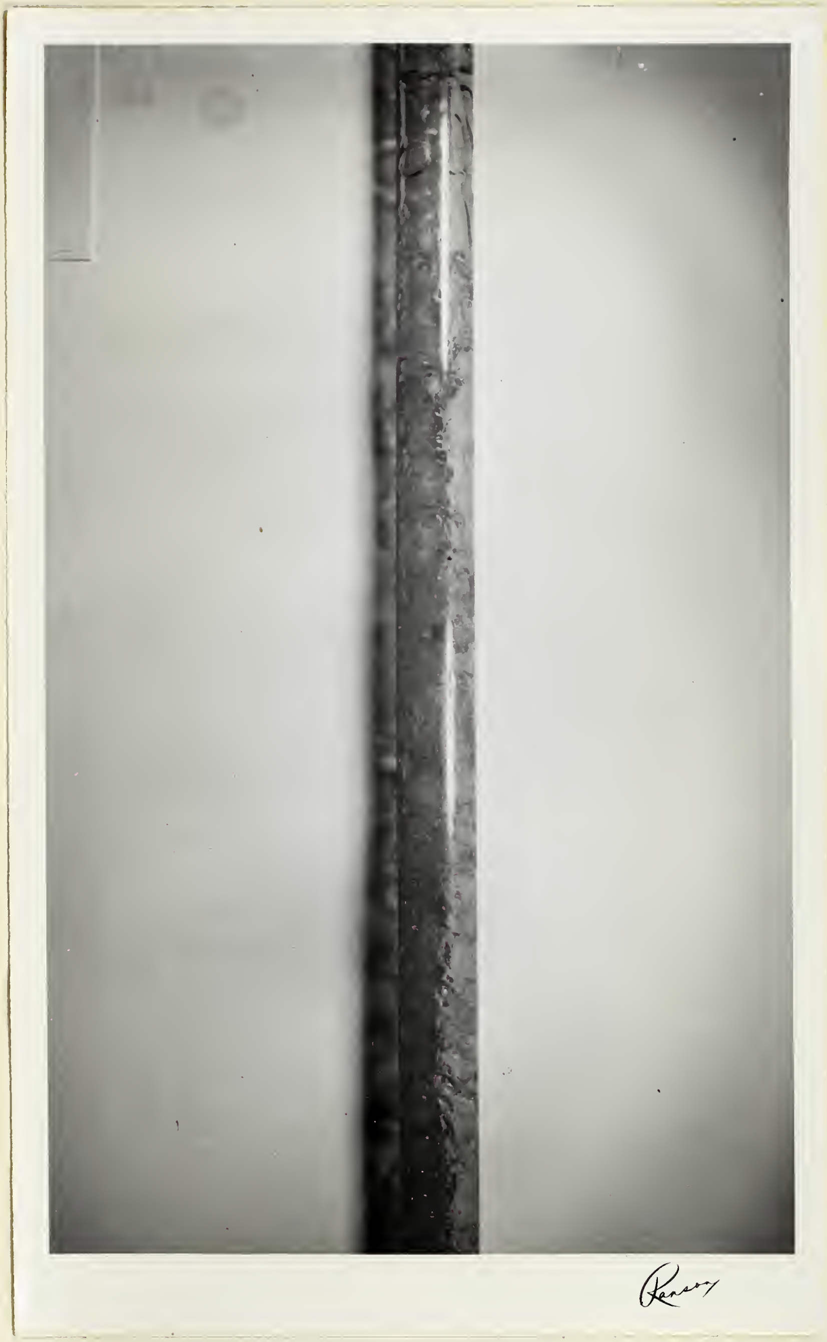

Fig. 15. Froth Flow.

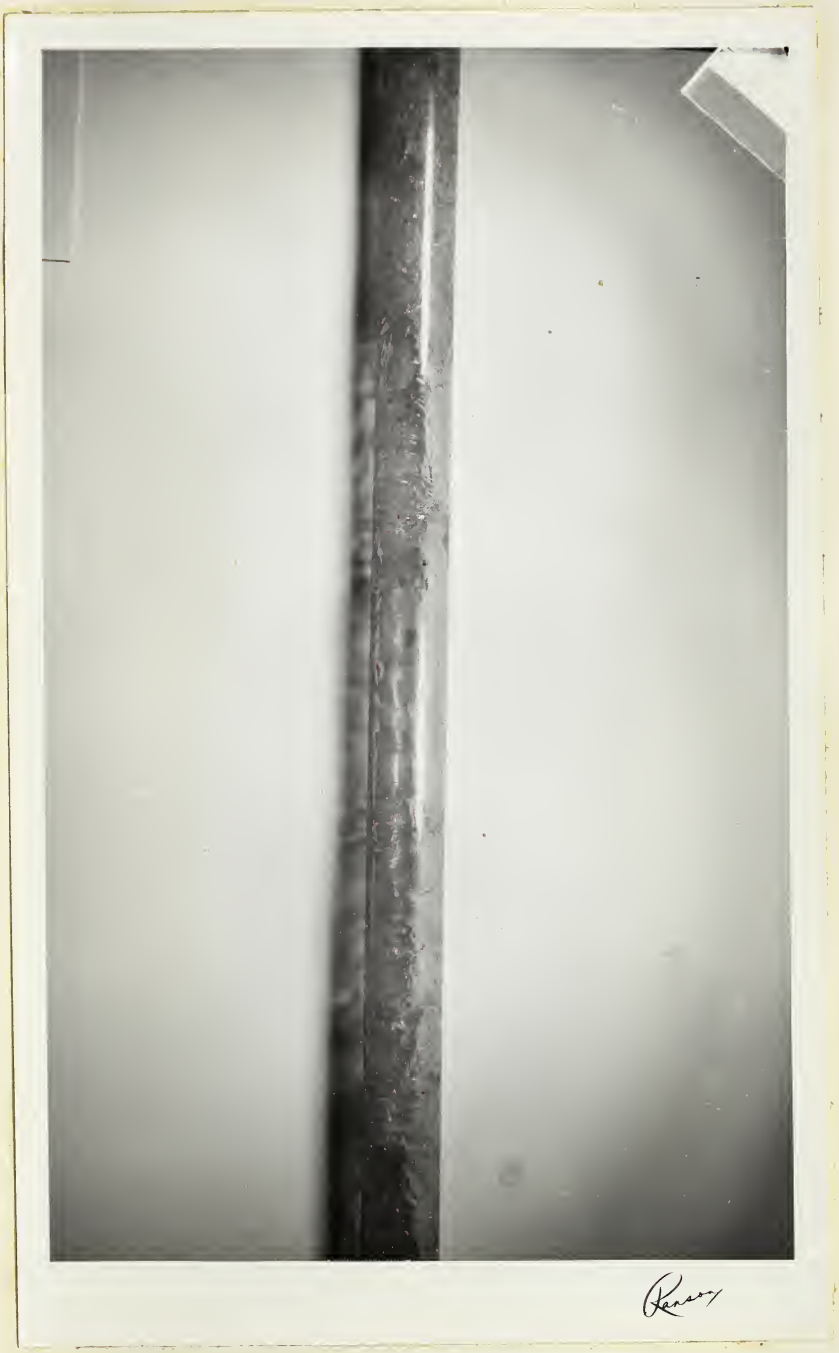

Fig. 16. Transition from Froth to Annular Film Flow.

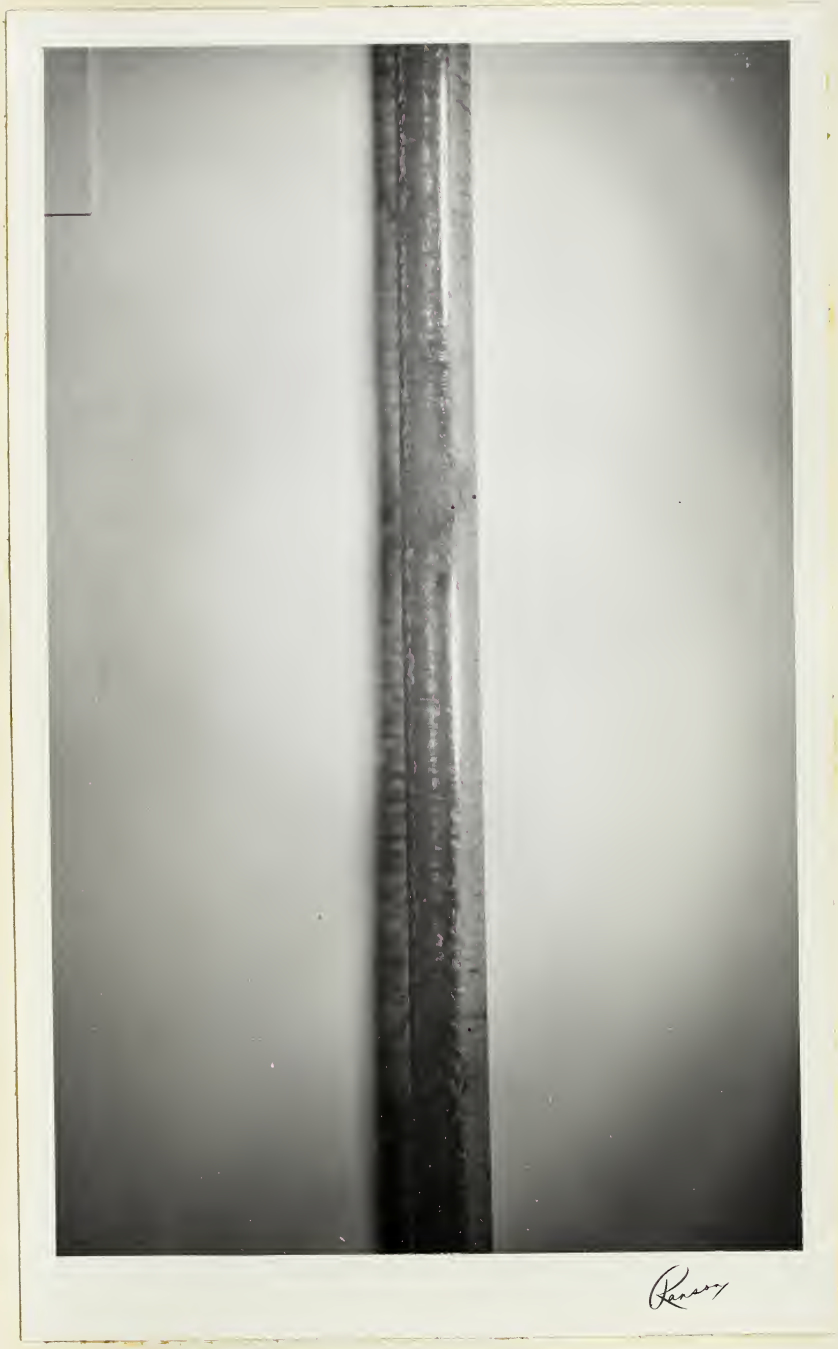

Fig. 17. Annular Film Flow.

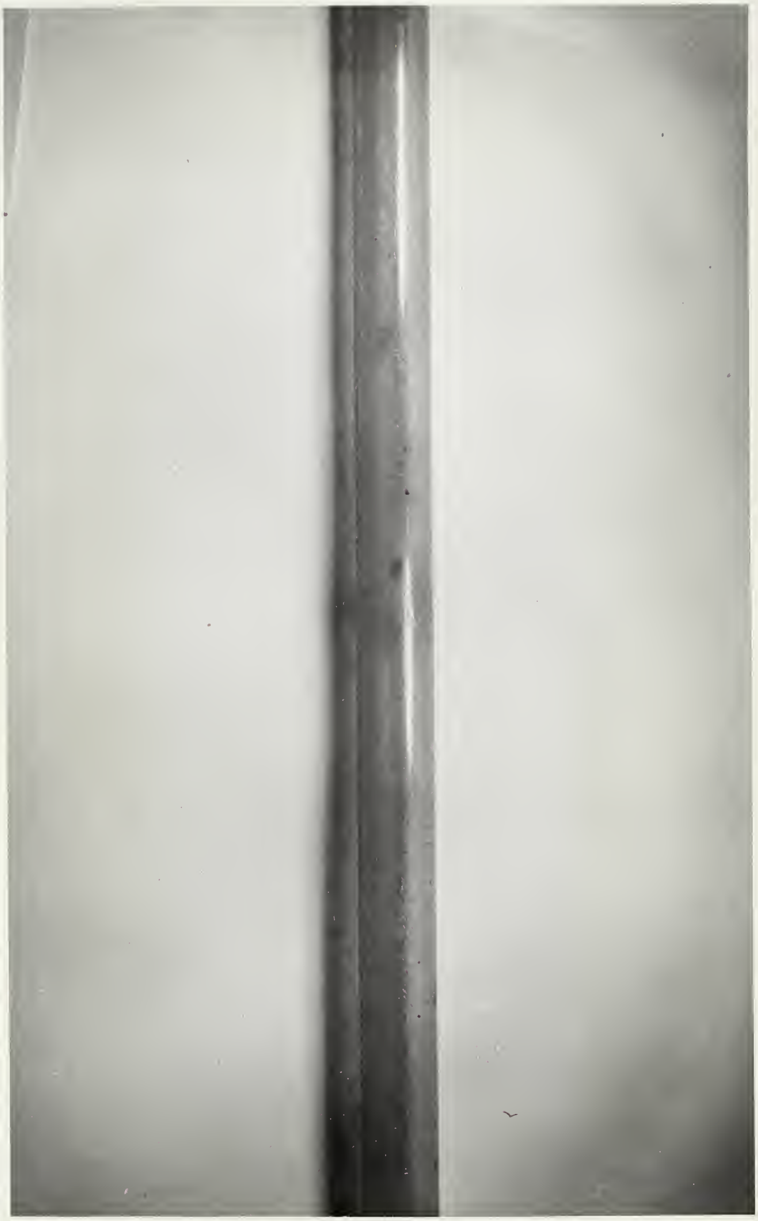

Fig. 18. Transition from Annular Film to Mist Flow.

measured pressure drop is largely due to the hydrostatic head of the column of water. Introducing air into the test section at increasing rates results in a rapid decrease in the measured pressure drop. This decrease continues until a minimum point is reached. Increasing the air rate beyond this point results in the pressure drop increasing to a maximum. From the introduction of air into the water through the pressure drop minimum and slightly beyond it, the slug type of flow pattern is observed. Between these maximum and minimum points the flow gradually changes from the slug type to the froth type. Further increasing the air rate causes the pressure drop to decrease again to a second minimum. Between the maximum and the second minimum the flow pattern changes from froth to annular film flow. At air rates beyond this second minimum, the pressure drop increases with increasing air rate to the highest air rate possible in the test equipment. Somewhere beyond the second minimum the flow pattern changes from the annular film to the mist type.

Although the general shape of the curves in the larger tube conform to those of Radford, greater values of the pressure drop at any discharge air-water ratio are found. These differences may be due to three things. The calibrations of the orifice plates used to measure the air flow were checked and higher values of the orifice constants were found. Previously, an air purge system was used to keep the different manometer lines free of water. This system was removed and the small separators were installed. The mid-point pressure in the test section was somewhat higher, i.e., 18 p.s.i.a. compared to 16.2 p.s.i.a.. Any one, or all three, of these changes may be the cause of the higher pressure drops.

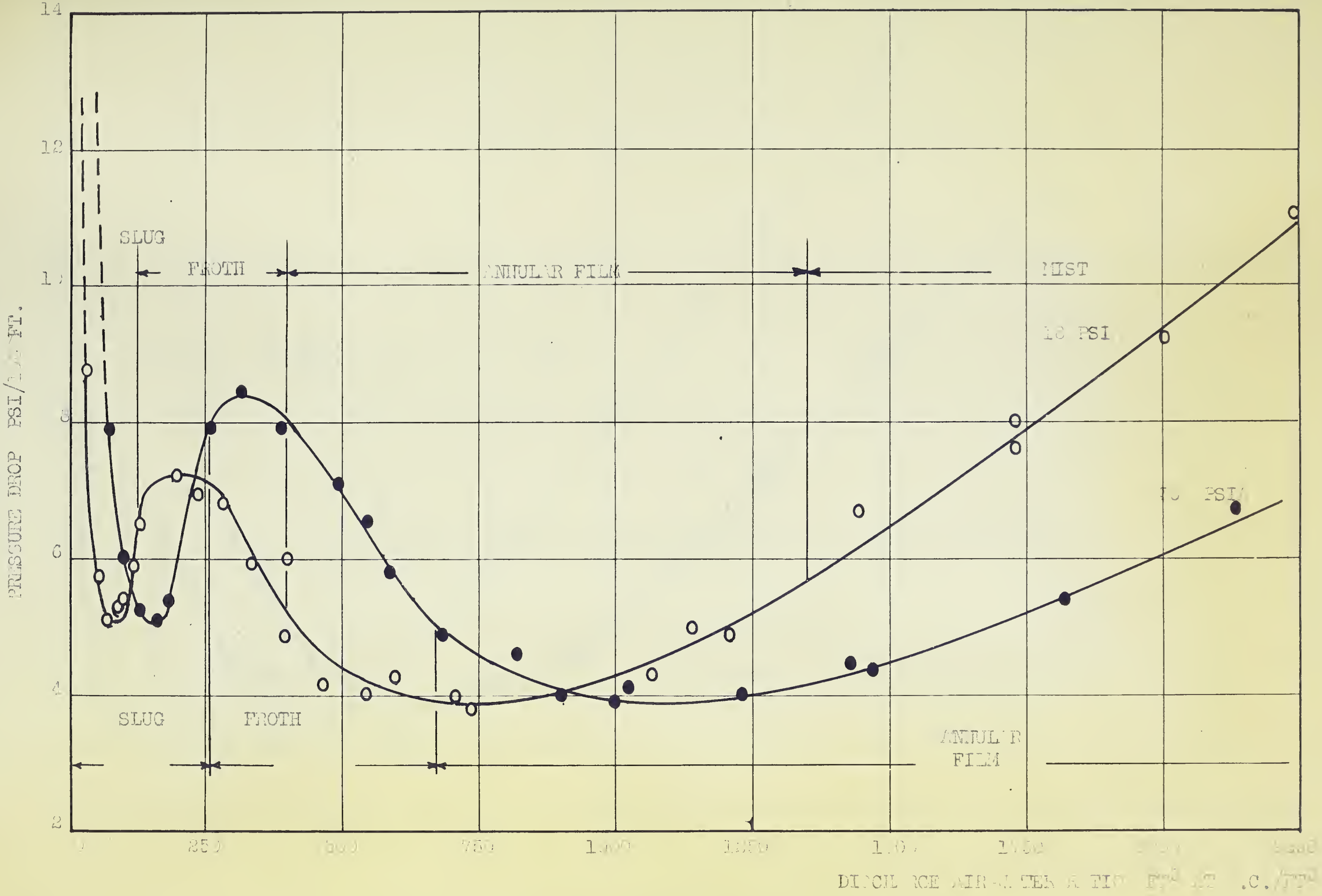

Fig. 19. Variation of Pressure Drop with Discharge Air-Water Ratio (1/2 inch Tube, Water Rate - 4.14 lbs./ft² sec.)

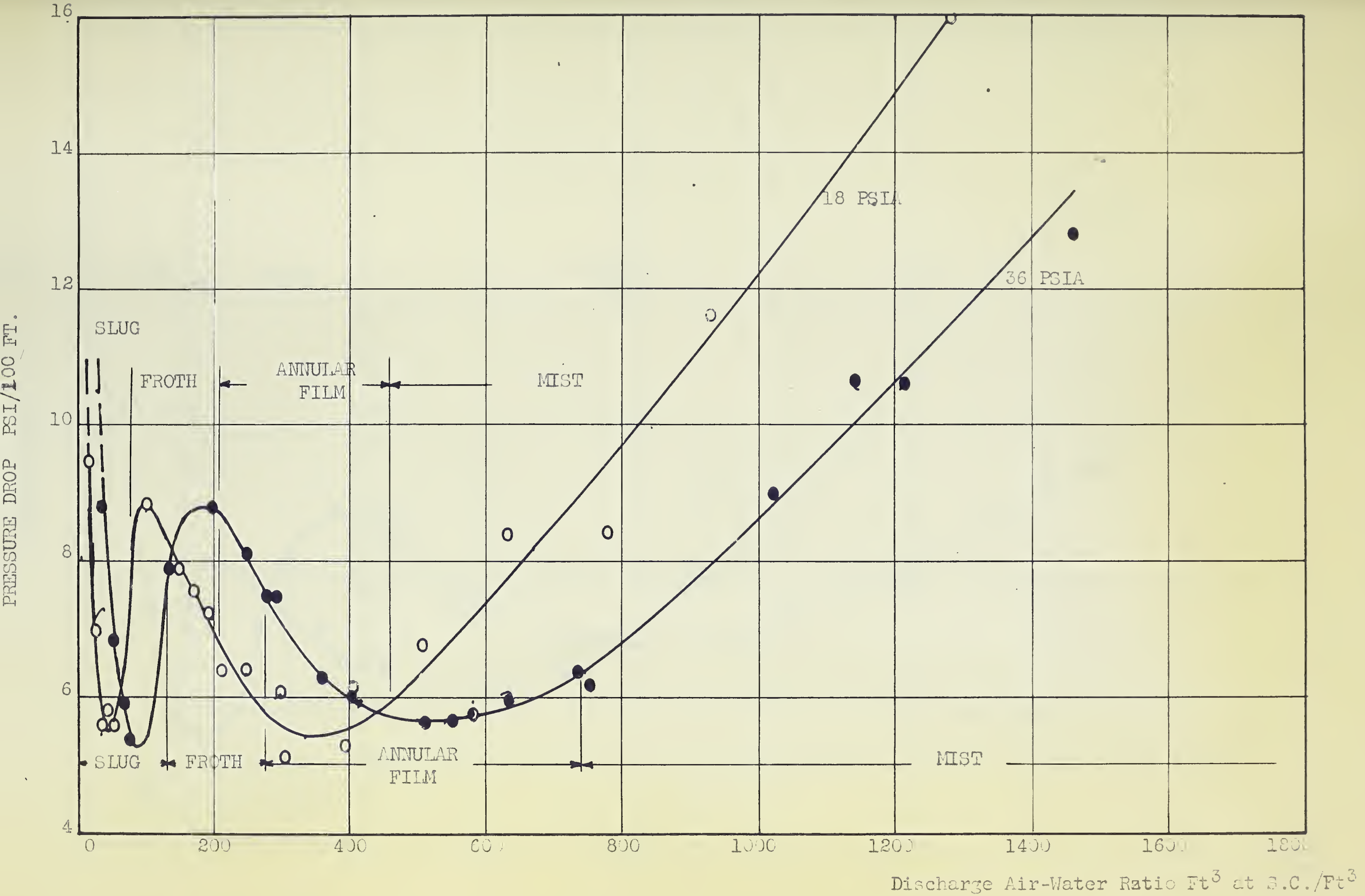

Fig. 20. Variation of Pressure Drop with Discharge Air-Water Ratio (1/2 inch Tube, Water Rate - 8.10 lbs./ft^2 sec.)

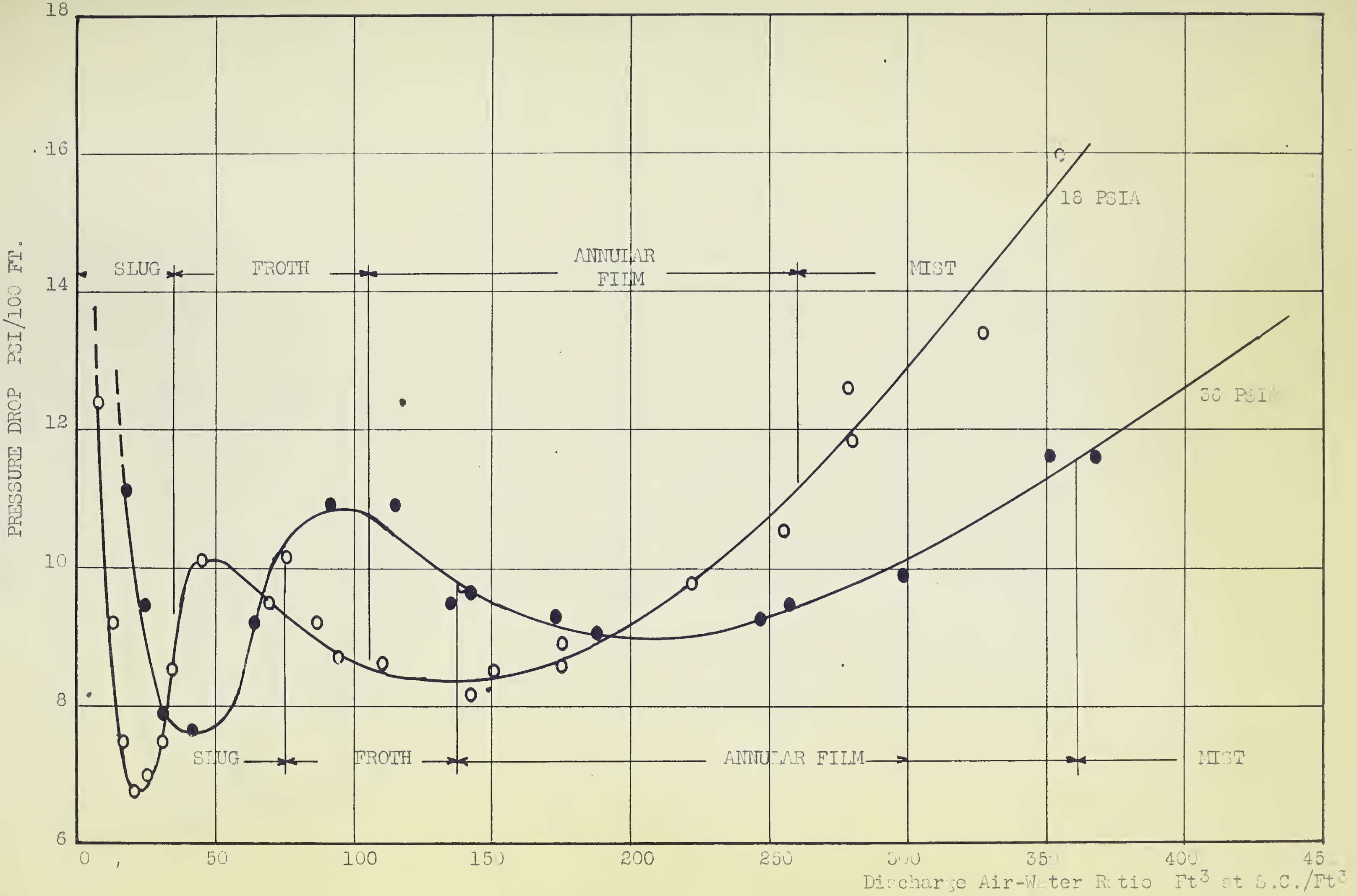

Fig. 21. Variation of Pressure Drop with Discharge Air-Water Ratio
(1/2 inch Tube, Water Rate - 17.6 lbs./ft^2 sec.)

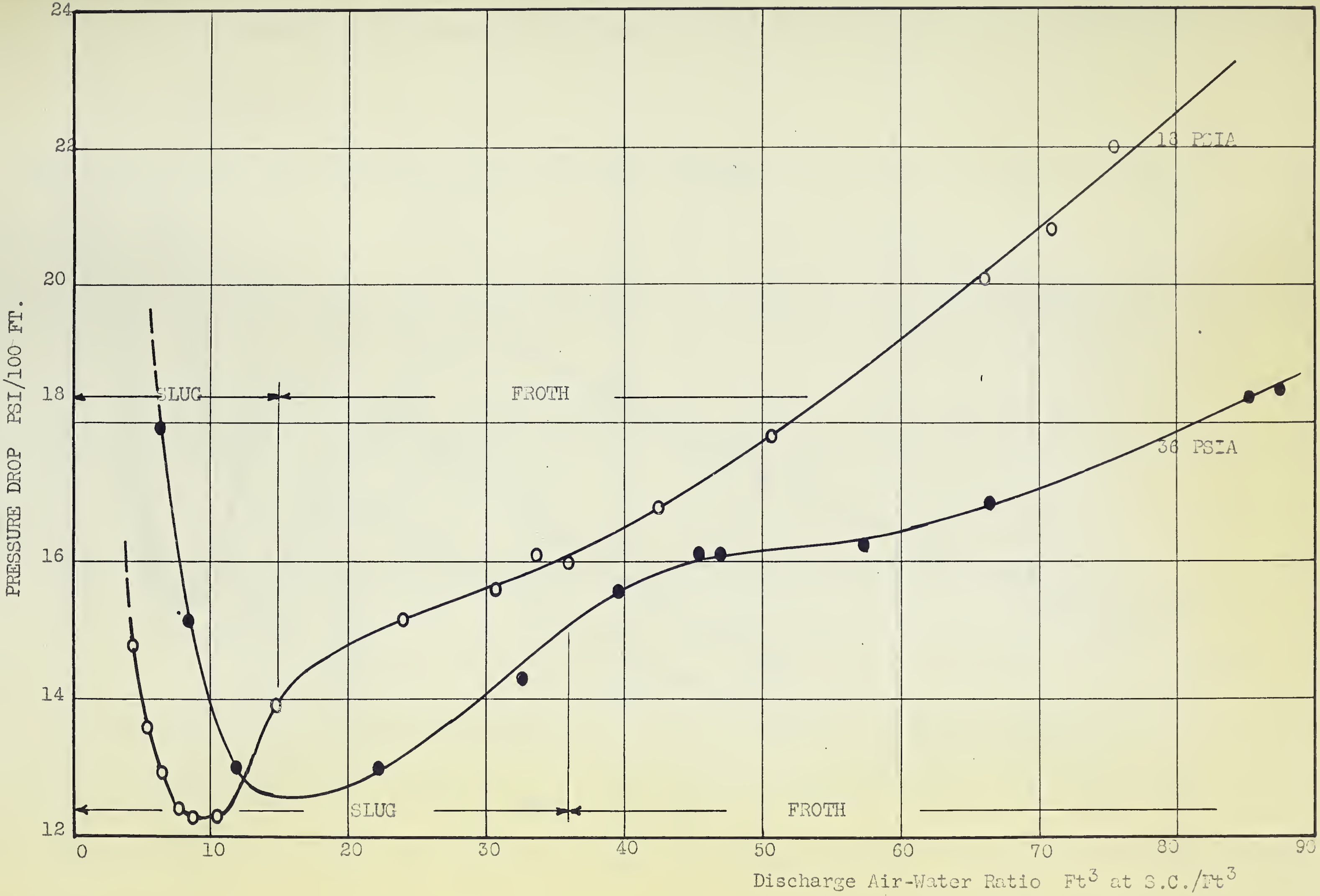

Fig. 22. Variation of Pressure Drop with Discharge Air-Water Ratio (1/2 inch Tube, Water Rate - 51.0 lbs./ft^2 sec.)

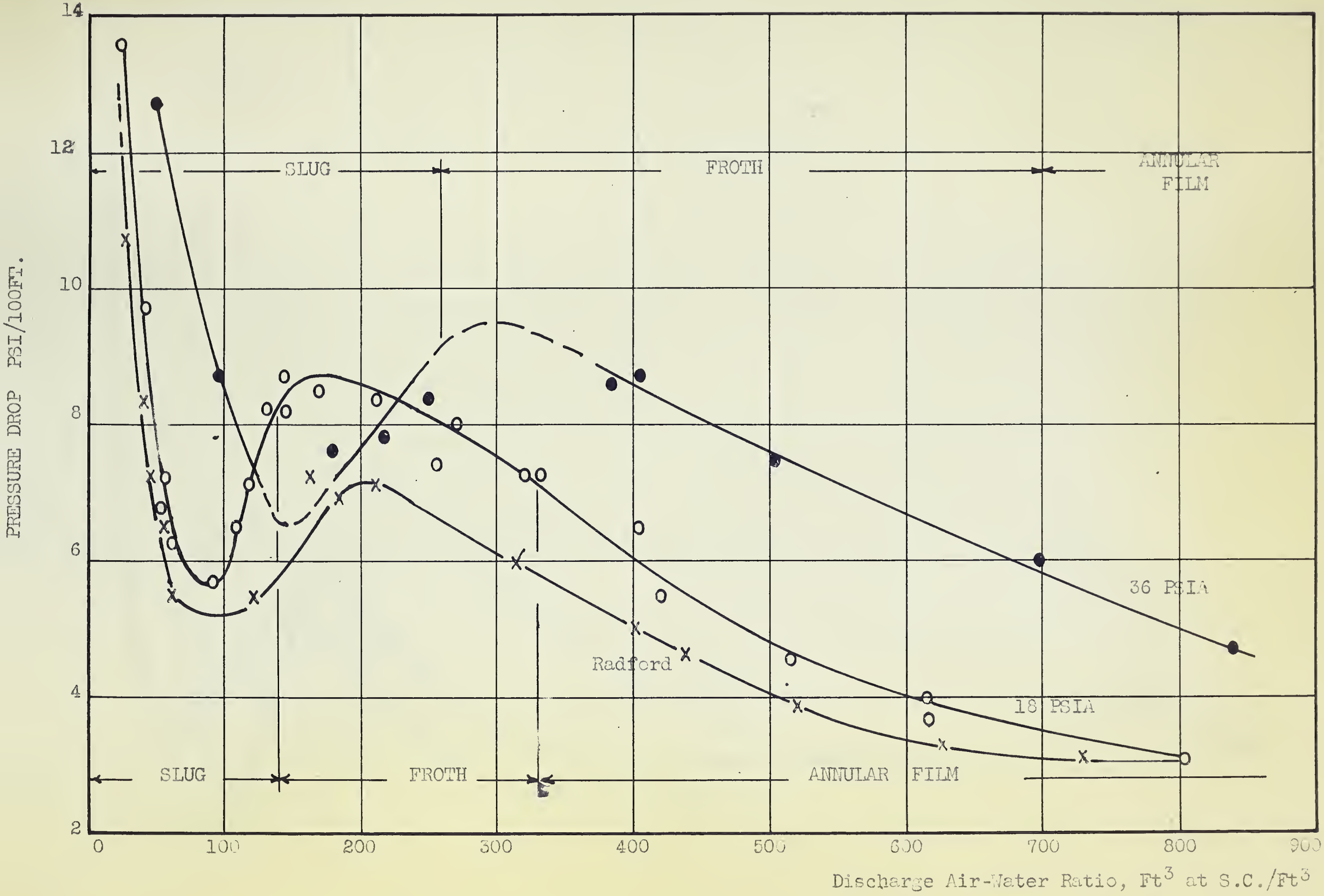

Fig. 23. Variation of Pressure Drop with Discharge Air-Water Ratio (1-inch Tube, Water Rate - 4.15 lbs./ft^2 sec.)

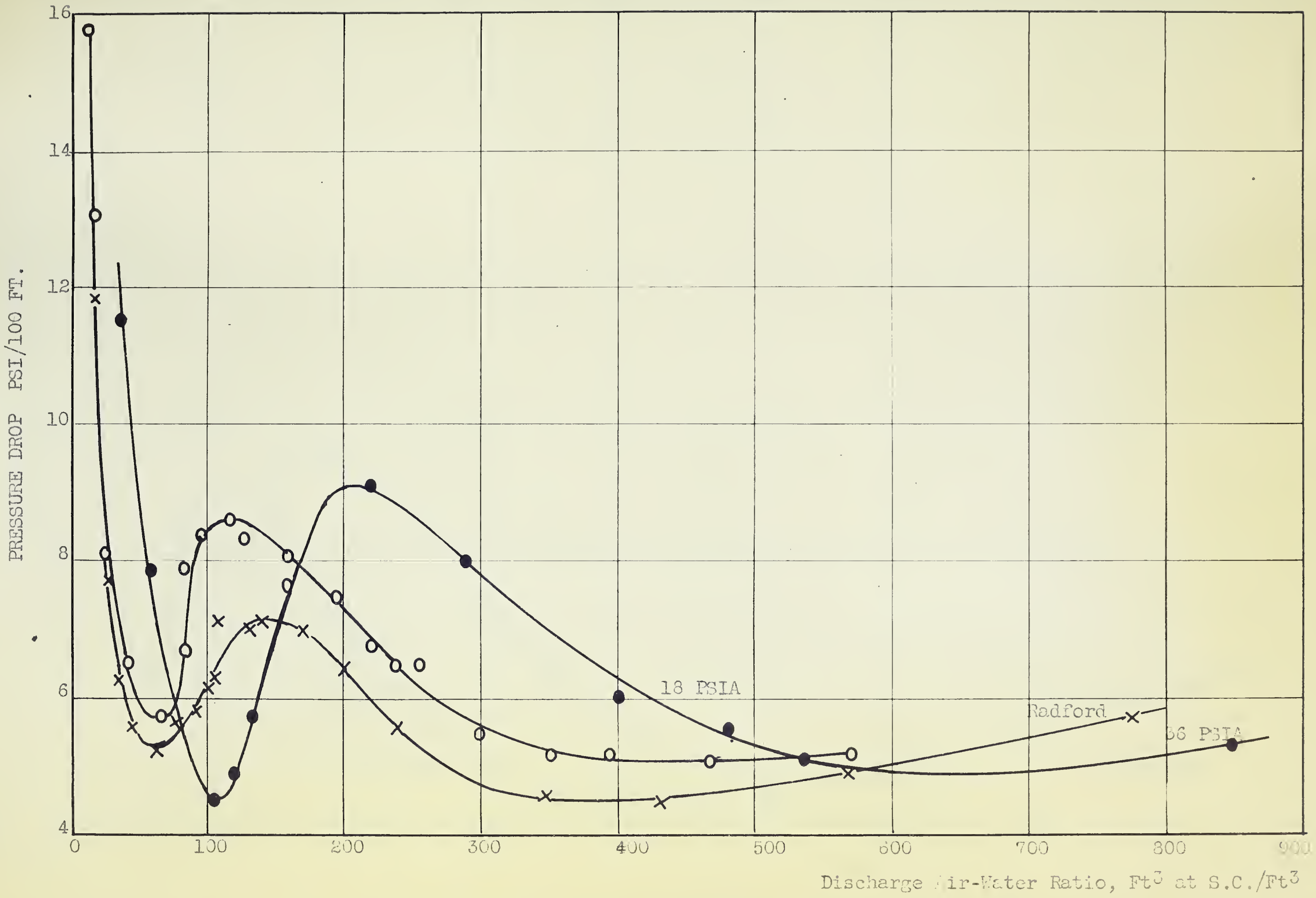

Fig. 24. Variation of Pressure Drop with Discharge Air-Water Ratio (1 inch Tube, Water Rate - 8.00 lbs./ft^2 sec.)

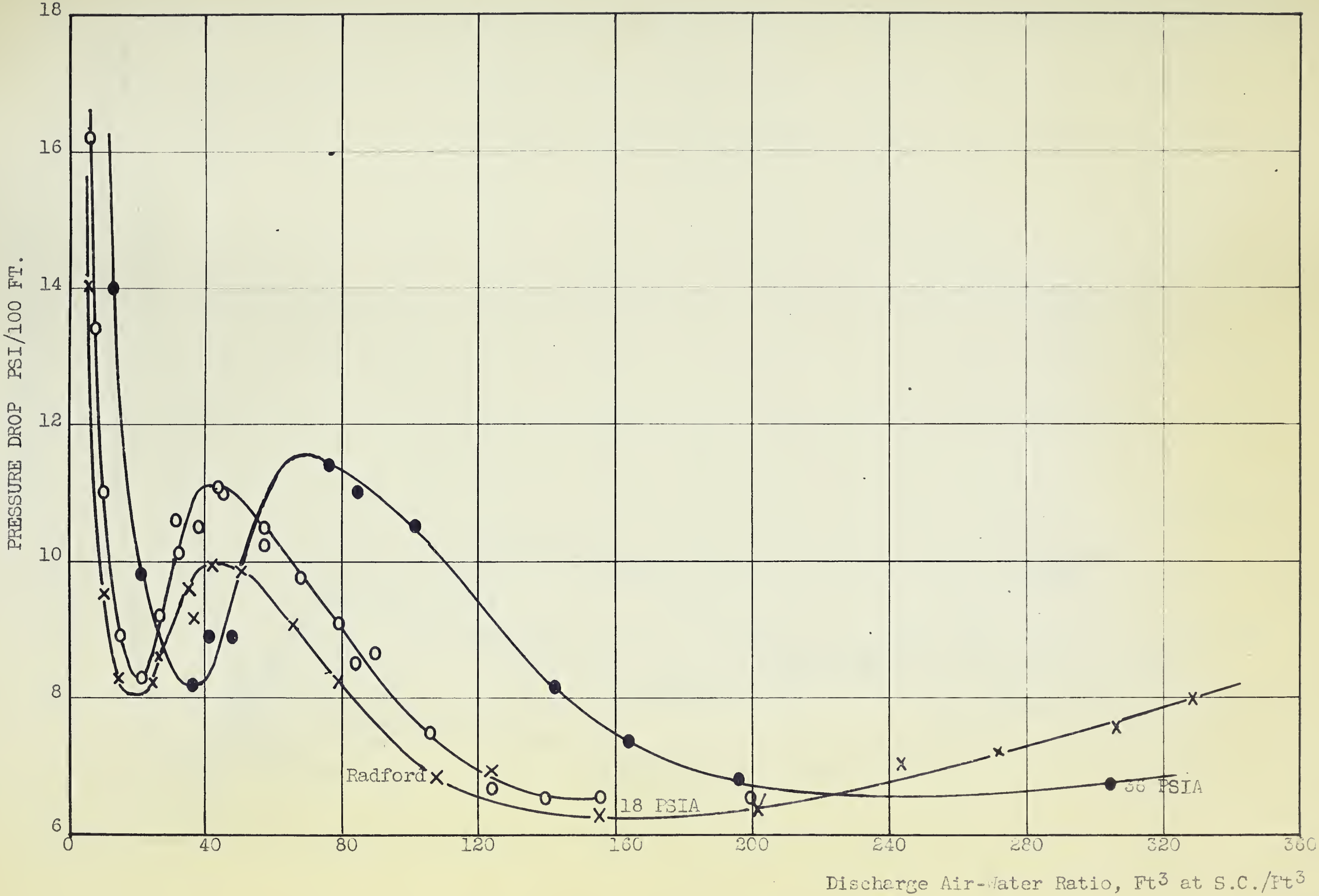

Fig. 25. Variation of Pressure Drop with Discharge Air-Water Ratio (1 inch Tube, Water Rate - 17.9 lbs./ft^2 sec.)

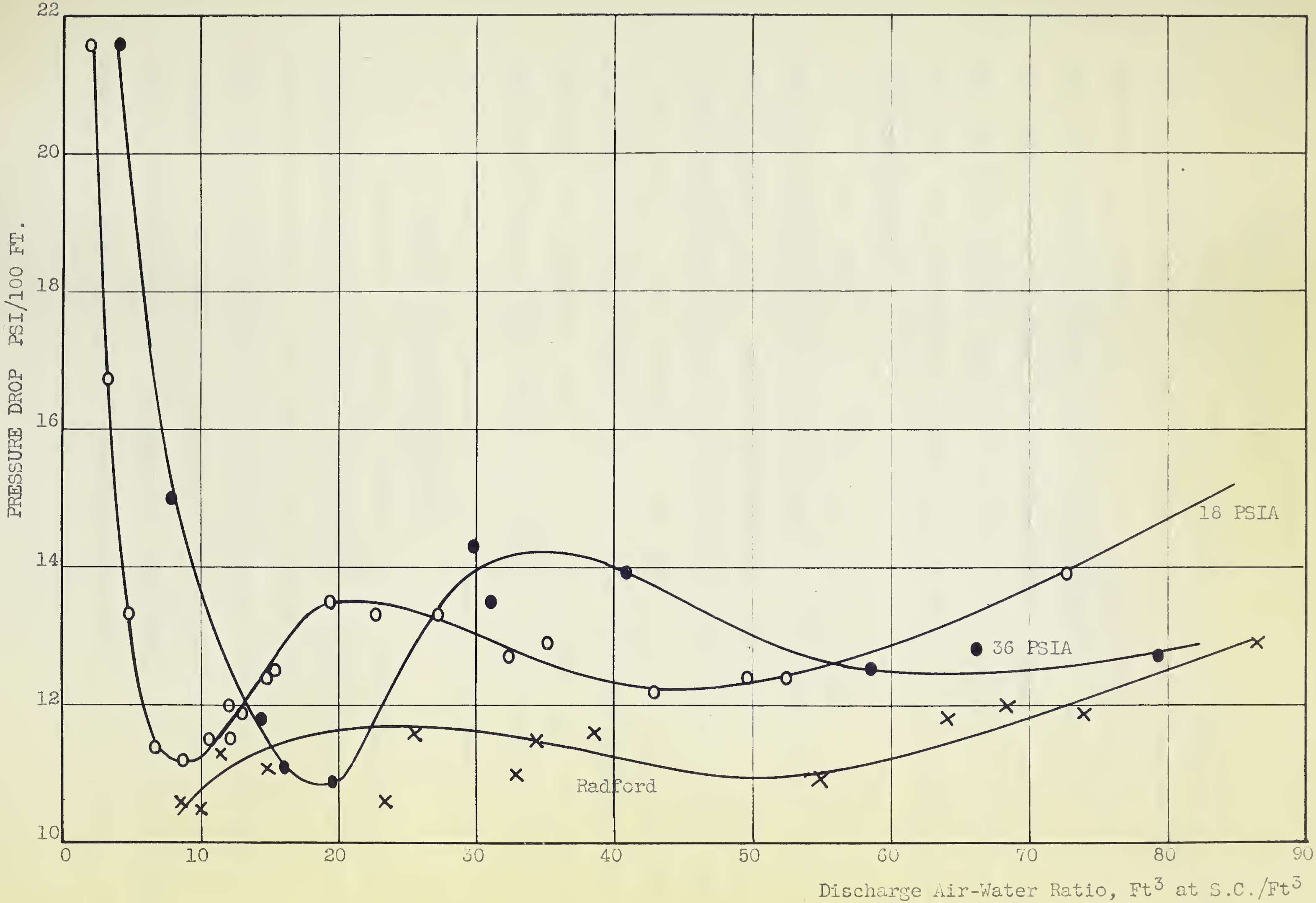

Fig. 26. Variation of Pressure Drop with Discharge Air-Water Ratio (1 inch Tube, Water Rate - 51.9 lbs./ft^3 sec.)

b. Effect of Water Rate.

The effect of varying the water rate is shown in Figs. 19 to 26. At the lowest water rate the pressure drop at the second minimum is lower than the pressure drop at the first minimum. With increasing water rate this situation changes until at the highest water rate used, only a bare suggestion of a second minimum occurs and at a greater pressure drop than the first minimum. This would confirm the observations in previous work (14). The disappearance of the second minimum is more pronounced in the smaller tube.

The effect of water rate is also shown in Figs. 27 and 28, in which the measured pressure drops at the first and second minimum points and the maximum are plotted against the water rate. The points are scattered but do show the definite increase in pressure drop with increasing water rate. In Figs. 29 and 30 the discharge air-water ratio at the minimum and maximum points are also plotted against the water rate. At lower water rates the discharge ratio decreases rapidly with increasing water rate. At higher water rates the decrease is more gradual and suggests that the discharge ratio at these inflection points would change very little at high water rates.

c. Effect of Gas Phase Density.

The effect of gas phase density at each of the four water rates in the two sizes of tubing is also shown in Figs. 19 to 26. The tests in both tubes were conducted at test section mid-point pressures of 18 and 36 p.s.i.a. Thus, the gas phase density at the higher pressure was twice that of the lower pressure. At the higher gas phase density the measured pressure drops at most ot the discharge air-water ratios are considerably different from those at the lower density. The two curves are out of phase with each other, When

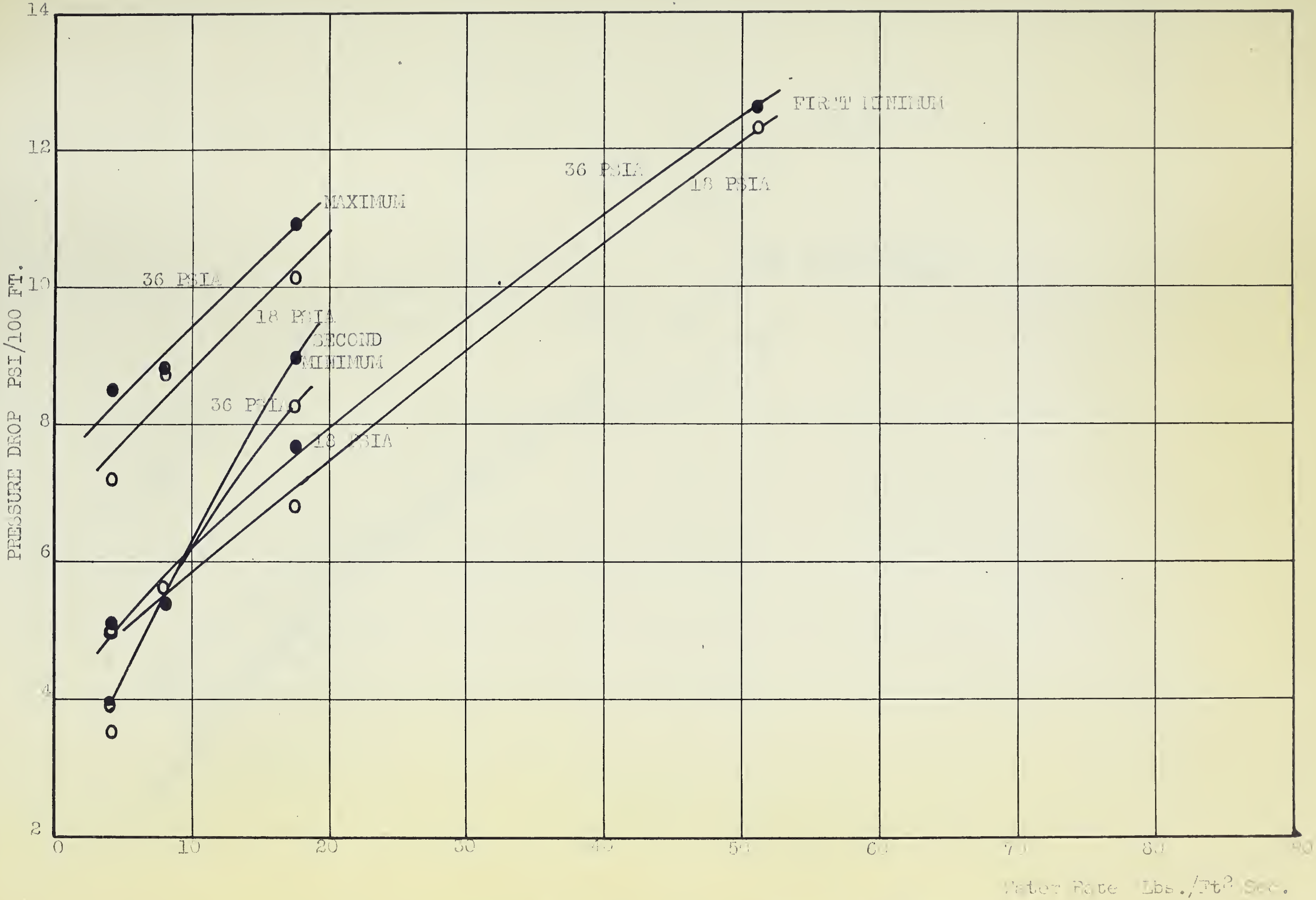

Fig. 37. Effect of Water Rate on the Maximum and Minimum Pressure Drops - 1/2 inch Tube.

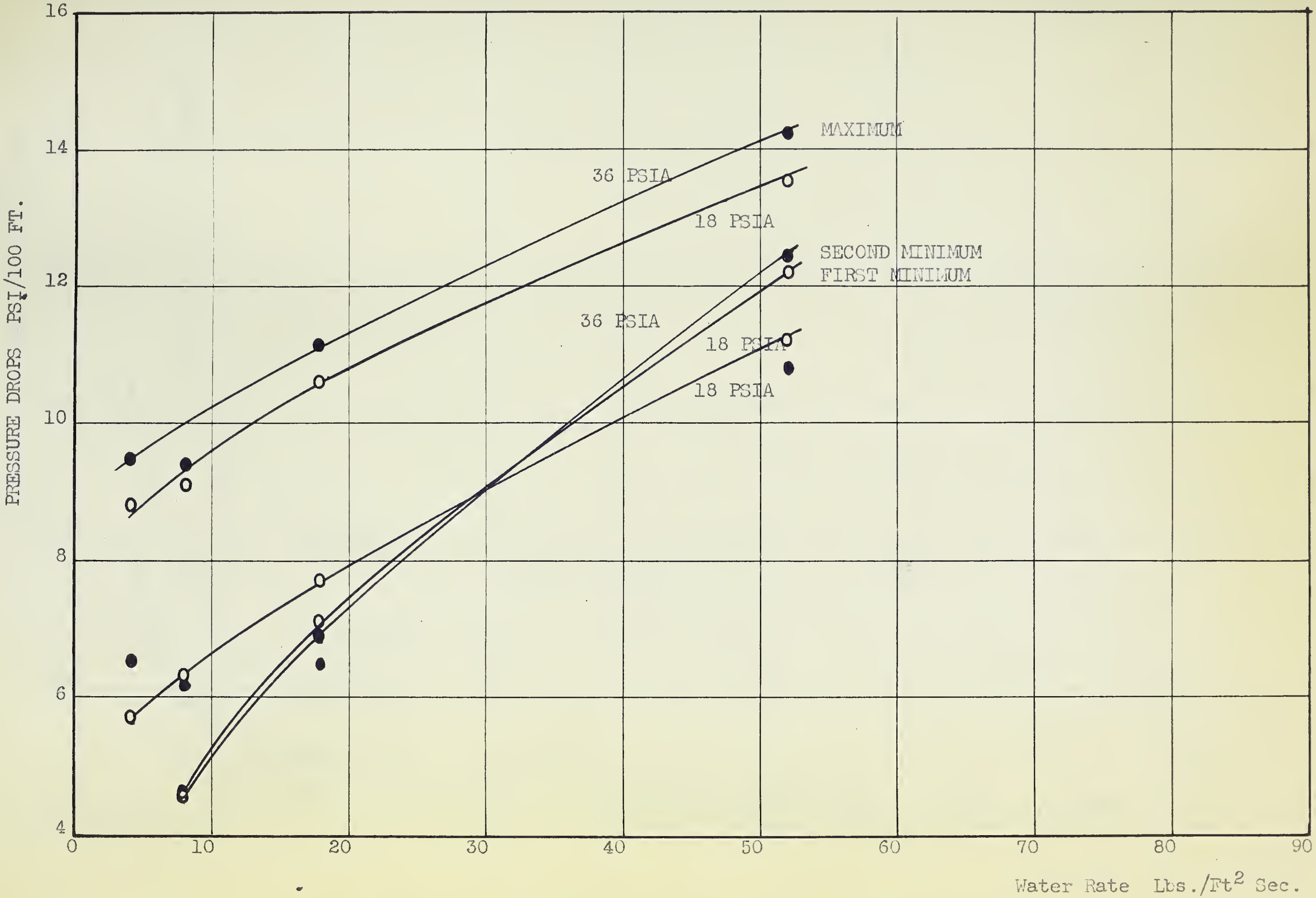

Fig. 28. Effect of Water Rate on the Maximum and Minimum Pressure Drops - 1-inch Tube.

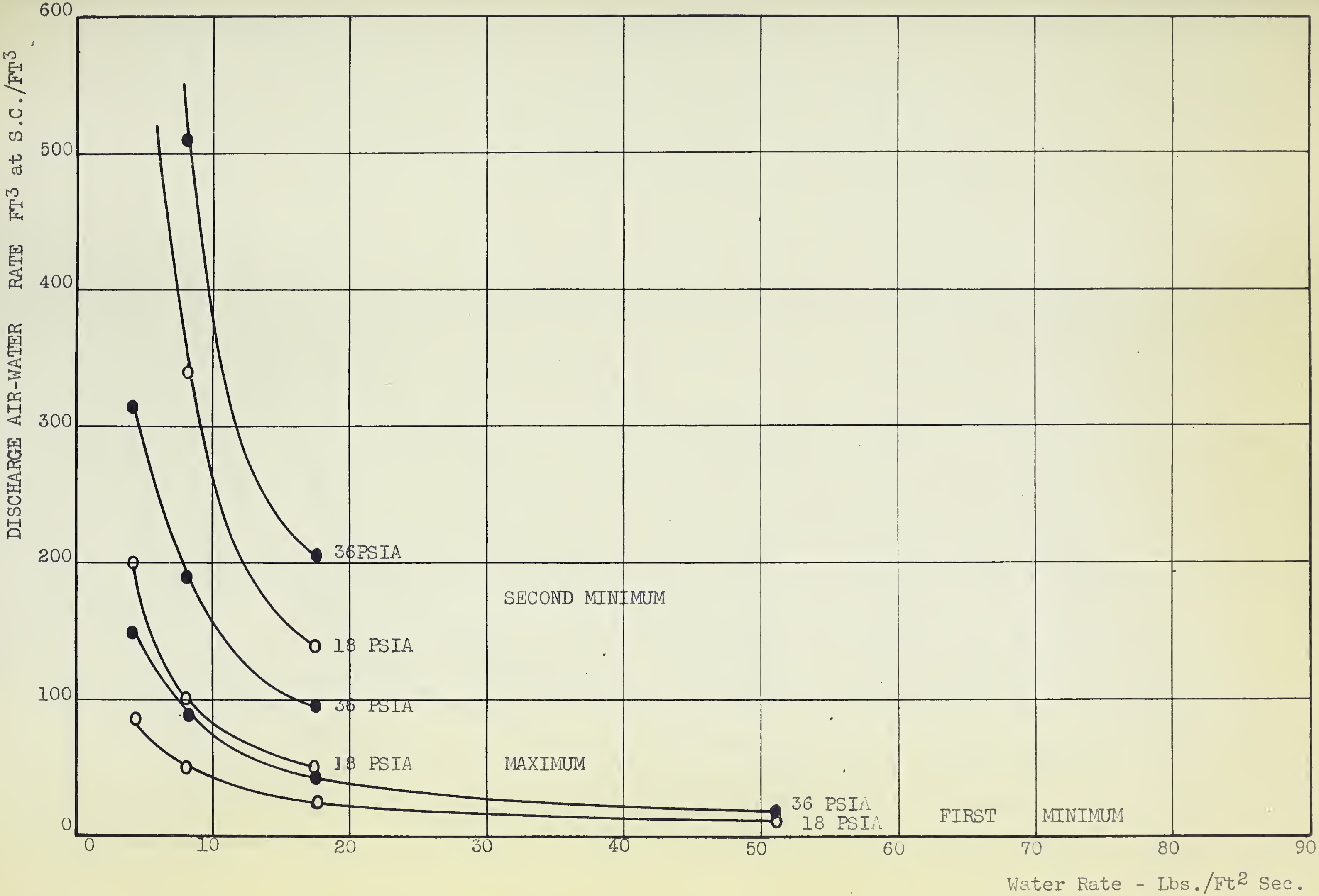

Fig. 29. Effect of Water Rate on the Discharge Air-Water Ratios Corresponding with the Maximum and Minimum

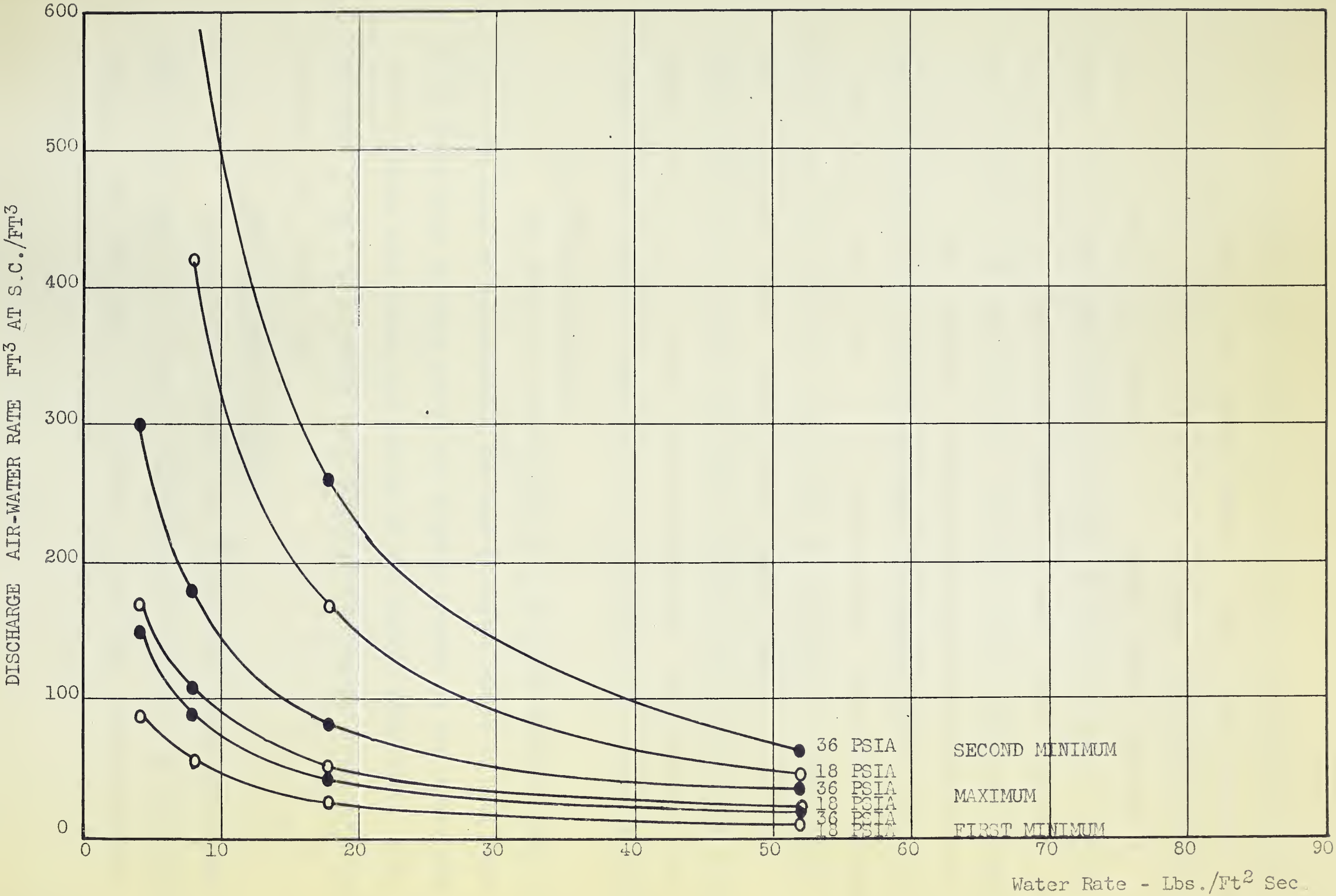

Fig. 30. Effect of Water Rate on the Discharge Air-Water Ratios Corresponding with the Maximum and Minimum Pressure Drops - 1 inch Tube.

the measured pressure drop reaches the first minimum at the lower density, the measured pressure drop at the higher density is about 35 per cent greater for the same air rate. As the air-water ratio increases, the measured pressure drop at the lower density increases to the maximum, whereas the measured pressure drop at the higher density continues to decrease until it reaches the first minimum at approximately the same air-water ratio at which the maximum is reached at the lower density. Increasing the air-water ratio results in the pressure drop decreasing to the second minimum and then increasing at the lower density while the pressure drop at the higher density increases to the maximum and then decreases to the second minimum. Thereafter, the higher density curve lags the lower density curve at increasing air-water ratios. As would be expected, the two minimum and the maximum points for the higher density flow occur at roughly twice the air-water ratios at which the corresponding inflection points at the lower density occur. The maximum for each of the 16 curves occurs at about twice the air-water ratio of the first minimum.

d. Effect of Diameter.

The effect of tubing diameter is not so pronounced. The inflection points occur at approximately the same air-water ratios in both tubes. The pressure drops at these points are slightly greater in the larger tube for the first three water rates, and smaller at the highest water rate. Beyond the second minimum the pressure drop increases more rapidly with increasing air rate in the smaller tube.

e. Effect of Surface Tension.

An exploratory run was made with a small amount of detergent added to the water in an attempt to determine the importance of the surface tension of the liquid phase on the pressure drop of the two-phase mixture.

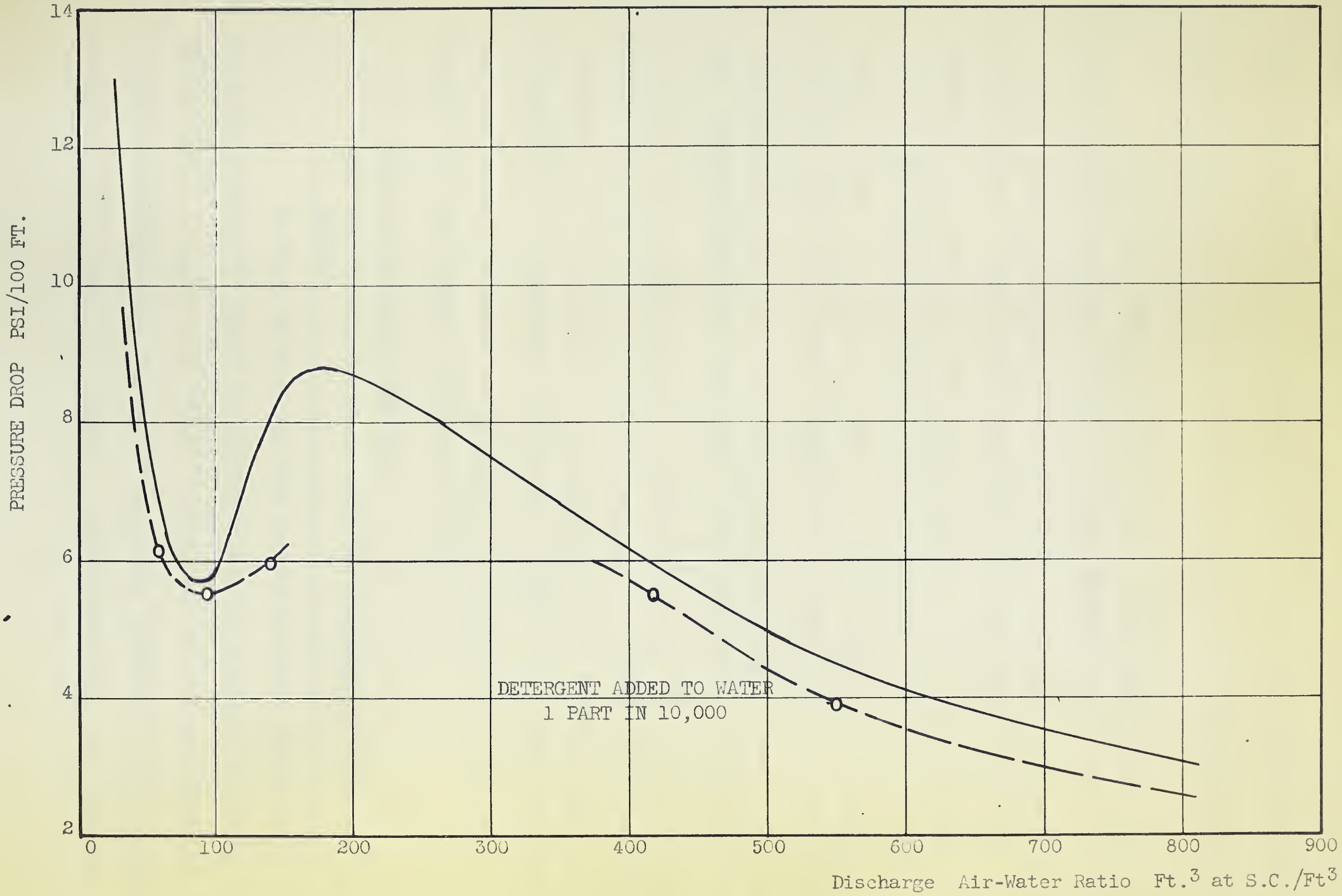

Fig. 31. Effect of Liquid Phase Surface Tension on the Pressure Drop Discharge Air-Water Ratio Curve (1-inch Tube, Water Rate - 4.15 lbs./ft^2 sec.)

Five runs were made at the lowest water rate in the larger tube with the test section mid-point pressure constant at 18 p.s.i.a. The results of these tests are plotted in Fig. 31.

A detergent (Tergitol Penetrant No. 4) was added to the water such that its concentration was 1 part in 10,000. The addition was made prior to the water mixing with the air. Surface tension measurements were made by the Du Nouy method on samples of the water plus detergent and the pure water. Relative to the pure water, the surface tension of the mixture was o.80.

The detergent caused the mixture to become a foam of small air bubbles in water not unlike soap suds. At low air rates, the flow pattern was one of slugs of air passing through this air-water foam. In the annular film region the water annulus was cloudy, suggesting that it was an air-water foam. It would appear that the effect of the detergent is to lower the pressure drop of the two-phase mixture, although not as much as had been expected. No data were taken at, or near, the maximum point in the froth region; hence the discontinuity of the curve. The maximum may be considerably lower with the addition of the detergent to the water. Higher concentrations of detergent were found to be impracticable because of excessive foam which made pressure drop measurements difficult to obtain.

3. Test Section Hold-Up Results.

(a) Test Section Air-Water Ratio vs. Discharge Air-Water Ratio Curves.

In Figs. 32 to 39 the test section air-water ratios (ft^3 air at mid-point pressure/ft^3 water) are plotted versus the discharge air-water ratios (ft^3 air at 14.4 p.s.i.a. and 60°F/ft^3 water). It will be noted that with increasing discharge ratios the test section ratio passes through a maximum coincident with the slug flow minimum on the pressure drop curve, decreases

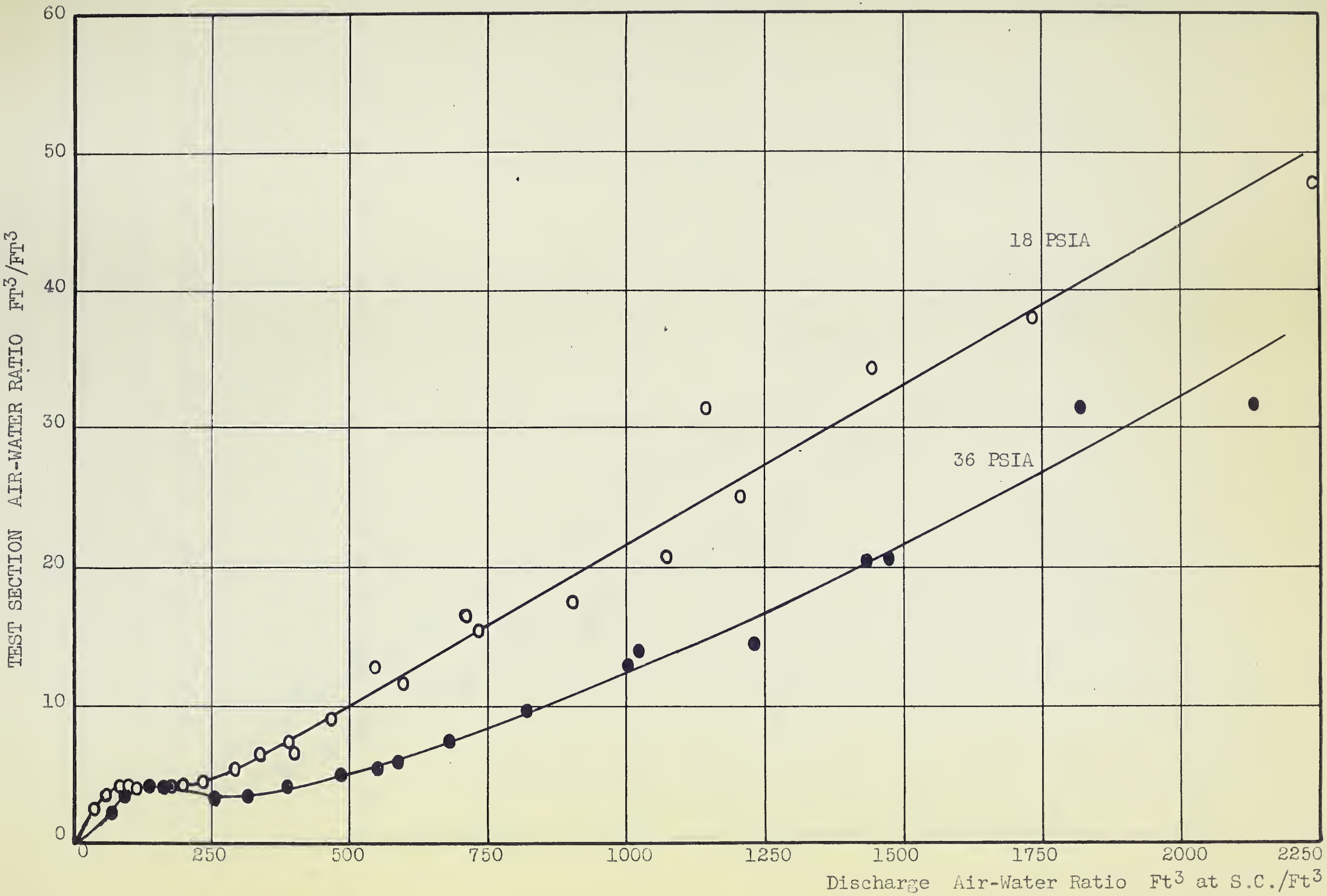

Fig. 32. Variation of Air-Water Ratio in the Test Section with Discharge Air-Water Ratio (1/2 inch Tube, Water Rate - 4.17 lbs./ft^2 sec.)

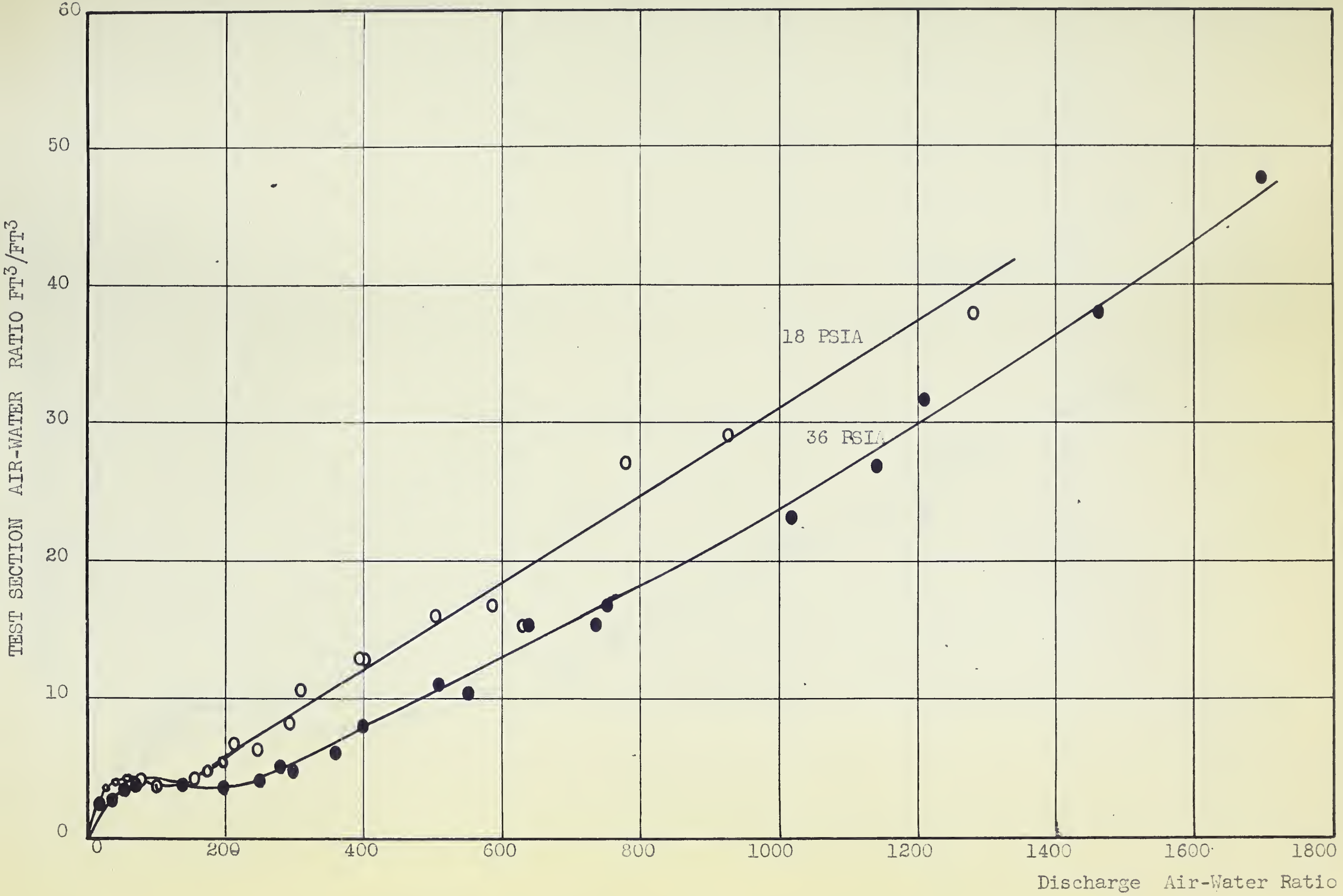

Fig. 33. Variation of Air-Water Ratio in the Test Section with Discharge Air-Water Ratio (1/2 inch Tube, Water Rate - 8.10 lbs./ft^2 sec.)

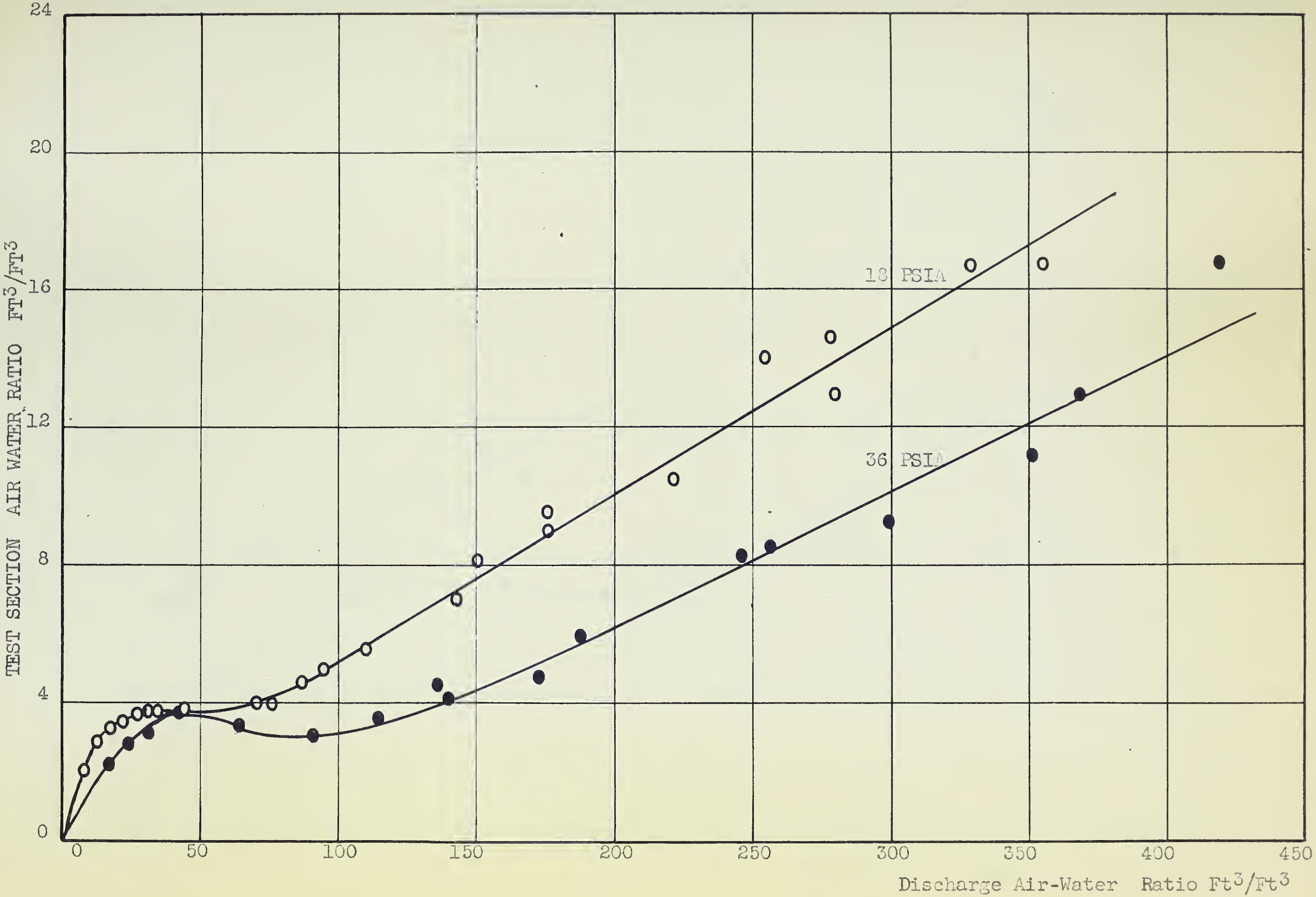

Fig. 34. Variation of Air-Water Ratio in the Test Section with Discharge Air-Water Ratio (1/2 inch Tube, Water Rate - 17.6 lbs./ft^2 sec.)

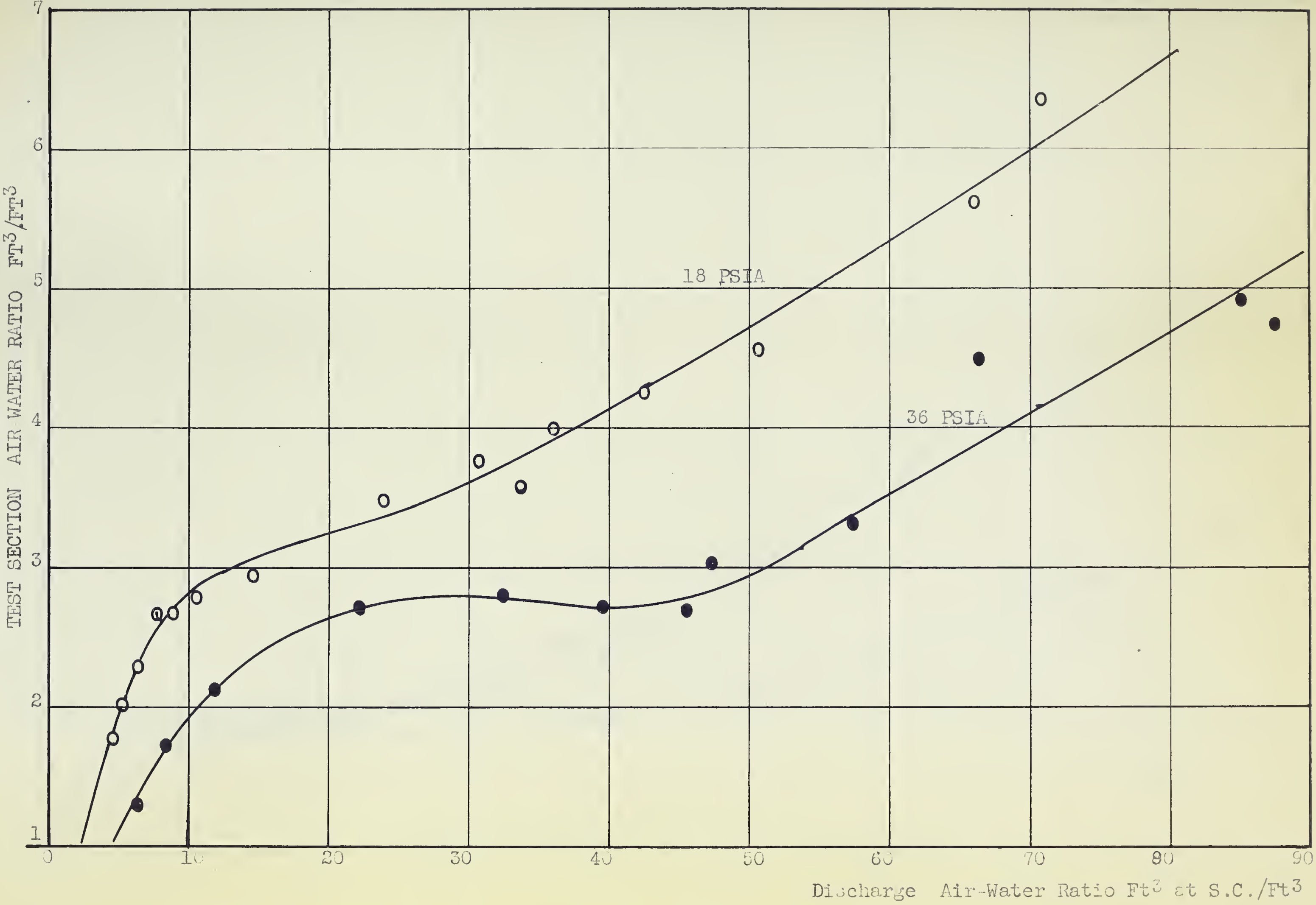

Fig. 35. Variation of Air Water Ratio in the Test Section with Discharge Air-Water Ratio (1/2 inch Tube, Water Rate - 51.0 lbs./ft^2 sec.)

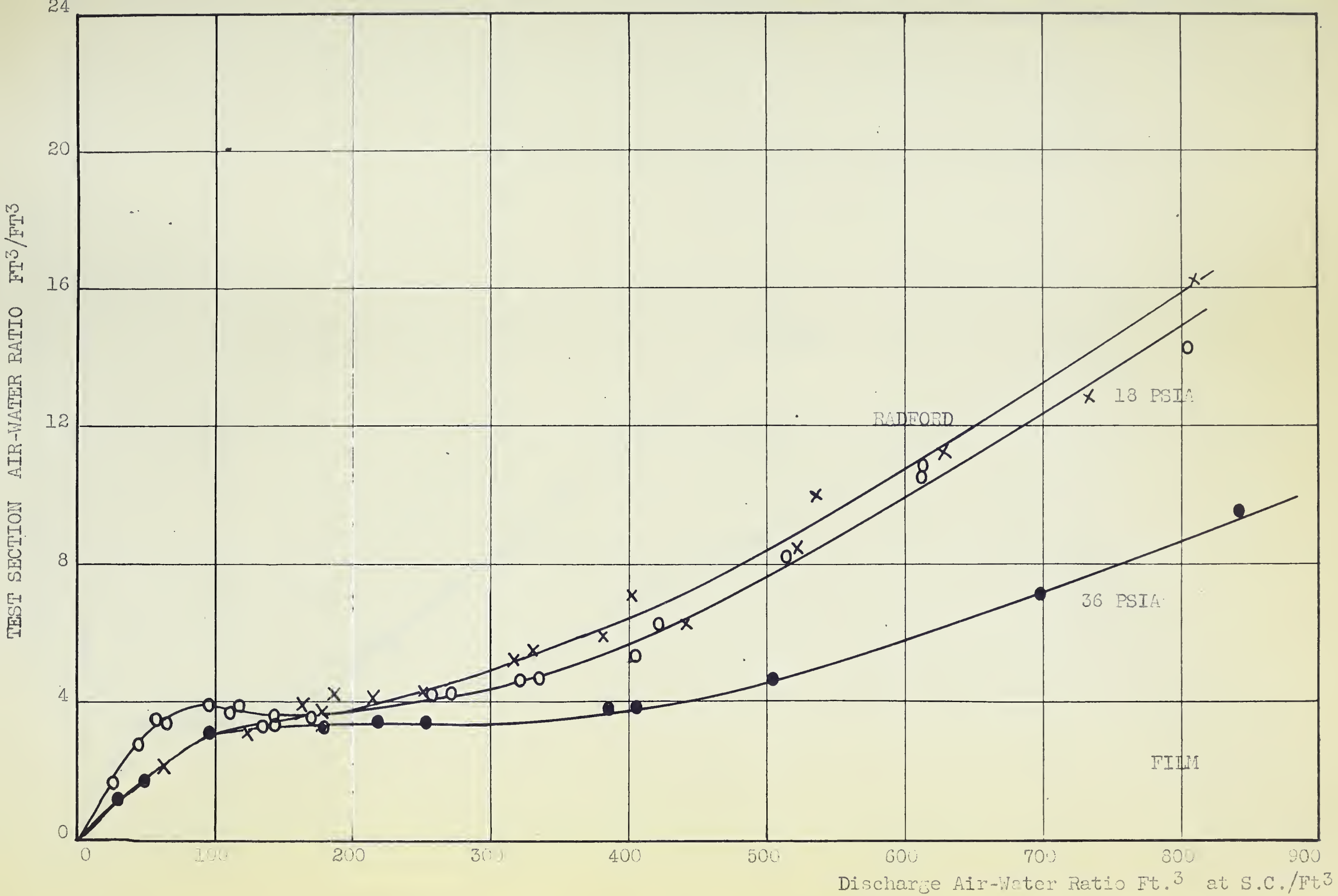

Fig. 36. Variation of Air Water Ratio in the Test Section with Discharge Air-Water Ratio (1 inch Tube, Water Rate 4.15 lbs./ft^2 sec.)

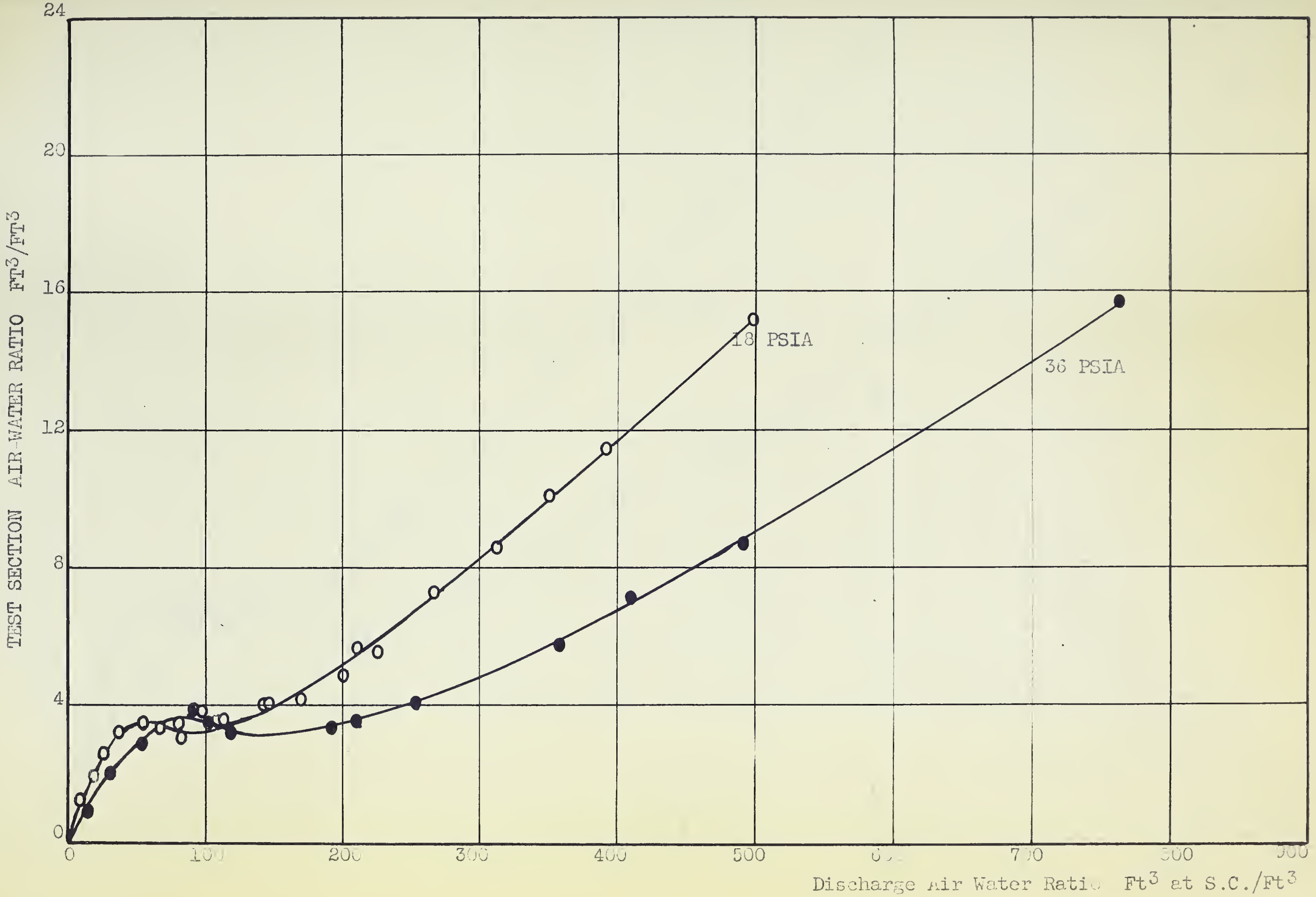

Fig. 37. Variation of Air Water Ratio in the Test Section with Discharge Air-Water Ratio (1 inch Tube, Water Rate - 8.00 lbs./ft^2 sec.)

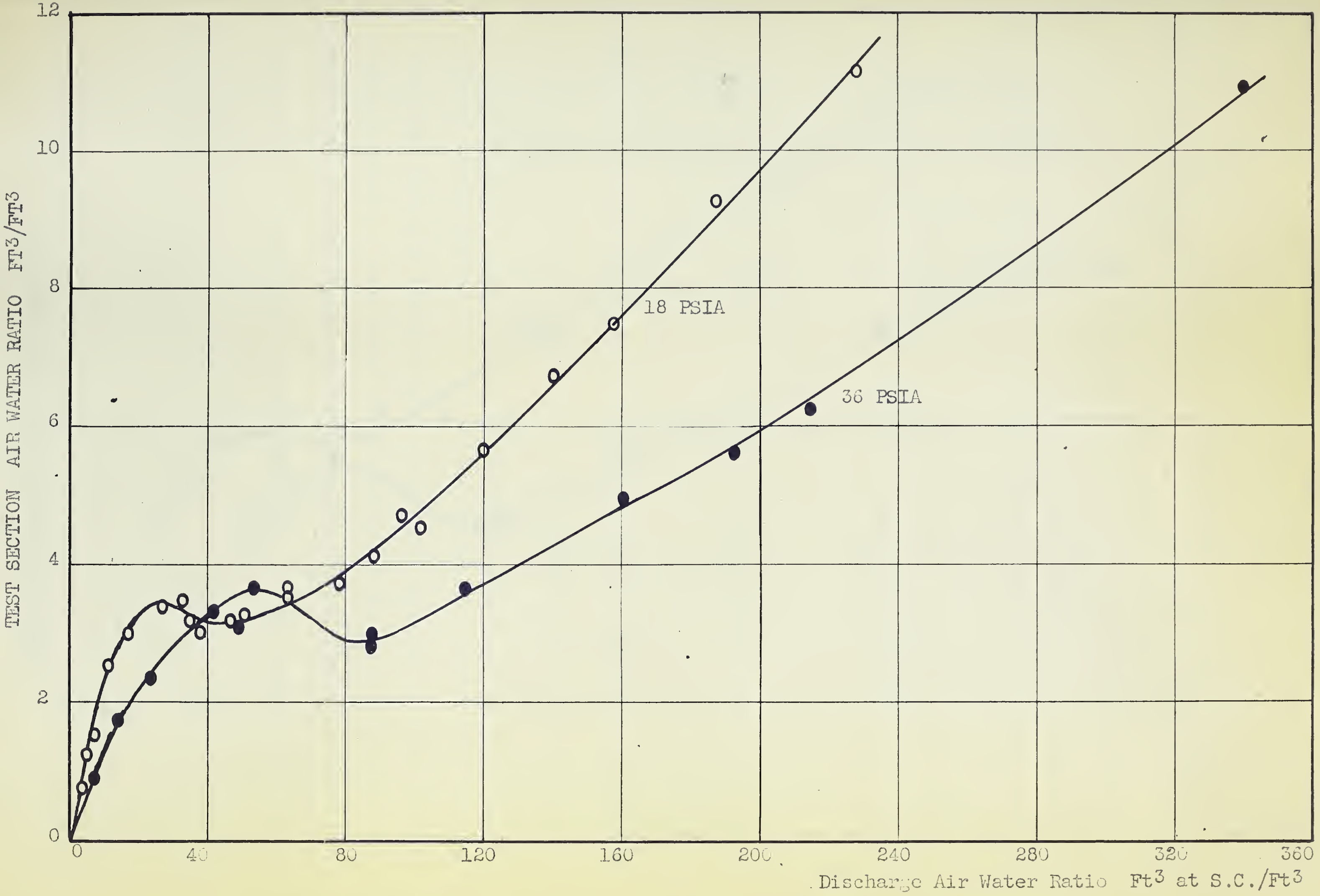

Fig. 38. Variation of Air-Water Ratio in the Test Section with Discharge Air-Water Ratio (1 inch Tube, Water Rate 17.9 lbs./ft^2 sec.)

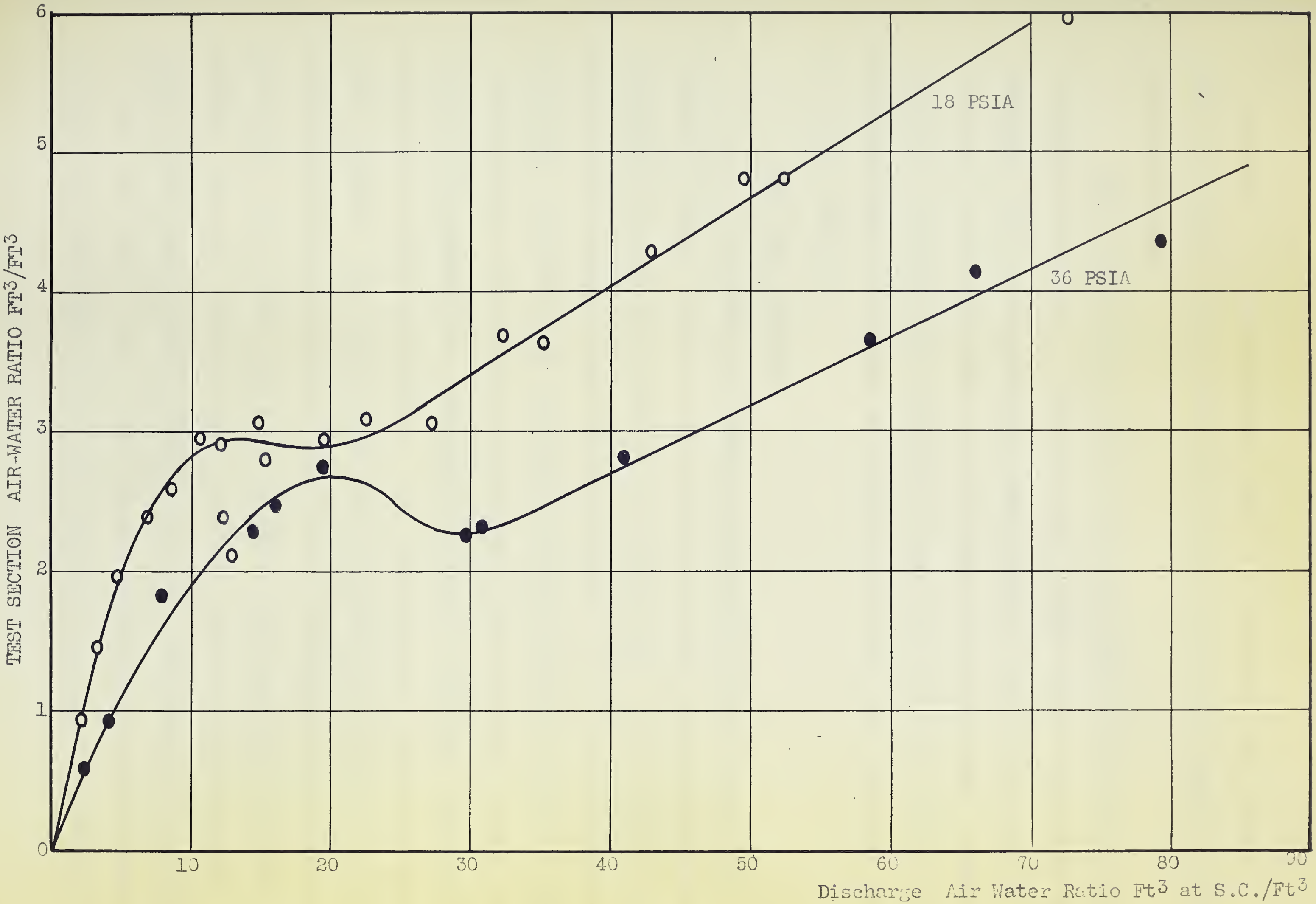

Fig. 39. Variation of Air Water Ratio in the Test Section with Discharge Air Water Ratio (1 inch Tube, Water Rate - 51.9 lbs./ft^2 sec.)

to a minimum at the same discharge ratio as the pressure drop maximum in the froth flow region, and then steadily increases through the annular film and mist flow regions.

The water particles, in the mist flow region, become smaller with increasing air rate and , if this air rate is high enough, they may become vaporized. The flow then would be single phase and the hold-up would be zero. It may well be that the test section air-water ratio (corrected to standard conditions) approaches the discharge air-water ratio at these high air rates and becomes very nearly equal to it just prior to the point where the water all becomes vaporized.

(b) Slip Velocity.

An attempt was made to calculate the slip velocity, i.e., the velocity of the air relative to the particles of water, using the results obtained in the mist flow region in the smaller tube. In this region the flow pattern is the simplest since the water appears to be in the form of discrete particles. An equation was developed expressing the slip velocity in terms of the discharge ratio, the test section ratio, the water rate and the cross-section of the empty tube. Velocities of spheres, ellipsoids, and tear-drop shaped particles of water falling in air were calculated and plotted against their diameters. From these curves the calculated slip velocities indicated water particles having diameters from 3/32 to 1/2 inches for tear-drop shaped particles, 5/32 to 27/32 inches for ellipsoids and even larger diameters for spheres. Since the calculated slip velocities increased with increasing air-rate, the particle diameters likewise increased. Observations of the diameters of water particles in the mist flow region indicated that these calculated diameters were much too large and that with increasing air rate the particles became

smaller. The results appear to indicate that the true mist flow condition probably had not been reached and that a thin annulus of water may have existed on the inside wall of the tube resulting in an error in the calculated slip velocity. Further study is evidently necessary in order to correlate liquid hold-up with the discharge air-water ratio.

c. Effects of Water Rate, Gas Phase Density and Tubing Diameter.

With increasing water rate the test section air-water ratios at the maximum and minimum points appear to decrease slightly.

At any discharge ratio the effect of doubling the gas phase density is to increase the test section ratio when these ratios at the two densities are compared at standard conditions. At the higher density the curves show the same maximum and minimum points corresponding with the first two inflection points on the pressure drop curves and lag those at the lower density.

Little or no difference is found between the test section ratios in the two tubes at any discharge ratio up to the highest air rates that were possible in the test equipment.

4. Correlation of Friction Factors.

a. Energy Balances.

In previous work (14) energy balances for air and water simultaneously entering and leaving an elemental section of vertical tubing were developed from the first law of thermodynamics. These energy balances were combined and, after assuming that the surface energy and kinetic energy terms were negligible, and that the inlet and outlet air-water ratios were equal, the resulting differential equation was integrated. Upon simplifying and transposing the terms, the equation became

$$-\left(\frac{P_2 - P_1}{X_2 - X_1}\right) = \frac{g}{\beta}\,\frac{(\frac{G}{L})_{av} + 1}{(\frac{G}{L}\,v_G)_{av} + v_L} + \frac{\Sigma F_L}{\Delta X\left[(\frac{G}{L}\,v_G)_{av} + v_L\right]}$$

where

P_1 = downstream pressure, lbs_f/ft^2

P_2 = upstream pressure, lbs_f/ft^3

X_1 = downstream pressure tap position above datum, ft.

X_2 = upstream pressure tap position above datum, ft.

g = acceleration due to gravity, $ft./sec^2$

β = proportionality constant, $\frac{lbs_m\ ft.}{lbs._f\ sec^2}$

G = saturated air rate, $\frac{lbs_m}{sec.}$,

L = water rate, $\frac{lbs_m}{sec.}$

v_G = specific volume of saturated air at flowing conditions, ft^3/lb_m

v_L = specific volume of water, ft^3/lb_m

ΣF_L = summation of all friction and other irreversibility losses, $\frac{lbs_f ft.}{lbs_m}$

ΔX = $X_2 - X_1$, ft.

The pressure gradient then is the sum of two terms. The first term $\frac{g}{\beta}\,\frac{(\frac{G}{L})_{av} + 1}{(\frac{G}{L}\,v_G)_{av} + v_L}$, representd the hydrostatic head per unit of height equivalent to the discharge mixture, and the second term, $\frac{\Sigma F_L}{\Delta X\left[(\frac{G}{L}\,v_G)_{av} + v_L\right]}$ represents the irreversibility effects per unit of height.

b. Determination of Friction Losses.

Using the above relationship, the friction loss, ΣF_L, is calculated at several points over a wide range on the smoothed pressure drop - discharge air-water ratio curves for each water rate at both gas phase densities in the two tubes. This ΣF_L, however, expresses the losses in terms of foot pounds force per pound mass of flowing water. Radford suggested that since the flow pattern appears dependent mainly on the air rate, any calculations of friction losses, friction factor and Reynolds number might be expressed in terms of the flowing air phase alone. This approach was also used by Carpenter (2), Gazley (4) and Jenkins (6) in their work on two-phase, two-component flow in vertical and horizontal tubes, at the University of Delaware. At this stage it would appear to be the most logical method. To obtain ΣF_G, the losses expressed in ft.lbs_f/lb_m of flowing air, ΣF_L is multiplied by the ratio of the mass rate of flow of water to air, i.e., $\Sigma F_G = \frac{L}{G} \Sigma F_L$. The measured pressure drop - discharge air-water ratio curve for the 4.15 lbs/ft^2 sec. water rate at the lower gas phase density in the larger tube is shown again in Fig. 40. The two components of this pressure drop, computed from the above equation, are also plotted. It will be noted that at low discharge ratios the hydrostatic head equivalent forms a large part of the measured pressure drop but quickly falls off to a very small value with increasing discharge ratios. The friction or irreversibility equivalent then accounts for virtually all of the pressure drop. At zero discharge ratio the measured pressure drop is 45.5 p.s.i./100 ft. mainly due to the hydrostatic head of the column of water.

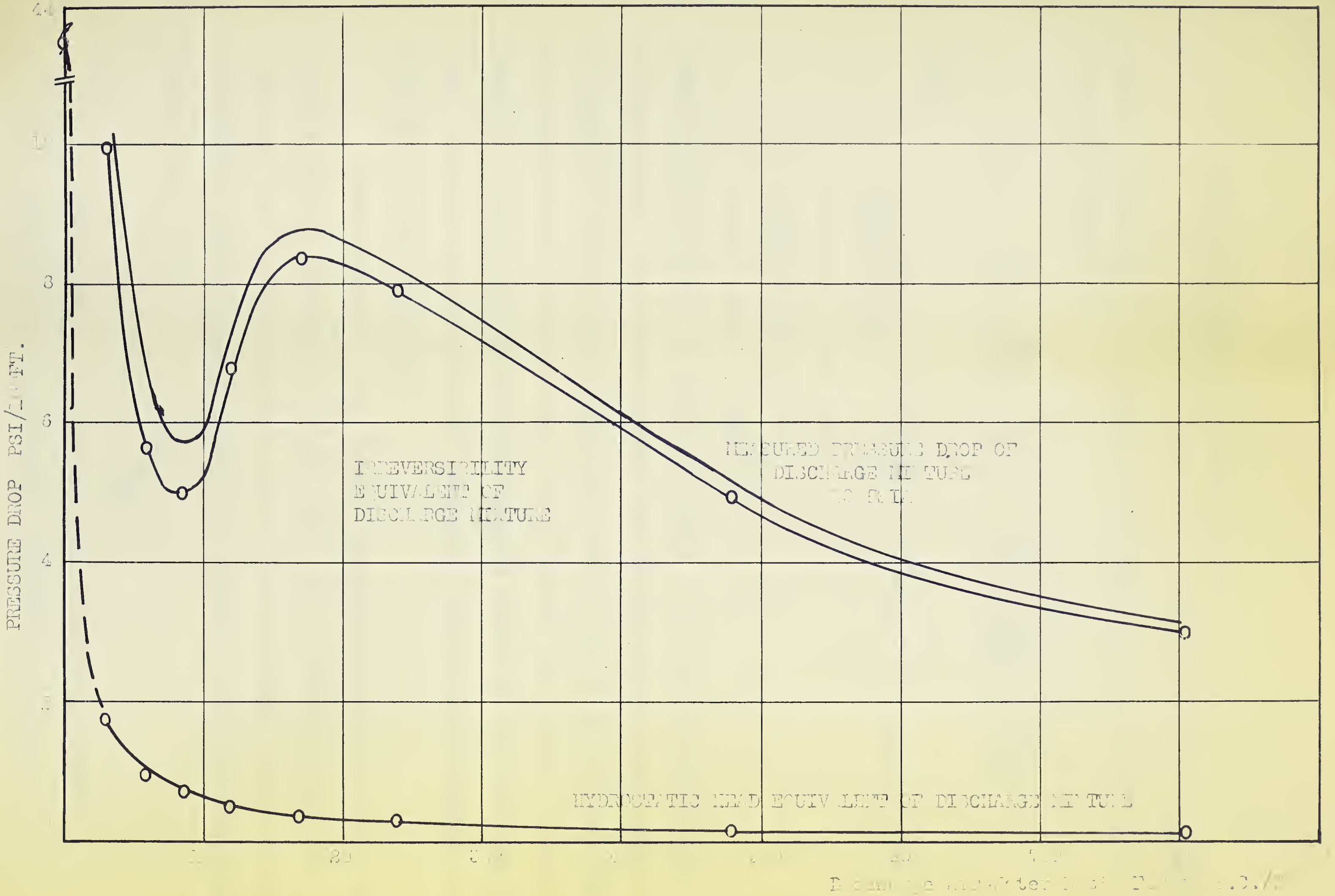

F[illegible] V[illegible] [illegible] Irreversibility
C[illegible] of Pressure Drop with Discharge [illegible] -Water
[illegible] ([illegible])

c. Determination of Friction Factor.

The determination of friction factors for the flowing two-phase mixtures is approached by analogy to single-phase flow in tubes. Thus a friction factor defined as

$$f_G = \frac{\beta}{2}\left(\frac{\Sigma F_G}{V_G^2}\right)\left(\frac{D}{N}\right) = \frac{\beta}{2}\left(\frac{DA^2}{v_G^2 N}\right)\left(\frac{\Sigma F_G}{G^2}\right)$$

where

V_G = gas phase velocity based on the empty cross section of the tube, ft./sec.

D = diameter of tube, ft.

N = length of tube, ft.

A = cross section of tube, ft^2

(Other items as defined in Part (a) above.) is used to correlate the friction losses. It is realized that this friction factor almost surely will be dependent upon the ratio of the mass rates of flow of the air and water, the gas phase density, the water rate, the tube diameter and length, the flow pattern of the two phase mixture, the surface tension of the liquid phase and other variables as well as the tube roughness and the Reynolds number as in the case of single phase flow.

Using values of ΣF_G computed from pressure drops from the smoothed pressure drop vs. discharge air-water ratio curves, friction factors are calculated from the above equation and are plotted in Figs. 41 and 42 against a superficial Reynolds number based on the flowing air, and the empty cross section, i.e.,

$$Re_G = \frac{D V_G \rho_G}{\mu_G}$$

where

ρ_G = specific weight of air at flowing conditions, lbs_m/ft^3

μ_G = viscosity of air at flowing conditions, $lbs_m/sec.ft.$

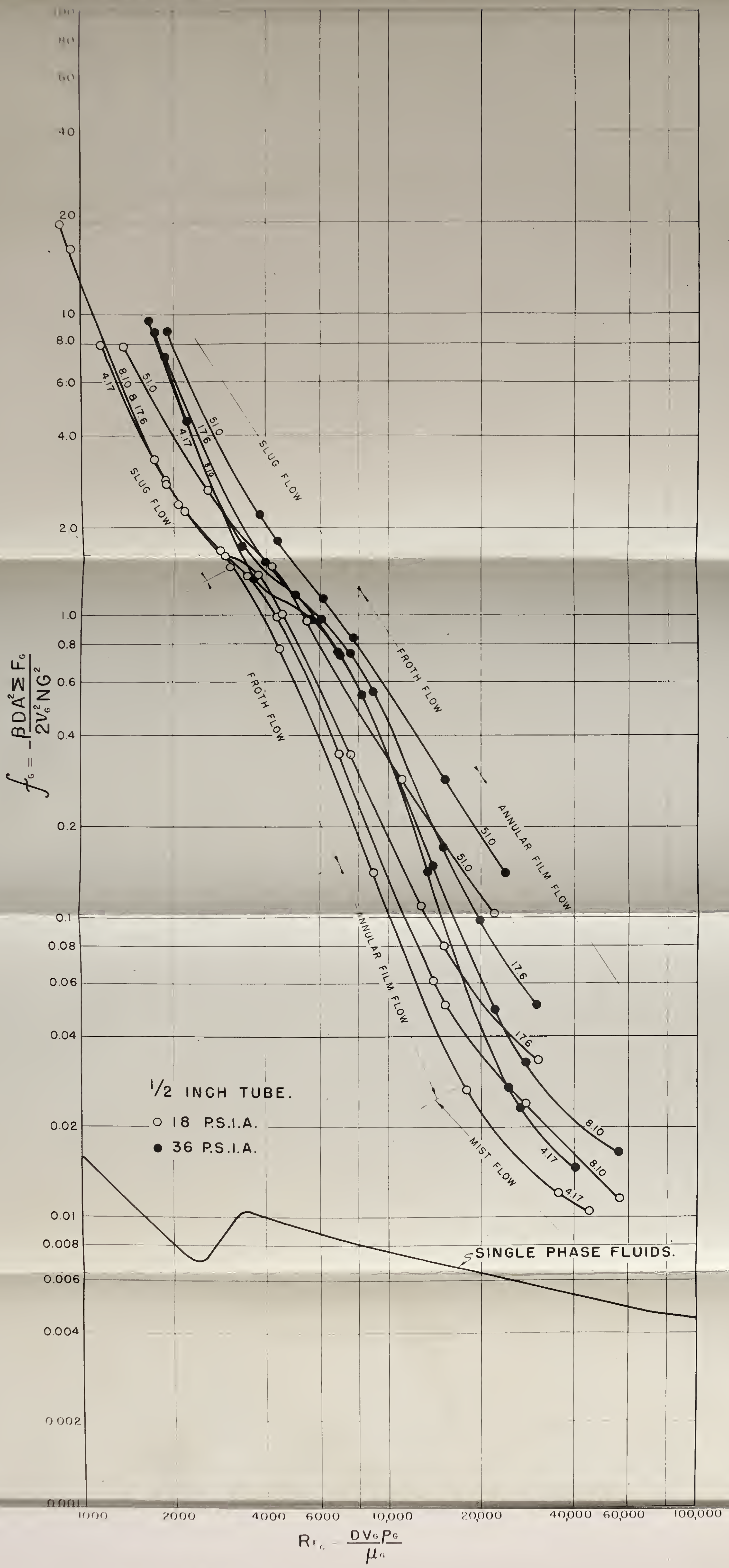

Fig. 41. Variation of Friction Factors with Reynolds Number - 1/2-inch Tube.

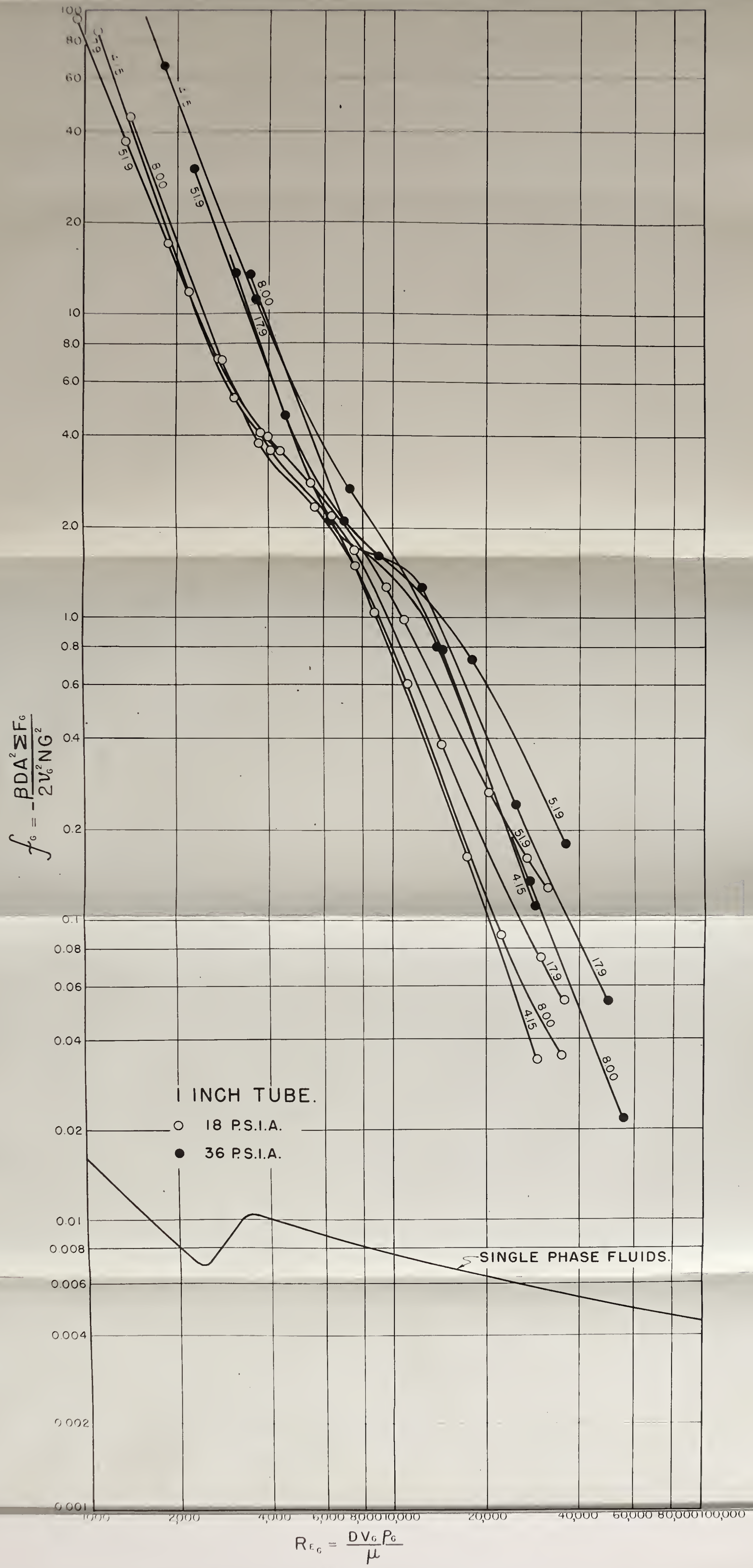

Fig. 42. Variation of Friction Factor with Reynolds Number - 1-inch Tube.

Two sets of curves are shown for each tube, these being for each gas phase density. The water rates are marked on each curve. For comparison, the friction factor curve for single phase fluids is also shown in each figure.

The most notable features of the curves are the magnitude of the friction factor at low Reynolds numbers and the change in the friction factor with increasing Reynolds numbers. At a Reynolds number of 1000, the friction factors for the two-phase flow are about 1,000 times greater than that for single-phase flow. With increasing Reynolds numbers the friction factor curves decrease rapidly in the slug flow range. In the transition from slug to froth flow, the curves all show a marked change in slope and the decrease in the friction factor is not so great. Thereafter, the rapid decrease in f_G continues again until the mist flow region is reached. In this region the decrease in f_G is again not so great and the curves show a gradual tendency to approach the curve for single phase fluid at Reynolds numbers greater than 100,000. This would be expected since at high discharge air-water ratios the single-phase condition is approximated. Over the range of Reynolds numbers studied, the slopes of the curves, disregarding the transition region and the mist flow region;,are all about -2.1.

In correlating the pressure drops for two-phase flow by means of a method analogous to that used for single-phase flow, it is appreciated that the former flow is complex and can not be solved completely by the methods used for the latter. After preparing the friction factor - Reynolds number curves, a parameter based upon the fraction of the tube filled with gas was plotted on them. At various assumed values of the ratio of the volume of gas in the tube to the total volume of the tube, i.e., the fraction of the tube filled with gas, the test section air-water ratio was calculated for each curve.

From Figs. 32 to 39 the corresponding discharge ratio was obtained and the Reynolds number was calculated. These ratios were plotted on each curve at their respective Reynolds numbers. It was thought that a series of curves might be obtained analogous to those for different relative roughnesses for single phase flow in pipes since it is felt that the test section air-water ratio may be the controlling factor in that part of the friction losses due to effect of interfacial roughness between the air and the water. The points, however, were scattered and no satisfactory curves joining all points of equal ratios could be obtained. Further investigation of the test section ratio is evidently necessary

Since a separate curve is obtained for each water rate at each of the gas phase densities in both tubes, it is obvious that these variables have considerable influence on the friction factor. Such a plot is of little value in solving two-phase flow problems unless the influence of each variable over a wide range has been determined. Only the effects of water rate, gas phase density and tubing diameter have been measured. These three variables are considered separately using cross-plots of Figs. 41 and 42.

d. Effect of Water Rate.

As a first attempt to analyze the effect of water rate, a cross plot of the friction factors at four different Reynolds numbers, 2000, 6000, 10,000 and 20,000 at the two gas phase densities in each tube versus the water rate, was prepared on semi-log graph paper. The values of the ordinate at W = 0 for the four Reynolds numbers were obtained from the curve for single-phase fluids in smooth pipes. However, on the semi-log paper the points were too crowded at the low water rates; hence it was felt that the

use of log log paper would show the curves better. In order to get around the difficulty of zero water flow, the friction factors are plotted against (W + 0.1) instead of W, as shown in Figs. 43 and 44. Strictly speaking, this results in a slight distortion in the curves as low values of W, but it does enable the curves to be plotted down to W = 0. Since no data are available for water rates between 0 and 4.15 lbs_m/ft^2 sec., the curves are dotted in this region and their positions are only assumptions. However, it is apparent that the addition of a slight amount of water to the flowing air results in a large increase in the friction factor, the increase being greatest at low Reynolds numbers. Increasing water rate in the range studied has little effect on the friction factor at low Reynolds numbers, especially in the larger tube. With increasing Reynolds numbers the effect of the water rate on the magnitude of the friction factor becomes smaller, but with increasing water rate the friction factor becomes greater. This is more pronounced in the smaller tube.

e. Effect of Gas Phase Density.

The friction factor at the four Reynolds numbers (2000, 6000, 10,000 and 20,000) for each water rate in both tubes are plotted against the ratios of the gas phase to the liquid phase density in Fig. 45. Since only two densities were used, the results cannot be extrapolated over a wide range of densities, The results do show, however, that at the higher density, the friction factors are higher, the increase being greater at the lowest and the highest Reynolds numbers. It would appear that the flow pattern greatly influences the results. The effect of flow pattern in the intermediate Reynolds number (6000) results in the smaller increase in the friction factor at the higher density. This is the transformation region from slug to froth flow.

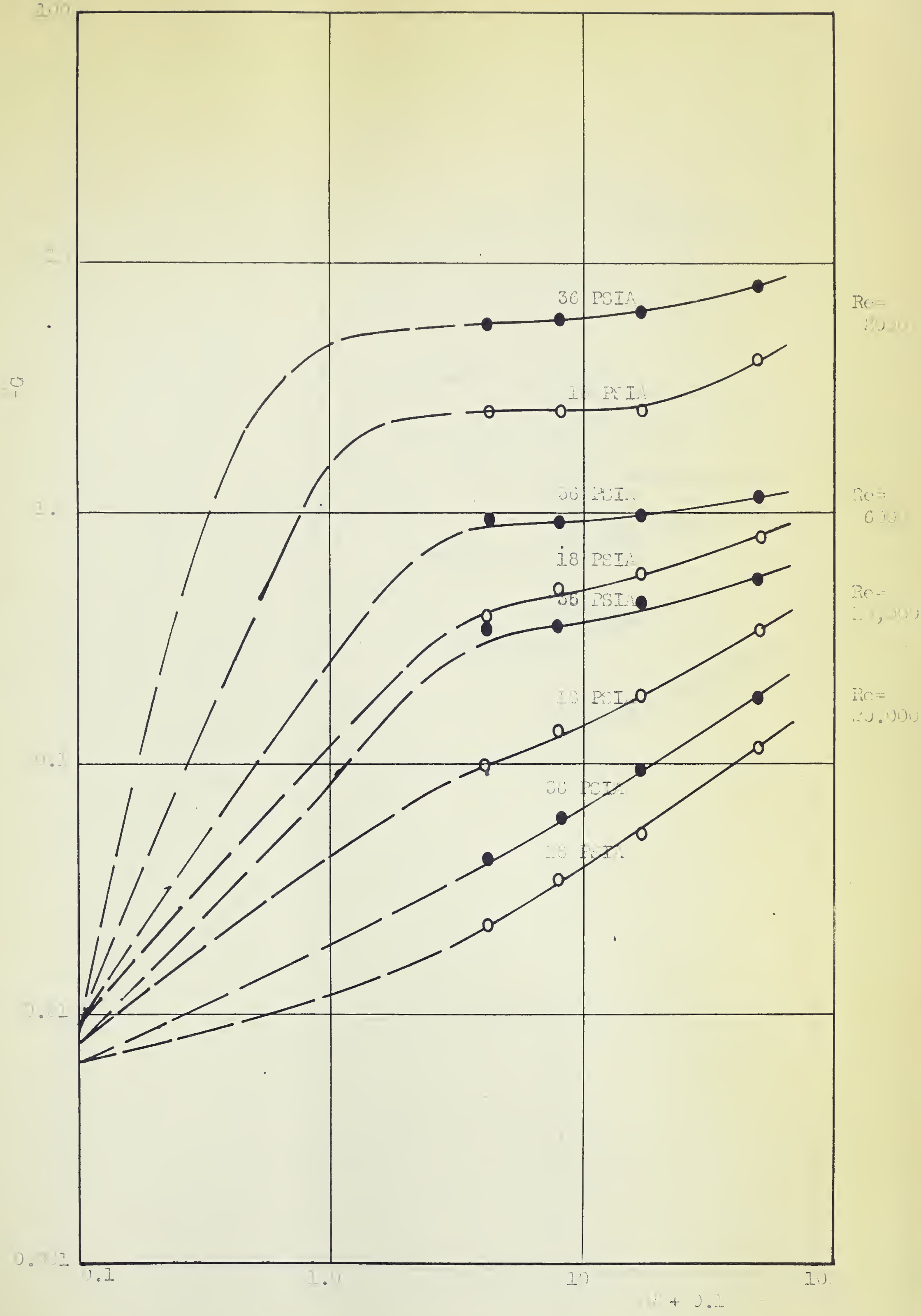

Fig. [illegible]. Effect of Water Rate on Friction Factor - 1/2-inch Tube.

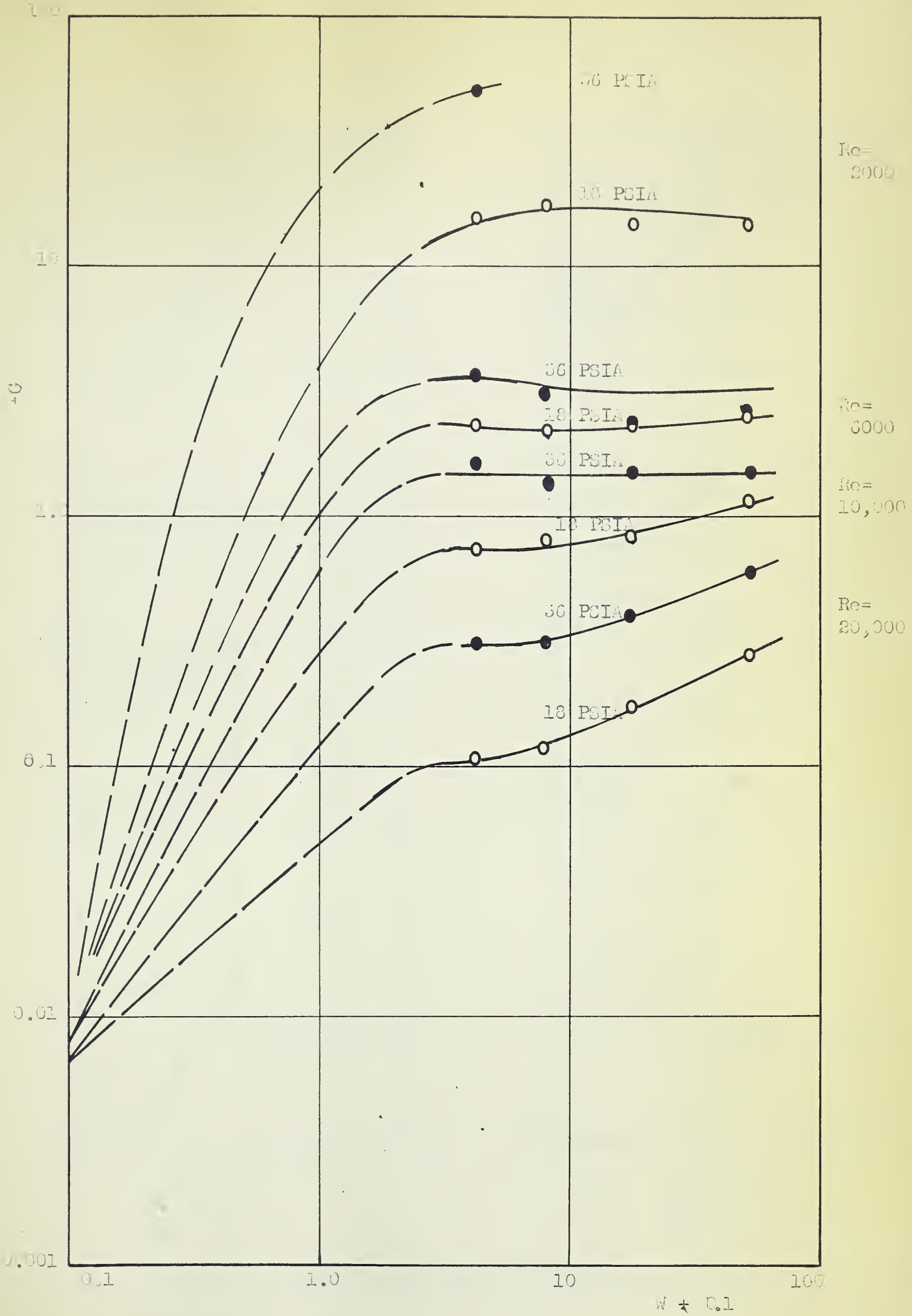

Fig. 44. Effect of Water Rate on Friction Factor - 1-inch Tube.

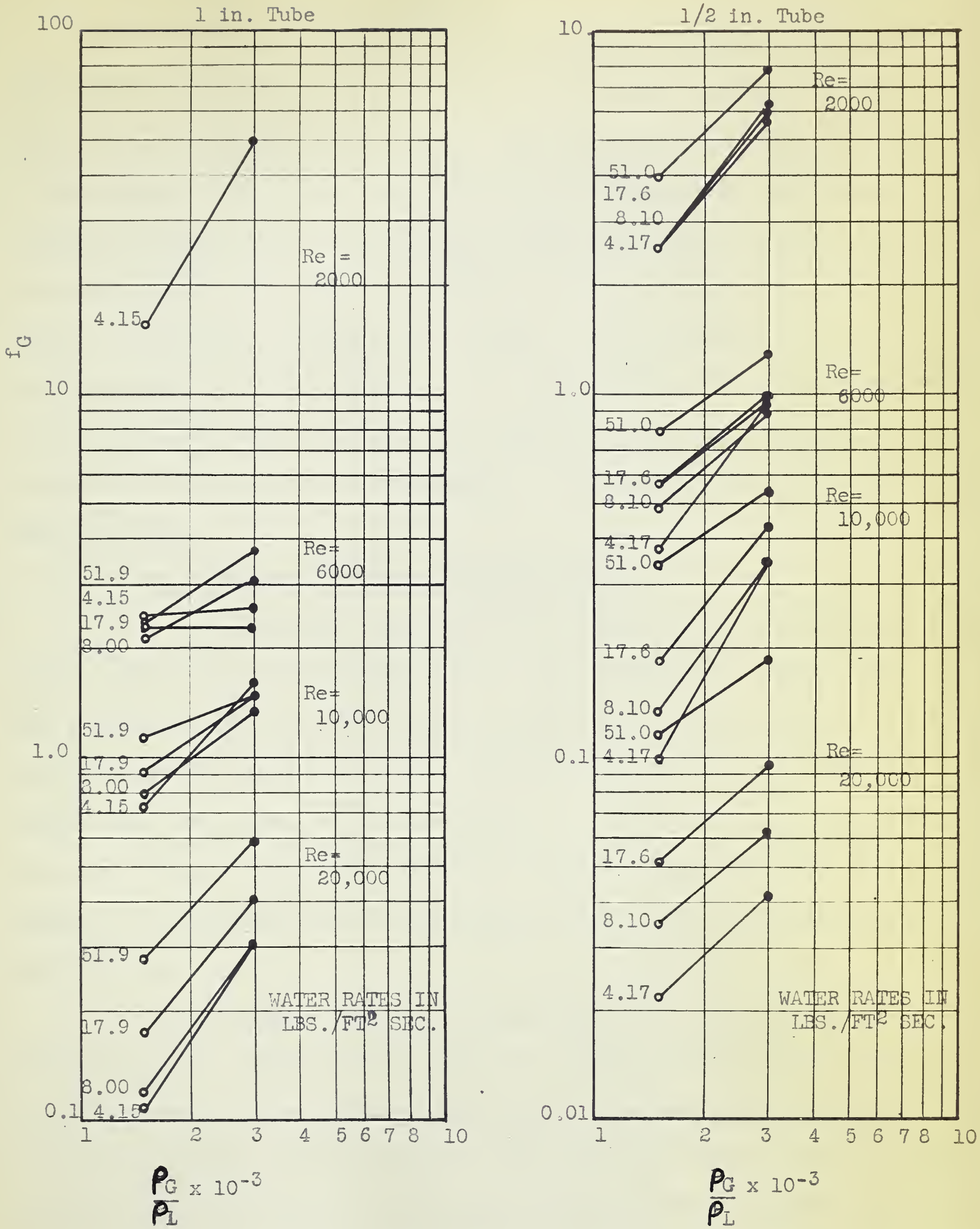

Fig. 45. Effect of Gas Phase Density on Friction Factor.

f. Effect of Tubing Diameter.

In Figs. 46 and 47, friction factors at Reynolds numbers of 2000, 6000, 10,000 and 20,000 are plotted against tube diameters for each water rate and each gas phase density. Friction factors are from 2 1/2 to 9 times higher in the larger tube than in the smaller tube. The increase appears to depend upon the water rate, the gas phase Reynolds number and the gas phase density, but shows no consistent pattern. At the lower gas phase density, the greatest increase in f_G between the two diameters is at a Reynolds number of 10,000, whereas at the higher density the greatest increase is at a Reynolds number of 20,000. As observed in Part (d), friction factors increase more rapidly with increasing water rate in the smaller tube than in the larger one.

(g) Summary of Friction Factor Results.

At low water rates the effect of water rate on the friction factors appears to be very great, but at higher water rates, the air rate and consequently the gas phase Reynolds number become more important. The magnitude of the effect of gas phase density on the friction factors is dependent upon the pattern of the flowing mixture, which is in turn dependent upon the flowing air rate. The effect of diameter is not consistent but appears to be dependent upon a combination of water rate, gas phase density and flow rate.

Thus it appears that the friction factors for two-phase vertical flow are complex. Because of the number of variables that influence these friction factors, a correlation of the effect of any one variable alone is difficult to obtain. Further studies of the effects of water rate, gas phase density and tubing diameter are evidently necessary before a general relation-

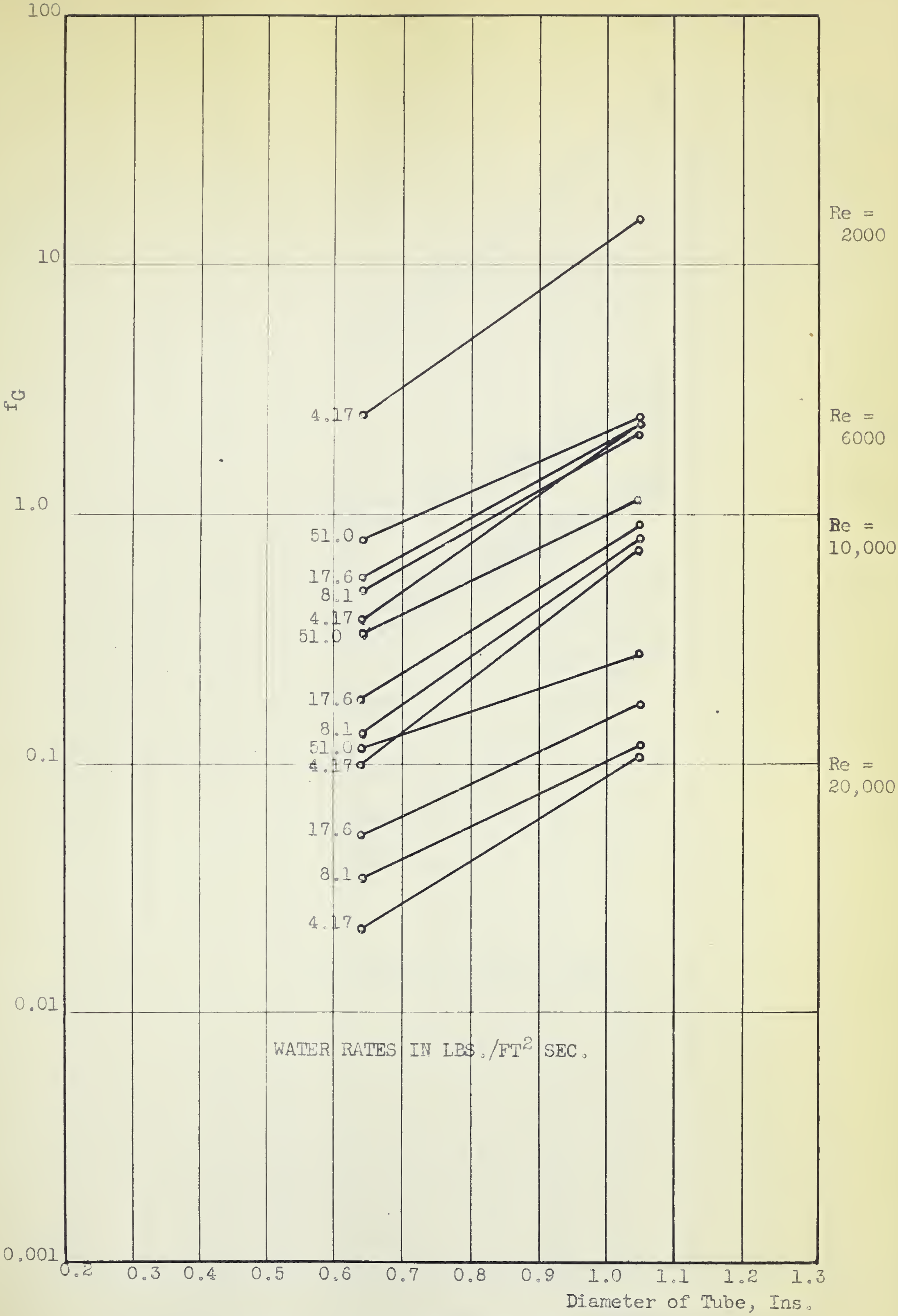

Fig. 46. Effect of Tube Diameter on Friction Factor - Mid-Point Pressure 18 p.s.i.a.

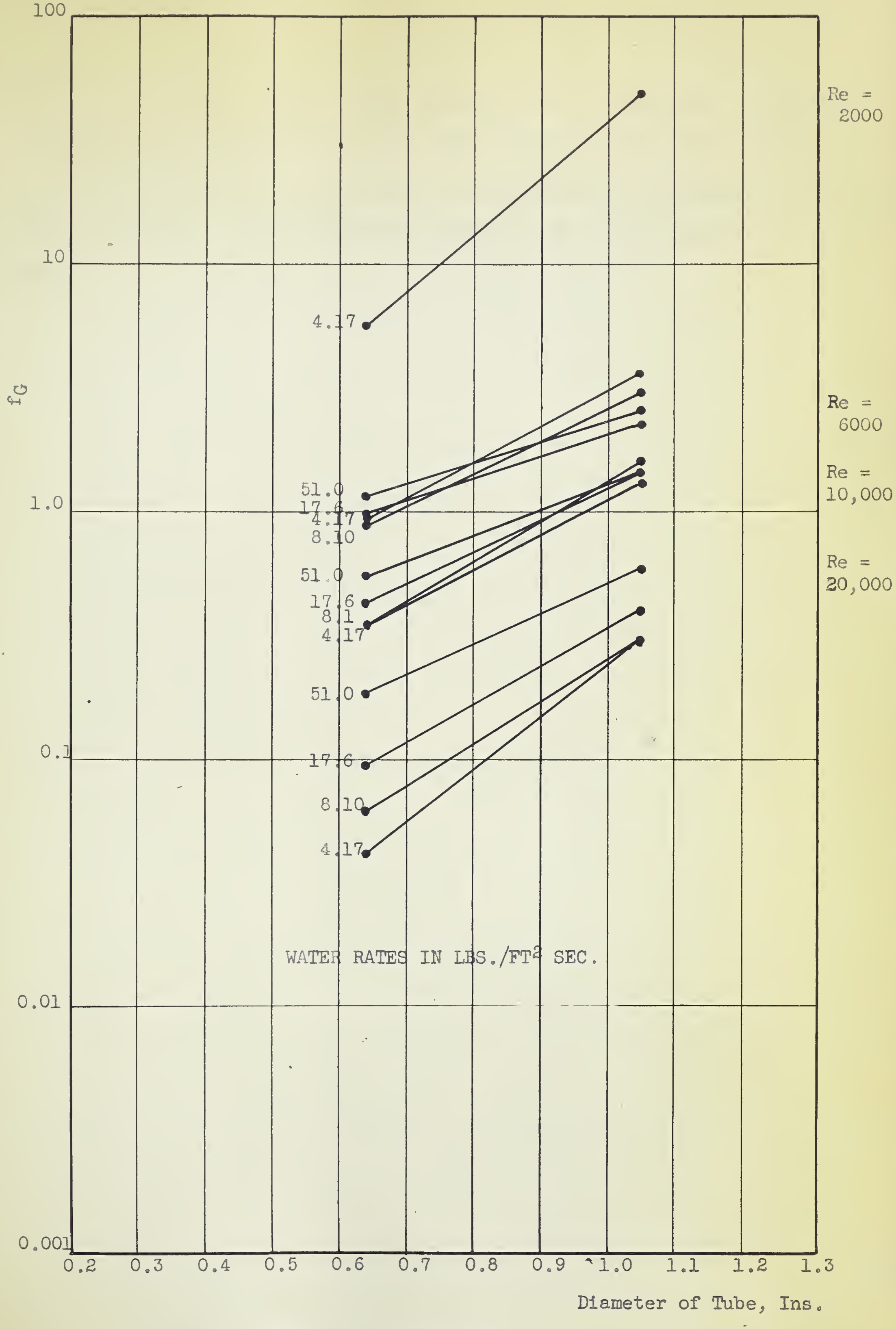

Fig. 47. Effect of Tube Diameter on Friction Factor - Mid-Point Pressure 36 p.s.i.a.

ship embracing all of the pertinent variables will be obtained. A detailed examination of the flow patterns and their effects on the other variables would be very helpful. Such an examination might shed information on interfacial roughness, i.e. the roughness effect of the liquid phase on the gas phase.

CHAPTER VIII

CONCLUSIONS

1. Studies have been conducted on the upward flow of air-water mixtures in vertical tubes embracing the following range of variables: tube diameter, 0.640-inch and 1.049-inch; test section mid-point pressure, 18.0 and 36.0 p.s.i.a.; gas rate, 0 to 0.97 ft^3/sec. at 14.4 p.s.i.a and 60°F.; liquid rate, 4.15, 8.00, 17.9 and 51.9 lbs/ft^2 sec. The following observations have been made:

a. The same series of flow patterns are found regardless of water rate, gas phase density, or tubing diameter. That is, as the air rate is increased, the flow pattern passes through the slug region, the froth region, the annulus film region and the mist region. The transition from one type to the next is gradual and does not occur at any definite air rate.

b. The measured pressure drop shows the same general trend for different water rates, gas phase densities, and tubing diameters. As the air rate is increased the pressure drop passes through a first minimum point, a maximum point, a second minimum point, and then increases steadily. The magnitude of the pressure drop, however, is greatly influenced by these variables. With increasing water rates the pressure drops at these inflection points become greater and the second minimum point disappears at high water rates. Doubling the gas phase density results in the pressure drop - discharge air-water ratio curve lagging the corresponding curve of the lower density. Tubing diameter shows only slight effects on the pressure drop. An exploratory run conducted with the surface tension of the liquid phase decreased to 80 per cent of that for water alone, shows only a small decrease in pressure drop.

c. The air-water ratio existing in the test sections increases to a maximum point, decrease slightly to a minimum point and then increase steadily with increasing discharge air-water ratios. These two inflection points occur at the same air-water ratios as the first two pressure drop inflection points but are reversed.

An attempt to determine the slip velocity of the gas phase past the liquid phase in the mist flow region shows that further studies of test section hold-up are required before this velocity can be properly calculated.

2. Using a method proposed by Radford in earlier work on gas-liquid flow, the measured pressure drops are separated into two components, the hydrostatic head losses and the friction losses. The hydrostatic head losses are only significant at low discharge air-water ratios and decrease rapidly with increasing discharge ratio. The friction losses, expressed in terms of the gas phase, are used to calculate friction factors based on the flowing gas phase. These friction factors, arbitrarily defined as

$$f_G = \frac{\beta}{2} \quad \frac{DA^2}{v_G^2 N} \quad \frac{\Sigma F_G}{G^2}$$

are plotted against superficial Reynolds numbers also calculated on the basis of the flowing gas phase occupying the entire cross-section of the tube. The results show that friction factors for two-phase flowing mixtures are as much as 1000 times greater than friction factors for single phase fluids at corresponding Reynolds numbers and that with increasing Reynolds numbers, the friction factors decrease sharply over the range studied. The curves all have a slope of approximately -2.1. This attempt to correlate the gas phase friction factor with the gas phase Reynolds number is only partially successful in that the data for each water rate, gas phase density and tube fall on

separate curves. The effects of these variables on the friction factor appear to be interrelated and are complex. No complete correlation of these variables is possible at this time and further studies of their effects are necessary.

APPENDIX A

CALIBRATIONS

TABLE I. EXPERIMENTAL DATA - CALIBRATION OF WATER ORIFICE PLATES

Orifice Plate No. 1

1	2	3	4		5
Test No.	Discharge	Time	Rate		Manometer Difference Inches CCl_4 under H_2O
	ml.	sec.	ml./sec.	ft^3/sec.	
1	447	105.6	4.24	1.50×10^{-4}	3.05
2	918	102.5	8.95	3.16 "	11.10
3	1745	146.2	11.92	4.21 "	19.75
4	1815	135.3	13.40	4.73 "	24.95
5	1900	117.2	16.22	5.73 "	43.70
6	1945	101.6	19.15	6.76 "	57.75
					Inches Hg under H_2O
7	1930	104.7	18.40	6.50×10^{-4}	2.60
8	1900	82.9	22.9	8.10 "	4.10
9	1865	37.4	49.9	17.6 "	19.50
10	1805	32.3	55.8	19.7 "	24.00

Orifice Plate No. 3

1	2	3	4		5
Test No.	Discharge ml.	Time sec.	Rate		Manometer Difference Inches Hg under H_2O
			ml./sec.	ft.^{3}/sec.	
1			83.6	29.5×10^{-4}	4.00
2	1920	18.6	103.4	36.5 "	5.95
3	1850	13.2	140	49.5 "	10.90
4	1860	9.8	190	67.1 "	19.95
5			239	84.5 "	31.50

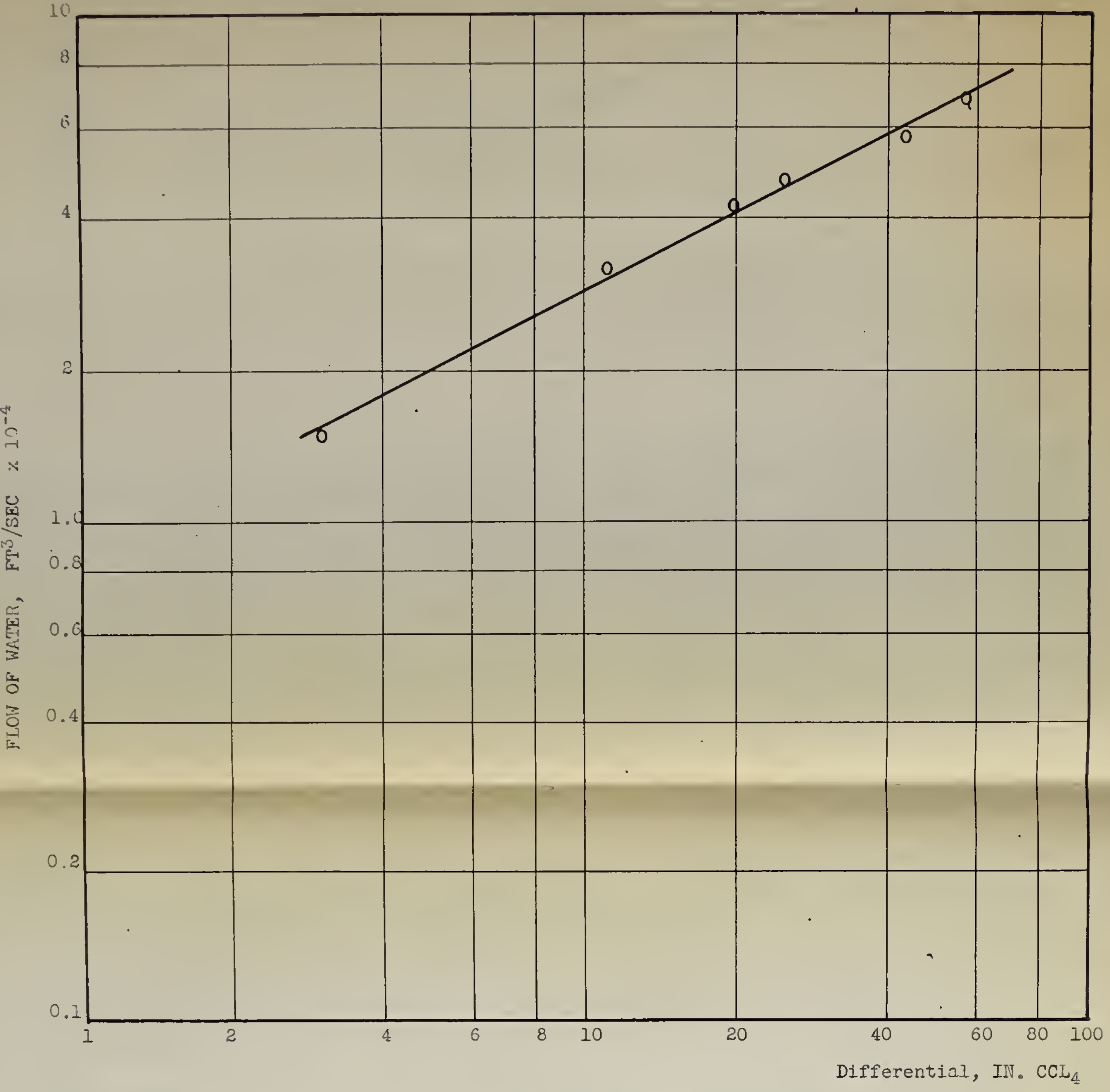

Fig, 48. Water Orifice Calibrations.

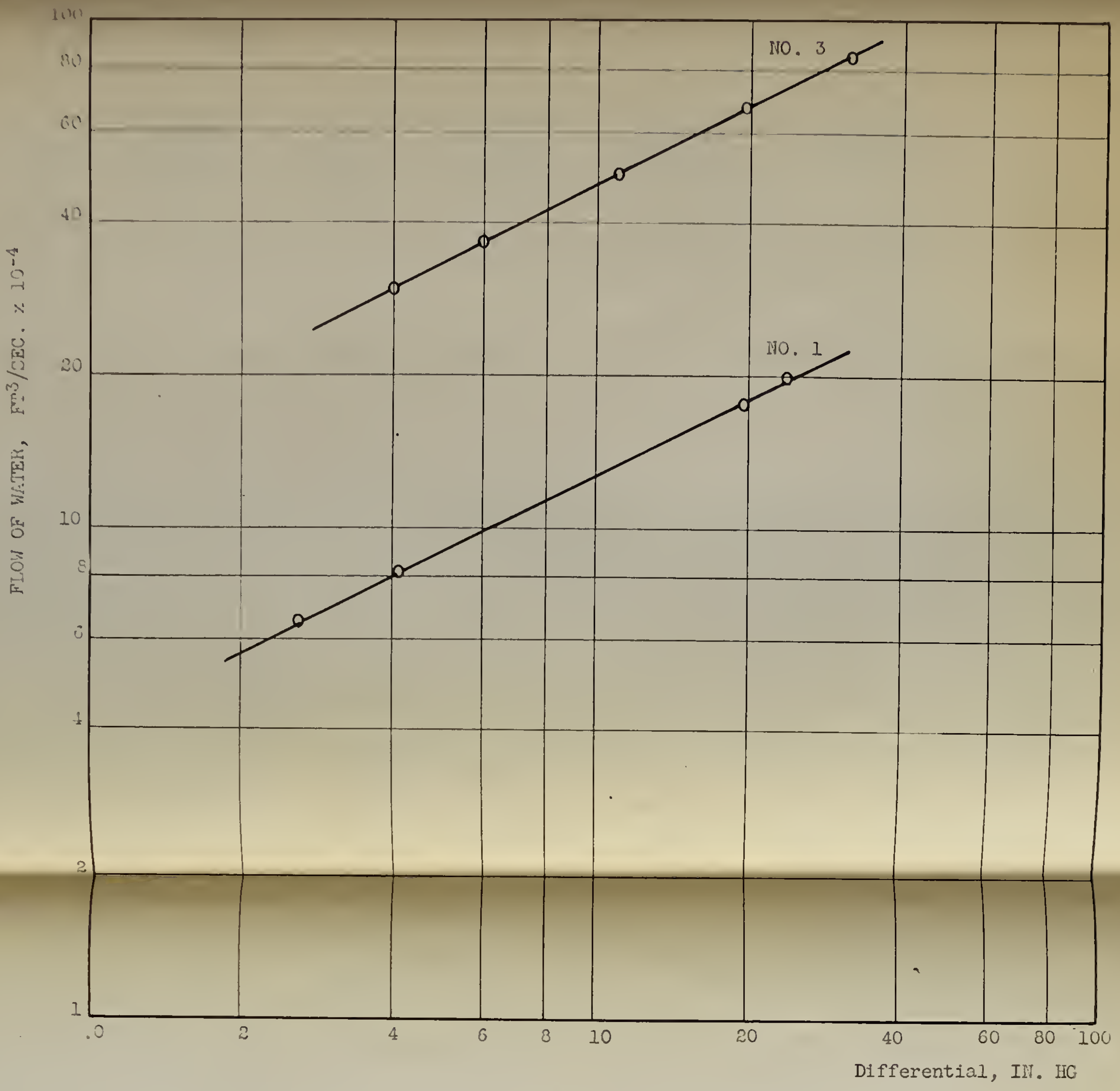

Fig. 49. Water Orifice Calibrations.

TABLE II. EXPERIMENTAL DATA - CALIBRATION OF AIR ORIFICE PLATES WITH CRITICAL FLOW PROVER

1	2	3	4	5	6	7
Air Orifice Plate No.	Pressure Upstream of Air Orifice P_f p.s.i.a.	Manometer Difference h_f Inches Hg under Air	Absolute Temp. in Critical Flow Prover T °R.	Pressure Upstream of Critical Flow Orifice P_c p.s.i.a.	Size of Critical Flow Orifice ins.	Critical Flow Orifice Coefficient
1	53.2	13.40	530	44.8	3/32	3.58
1	57.7	14.80	532	48.5	3/32	3.58
1	62.5	16.03	532	52.6	3/32	3.58
1	72.4	18.75	532	61.2	3/32	3.58
1	73.4	18.82	530	62.3	3/32	3.58
1	77.4	20.20	531	65.8	3/32	3.58
2	50.3	8.84	532	44.2	1/8	6.45
2	54.4	9.41	531	47.9	1/8	6.45
2	65.8	11.45	531	58.2	1/8	6.45
2	67.0	11.89	530	59.4	1/8	6.45
2	71.3	12.60	530	62.7	1/8	6.45
2	73.2	13.08	530	64.7	1/8	6.45
3	51.7	13.98	528	43.3	3/16	14.79
3	57.8	15.30	528	48.2	3/16	14.79
3	67.8	18.35	528	57.1	3/16	14.79
3	69.8	19.50	529	58.5	3/16	14.79
3	76.2	21.40	529	63.7	3/16	14.79
3	70.6	19.60	526	59.0	3/16	14.79
4	50.9	10.23	527	43.9	1/4	26.55
4	56.6	11.38	527	48.8	1/4	26.55
4	62.1	12.48	527	53.6	1/4	26.55

TABLE III. CALCULATED RESULTS - CALIBRATION OF AIR ORIFICE PLATES WITH CRITICAL FLOW PROVER

1	2	3	4	5
Air Orifice Plate No.	Q_c^* - Air Rate M ft^3/day	Q_o - Air Rate ft^3/sec.	$\sqrt{\frac{h_f P_f}{T}}$	K**- Air Orifice Coefficient
1	6.97	.0807	1.16	.0696
1	7.52	.0870	1.26	.0688
1	8.15	.0943	1.37	.0687
1	9.48	.110	1.60	.0687
1	9.69	.112	1.61	.0695
1	10.2	.118	1.72	.0688
				Ave. .0690
2	12.5	.143	.914	.157
2	13.4	.155	.982	.158
2	16.3	.189	1.18	.158
2	16.6	.193	1.23	.157
2	17.6	.203	1.30	.156
2	18.1	.210	1.34	.156
2				Ave. .157
3	27.9	.322	1.17	.275
3	31.0	.359	1.29	.277
3	36.8	.425	1.54	.277
3	37.6	.436	1.60	.272
3	41.0	.475	1.76	.271
3	38.0	.440	1.62	.271
				Ave. .274
4	50.7	.587	.994	.591
4	56.4	.653	1.11	.591
4	62.0	.718	1.21	.592
				Ave. .591

$$*Q_c = \frac{CP_c}{\sqrt{ST}}$$

$$**K = \frac{Q_o}{\sqrt{\frac{h_f P_f}{T}}}$$

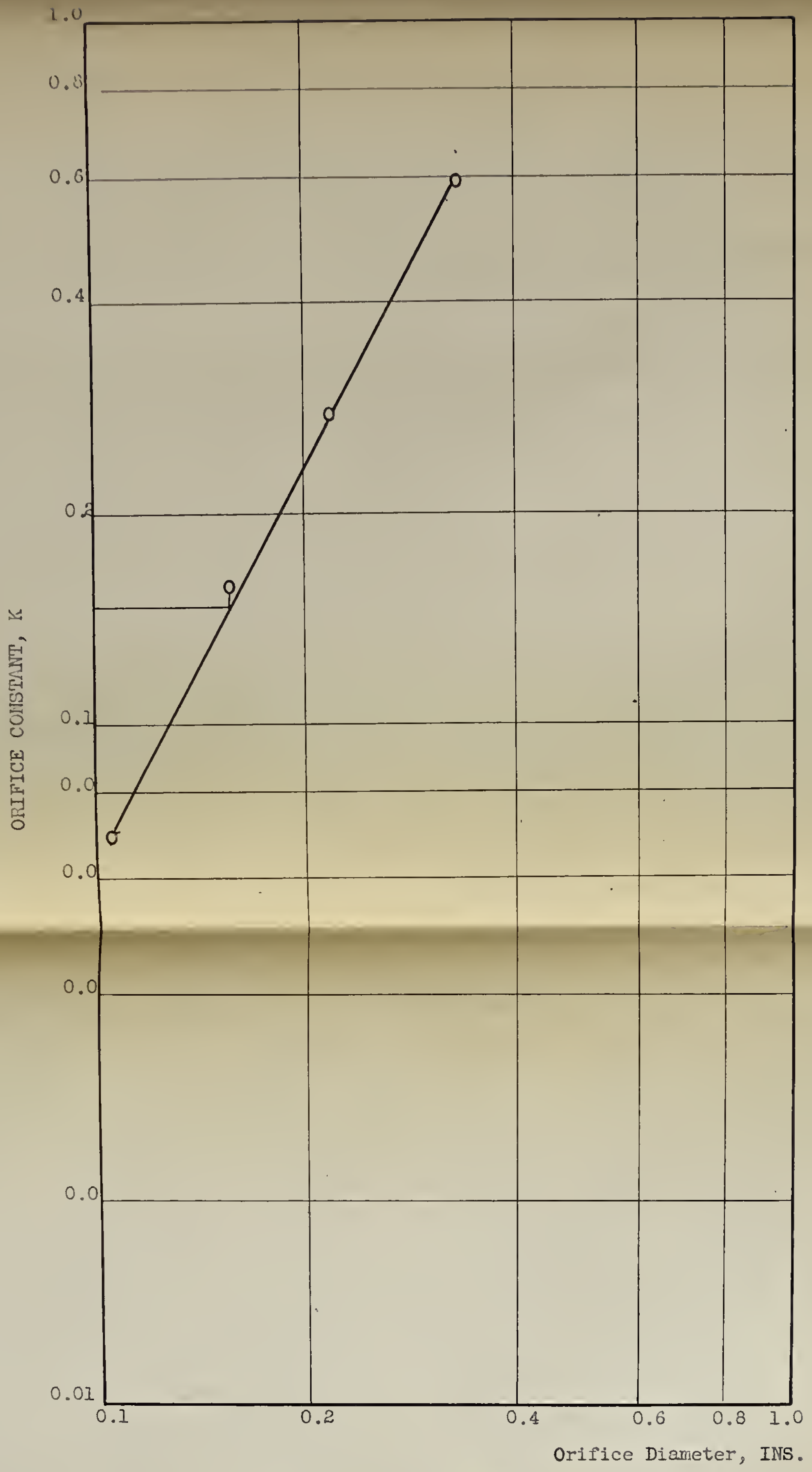

Fig. 50. Air Orifice Calibrations.

APPENDIX B

EXPERIMENTAL DATA

TABLE IV. SUPPLEMENTARY DATA

Transparent Butyrate Tubes

	Nominal 1/2-inch	Nominal 1-inch
Inside Diameter of Tubes..........	0.640 in. ± .005 in.	1.049 in. ± .005 in.
Length of Test Section...........	22.78 in. ± .02 ft.	22.88 ft. ± .02 ft.
Tube Volume between Plug Valves...	1950 ml.	5340 ml.

TABLE V. SINGLE PHASE WATER FLOW EXPERIMENTAL DATA (1/2-INCH TUBE)

1	2	3	4	
Test No.	Water Temp. °F.	Water Rate ft^3/sec. at 60°F.	Pressure Drop Manometer Difference	
			cm. CCl_4 under H_2O	cm. Hg under H_2O
1	66	29.2 x 10^{-4}	21.40	
2	67	36.8 "	31.25	
3	68	42.0 "	39.20	
4	67	33.0 "	26.00	
5	65	48.0 "	50.55	
6	63	58.5 "	72.20	
7	62	63.0 "	83.85	
8	76	66.5 "		4.05
9	70	84.0 "		6.20
10	69	95.0 "		7.65
11	67	119 "		12.30
12	65	167 "		22.35
13	64	222 "		37.15
14	64	263 "		50.45
15	64	317 "		70.30

TABLE VI. SINGLE-PHASE AIR FLOW EXPERIMENTAL DATA

1	2	3	4	5	6	
Test No.	Test Section	Mid-Point Pressure p.s.i.a.	Air Rate $ft^3/sec.$ at 14.4 p.s.i.a. and 60°F.	Air Temp. °R.	Pressure Drop Manometer Difference	
					cm. H_2O under air	cm. Hg under air
307	1/2 in.	36	.128	525	8.80	
308	"	36	.153	525	13.1	
309	"	36	.187	525	16.8	
310	"	36	.221	525	22.5	
311	"	36	.332	525	46.0	
312	"	36	.482	525	87.3	
313	"	36	.599	525		9.35
314	"	36	.780	525		14.45
315	"	36	.920	525		19.00
316	"	36	.157	525	11.9	
317	"	36	.217	525	22.0	
318	"	36	.274	525	31.8	
319	"	36	.350	525	45.5	
320	"	36	.409	525	59.5	
327	"	18	.0930	525	8.80	
328	"	18	.114	525	13.75	
329	"	18	.142	525	18.75	
330	"	18	.173	525	24.3	
331	"	18	.109	524	13.95	
332	"	18	.163	524	25.9	
333	"	18	.219	524	40.2	
334	"	18	.282	524	59.1	
335	"	18	.329	524	75.0	
336	"	18	.244	524	52.65	
337	"	18	.360	525		7.4
338	"	18	.514	525		13.6
343	1 in.	36	.733	527	16.7	
344	"	36	.622	530	12.8	
345	"	18	.530	531	9.05	
412	"	18	.476	527	14.3	
413	"	18	.647	527	23.6	

TABLE VII. TWO-PHASE FLOW EXPERIMENTAL DATA

1	2	3		4	5	6	7	8
Test No.	Test Section	Water Rate		Mid-Point Pressure p.s.i.a.	Air Rate $ft.^3/sec.$ at 14.4 p.s.i.a. and 60°F.	Measured Pressure Drop Cm. Hg under air	Volume Air Between Plug Valves ml.	Volume H_2O Between Plug Valves ml.
		$ft.^3/sec.$	$lbs./ft.^2sec.$					
157	1/2 in.	.000149	4.17	18	.00491	10.4	1425	525
158	"	.000149	4.17	18	.00766	6.8	1530	420
159	"	.000149	4.17	18	.0189	7.7	1585	365
160	"	.000149	4.17	18	.0105	6.0	1575	375
161	"	.000149	4.17	18	.0125	6.2	1590	360
162	"	.000149	4.17	18	.0148	6.4	1595	355
163	"	.000149	4.17	18	.0172	7.0	1570	380
164	"	.000149	4.17	18	.0287	8.5	1585	365
165	"	.000149	4.17	18	.0424	8.0	1645	305
166	"	.000149	4.17	18	.0347	8.2	1615	335
167	"	.000149	4.17	18	.0503	7.0	1700	250
168	"	.000149	4.17	18	.0581	5.8	1720	230
169	"	.000149	4.17	18	.0693	4.95	1760	190
170	"	.000149	4.17	18	.0810	4.75	1810	140
171	"	.000149	4.17	18	.0601	7.1	1690	260
172	"	.000149	4.17	18	.0882	5.1	1795	155
173	"	.000149	4.17	18	.1095	4.5	1830	120
174	"	.000149	4.17	18	.133	4.75	1845	105
175	"	.000149	4.17	18	.159	5.1	1860	90
176	"	.000149	4.17	18	.180	5.8	1875	75
177	"	.000149	4.17	18	.106	4.75	1840	110
178	"	.000149	4.17	18	.170	5.9	1890	60
179	"	.000149	4.17	18	.214	7.9	1895	55
180	"	.000149	4.17	18	.258	8.96	1900	50
181	"	.000149	4.17	18	.298	10.95	1920	30
182	"	.000149	4.17	18	.334	13.05	1910	40
183	"	.000149	4.17	18	.258	9.5	1920	30

TABLE VII (Continued)

207	1/2 in.	.000149	4.17	36	.0264	6.4	1585	365
208	"	.000149	4.17	36	.0378	9.3	1510	440
209	"	.000149	4.17	36	.0468	10.0	1525	425
210	"	.000149	4.17	36	.0576	9.3	1570	380
211	"	.000149	4.17	36	.0732	8.35	1640	310
212	"	.000149	4.17	36	.0871	6.85	1670	380
213	"	.000149	4.17	36	.102	5.8	1725	225
214	"	.000149	4.17	36	.0815	7.75	1650	300
215	"	.000149	4.17	36	.122	5.4	1770	180
216	"	.000149	4.17	36	.151	4.85	1820	130
217	"	.000149	4.17	36	.184	4.7	1825	125
218	"	.000149	4.17	36	.219	5.15	1860	90
219	"	.000149	4.17	36	.149	4.6	1810	140
220	"	.000149	4.17	36	.213	5.3	1860	90
221	"	.000149	4.17	36	.271	6.4	1890	60
224	"	.000149	4.17	36	.318	7.9	1890	60
229	"	.000149	4.17	36	.0103	9.35	1440	510
230	"	.000149	4.17	36	.0142	7.1	1530	420
231	"	.000149	4.17	36	.0190	6.2	1580	370
232	"	.000149	4.17	36	.0239	6.0	1570	380
185	1/2 in.	.000290	8.10	18	.0050	11.2	1355	595
186	"	.000290	8.10	18	.00753	8.3	1520	430
187	"	.000290	8.10	18	.0107	6.6	1550	400
188	"	.000290	8.10	18	.0133	6.85	1560	390
189	"	.000290	8.10	18	.0161	6.6	1570	380
190	"	.000290	8.10	18	.0170	6.8	1550	400
191	"	.000290	8.10	18	.0291	10.4	1550	400
192	"	.000290	8.10	18	.0438	9.3	1580	370
193	"	.000290	8.10	18	.0566	8.5	1645	305
194	"	.000290	8.10	18	.0494	9.0	1615	335
195	"	.000290	8.10	18	.0717	7.6	1685	265
196	"	.000290	8.10	18	.0855	7.2	1735	215
197	"	.000290	8.10	18	.0611	7.6	1695	255
198	"	.000290	8.10	18	.0900	6.1	1780	170
199	"	.000290	8.10	18	.114	6.25	1810	140

TABLE VII (Continued)

200	1/2 in.	.000290	8.10	18	.146	8.0	1835	115
201	"	.000290	8.10	18	.182	9.9	1830	120
202	"	.000290	8.10	18	.118	7.2	1810	140
202	"	.000290	8.10	18	.168	6.8	1840	110
204	"	.000290	8.10	18	.225	9.9	1880	70
205	"	.000290	8.10	18	.269	13.7	1885	65
206	"	.000290	8.10	18	.374	18.9	1900	50
233	1/2 in.	.000290	8.10	36	.0102	10.4	1395	555
234	"	.000290	8.10	36	.0152	8.1	1515	435
235	"	.000290	8.10	36	.0193	7.0	1545	405
236	"	.000290	8.10	36	.0221	6.4	1560	390
237	"	.000290	8.10	36	.0392	9.35	1535	415
238	"	.000290	8.10	36	.0580	10.4	1530	420
239	"	.000290	8.10	36	.0721	9.6	1570	380
240	"	.000290	8.10	36	.0865	8.9	1620	330
241	"	.000290	8.10	36	.104	7.45	1675	275
242	"	.000290	8.10	36	.0808	8.9	1630	320
243	"	.000290	8.10	36	.117	7.15	1735	215
244	"	.000290	8.10	36	.149	6.7	1790	160
245	"	.000290	8.10	36	.183	7.05	1830	120
246	"	.000290	8.10	36	.219	7.35	1840	110
247	"	0000290	8.10	36	.159	6.7	1780	170
248	"	.000290	8.10	36	.216	7.55	1830	120
249	"	.000290	8.10	36	.296	10.6	1870	80
250	"	.000290	8.10	36	.352	12.5	1890	60
251	"	.000290	8.10	36	.423	15.15	1900	50
252	"	.000290	8.10	36	.332	12.5	1880	70
115	1/2 in.	.00063	17.6.	18	.00474	14.7	1280	670
116	"	.00063	17.6	18	.00760	10.9	1450	500
117	"	.00063	17.6	18	.00997	8.8	1490	460
118	"	.00063	17.6	18	.0132	8.0	1520	430
119	"	.00063	17.6	18	.0160	8.3	1535	415
120	"	.00063	17.6	18	.0195	8.9	1540	410

TABLE VII (Continued)

121	1/2 in.	.000630	17.6	18	.0216	10.1	1535	415
122	"	.00063	17.6	18	.0282	11.9	1540	410
123	"	.00063	17.6	18	.0436	11.2	1560	390
124	"	.00063	17.6	18	.0544	10.9	1600	350
125	"	.00063	17.6	18	.0701	10.2	1650	300
126	"	.00063	17.6	18	.0896	9.7	1705	245
127	"	.00063	17.6	18	.0481	12.0	1555	395
128	"	.00063	17.6	18	.0596	10.3	1625	325
129	"	.00063	17.6	18	.0946	10.0	1735	215
130	"	.00063	17.6	18	.110	10.2	1755	195
131	"	.00063	17.6	18	.140	7.6	1780	170
132	"	.00063	17.6	18	.160	12.4	1820	130
133	"	.00063	17.6	18	.176	14.0	1810	140
134	"	.00063	17.6	18	.206	15.8	1840	110
135	"	.00063	17.6	18	.111	10.5	1765	185
136	"	.00063	17.6	18	.175	14.9	1825	125
137	"	.00063	17.6	18	.224	18.9	1840	110
257	1/2 in.	.00063	17.6	36	.0400	10.8	1505	445
258	"	.00063	17.6	36	.0568	12.9	1465	485
259	"	.00063	17.6	36	.0718	12.9	1525	425
260	"	.00063	17.6	36	.0886	11.5	1565	385
261	"	.00063	17.6	36	.109	10.95	1610	340
262	"	.00063	17.6	36	.0849	11.15	1590	360
263	"	.00063	17.6	36	.118	10.7	1670	280
264	"	.00063	17.6	36	.162	11.2	1745	205
265	"	.00063	17.6	36	.188	11.7	1760	190
266	"	.00063	17.6	36	.221	13.7	1790	160
267	"	.00063	17.6	36	.155	10.9	1740	210
268	"	.00063	17.6	36	.232	13.75	1810	140
276	"	.00063	17.6	36	.0105	13.15	1335	615
277	"	.00063	17.6	36	.0146	11.15	1435	515
278	"	.00063	17.6	36	.0199	9.35	1470	480
279	"	.00063	17.6	36	.0263	9.05	1530	420

TABLE VII (Continued)

140	1/2 in .	.00183	51.0	18	.0099	16.1	1305	645
141	"	.00183	51.0	18	.0118	15.3	1355	595
142	"	.00183	51.0	18	.0144	14.7	1420	530
143	"	.00183	51.0	18	.0160	14.5	1420	530
144	"	.00183	51.0	18	.0193	14.5	1435	515
145	"	.00183	51.0	18	.0080	17.5	1245	705
146	"	.00183	51.0	18	.0271	16.4	1455	495
147	"	.00183	51.0	18	.0439	17.9	1515	435
148	"	.00183	51.0	18	.0561	18.4	1540	410
149	"	.00183	51.0	18	.0663	18.9	1560	390
150	"	.00183	51.0	18	.0789	19.9	1580	370
151	"	.00183	51.0	18	.138	26.0	1710	240
152	"	.00183	51.0	18	.121	23.7	1655	295
153	"	.00183	51.0	18	.0617	19.0	1525	425
154	"	.00183	51.0	18	.0927	21.0	1600	350
155	"	.00183	51.0	18	.130	24.6	1685	265
280	1/2 in.	.00183	51.0	36	.0113	21.1	1100	850
281	"	.00183	51.0	36	.0152	17.8	1235	715
282	"	.00183	51.0	36	.0219	15.35	1325	625
283	"	.00183	51.0	36	.0406	15.3	1425	525
284	"	.00183	51.0	36	.0595	16.8	1435	515
285	"	.00183	51.0	36	.0724	18.45	1425	525
286	"	.00183	51.0	36	.0865	19.0	1465	485
287	"	.00183	51.0	36	.105	19.2	1500	450
288	"	.00183	51.0	36	.0830	19.0	1425	525
289	"	.00183	51.0	36	.121	19.9	1595	355
290	"	.00183	51.0	36	.156	21.7	1620	330
27	1 in.	.00040	4.15	18	.00930	16.2	3340	2000
28	"	.00040	4.15	18	.0246	7.5	4120	1220
29	"	.00040	4.15	18	.0221	8.1	4170	1170
30	"	.00040	4.15	18	.0369	6.8	4270	1070
31	"	.00040	4.15	18	.0473	8.5	4260	1080
32	"	.00040	4.15	18	.0440	7.7	4200	1140
33	"	.00040	4.15	18	.0578	10.3	4120	1220

TABLE VII (Continued)

34	1 in.	.00040	4.15	18	.0529	9.8	4080	1260
35	"	.00040	4.15	18	.0678	10.1	4180	1160
36	"	.00040	4.15	18	.0851	10.0	4250	1090
37	"	.00040	4.15	18	.108	9.5	4320	1020
38	"	.00040	4.15	18	.129	8.7	4410	930
39	"	.00040	4.15	18	.162	7.7	4500	840
40	"	.00040	4.15	18	.168	6.5	4610	730
41	"	.00040	4.15	18	.103	8.8	4320	1020
42	"	.00040	4.15	18	.206	5.4	4760	580
43	"	.00040	4.15	18	.247	4.4	4890	450
44	"	.00040	4.15	18	.247	4.8	4880	460
45	"	.00040	4.15	18	.322	3.7	4990	350
46	"	.00040	4.15	18	.133	8.7	4410	930
47	"	.00040	4.15	18	.0580	9.8	4170	1170
48	"	.00040	4.15	18	.0171	11.5	3940	1400
395	1 in.	.00040	4.15	36	.0198	15.1	3380	1960
396	"	.00040	4.15	36	.0382	10.3	4040	1300
397	"	.00040	4.15	36	.0718	9.05	4100	1240
398	"	.00040	4.15	36	.101	10.0	4140	1200
399	"	.00040	4.15	36	.0873	9.3	4130	1210
400	"	.00040	4.15	36	.154	10.2	4230	1110
401	"	.00040	4.15	36	.202	8.85	4410	930
402	"	.00040	4.15	36	.337	5.6	4830	510
405	"	.00040	4.15	36	.163	10.35	4240	1100
406	"	.00040	4.15	36	.279	7.1	4680	660
51	1 in.	.00077	8.00	18	.0112	16.9	3140	2200
52	"	.00077	8.00	18	.0147	13.6	3540	1800
53	"	.00077	8.00	18	.0196	10.7	3870	1470
54	"	.00077	8.00	18	.0289	8.2	4080	1260
55	"	.00077	8.00	18	.0417	7.5	4150	1190
56	"	.00077	8.00	18	.0526	8.6	4100	1240
57	"	.00077	8.00	18	.0630	9.6	4050	1290
58	"	.00077	8.00	18	.0746	10.1	4240	1100

TABLE VII (Continued)

59	1 in.	.00077	8.00	18	.0833	10.8	4160	1180
60	"	.00077	8.00	18	.0616	10.2	4160	1180
61	"	.00077	8.00	18	.0869	10.7	4180	1160
62	"	.00077	8.00	18	.111	10.1	4290	1050
63	"	.00077	8.00	18	.132	9.2	4310	1030
64	"	.00077	8.00	18	.153	8.4	4410	930
65	"	.00077	8.00	18	.173	7.9	4520	820
66	"	.00077	8.00	18	.112	9.8	4290	1050
67	"	.00077	8.00	18	.162	7.7	4540	800
68	"	.00077	8.00	18	.204	6.5	4700	640
69	"	.00077	8.00	18	.270	5.4	4860	480
70	"	.00077	8.00	18	.240	5.6	4780	560
71	"	.00077	8.00	18	.300	5.4	4910	430
72	"	.00077	8.00	18	.385	5.4	5010	330
351	1 in.	.00077	8.00	36	0.164	10.65	4170	1170
352	"	.00077	8.00	36	.274	7.3	4550	790
353	"	.00077	8.00	36	.378	5.7	4790	550
354	"	.00077	8.00	36	.316	6.4	4680	660
355	"	.00077	8.00	36	.587	5.65	5020	320
357	"	.00077	8.00	36	.0788	8.2	4170	1170
359	"	.00077	8.00	36	.196	10.1	4270	1070
360	"	.00077	8.00	36	.148	11.2	4120	1220
361	"	.00077	8.00	36	.0412	9.3	3970	1370
362	"	.00077	8.00	36	.0702	7.4	4260	1080
363	"	.00077	8.00	36	.0924	8.2	4050	1290
365	"	.00077	8.00	36	.0241	14.3	3600	1740
74	1 in.	.00172	17.9	18	.00870	21.1	2930	2410
75	"	.00172	17.9	18	.0117	18.0	3240	2100
76	"	.00172	17.9	18	.0184	12.0	3830	1510
77	"	.00172	17.9	18	.0282	10.1	4000	1340
78	"	.00172	17.9	18	.0460	9.2	4120	1220
79	"	.00172	17.9	18	.0574	11.8	4140	1200
80	"	.00172	17.9	18	.0662	12.4	4010	1330
81	"	.00172	17.9	18	.0808	12.6	4060	1280

TABLE VII (Continued)

82	1 in.	.00172	17.9	18	.0595	10.3	4060	1280
83	"	.00172	17.9	18	.0878	12.2	4090	1250
84	"	.00172	17.9	18	.110	12.0	4170	1170
85	"	.00172	17.9	18	.135	11.3	4210	1130
86	"	.00172	17.9	18	.153	10.5	4300	1040
87	"	.00172	17.9	18	.175	10.1	4370	970
88	"	.00172	17.9	18	.110	11.5	4190	1150
89	"	.00172	17.9	18	.165	10.1	4410	930
90	"	.00172	17.9	18	.207	8.9	4540	800
91	"	.00172	17.9	18	.272	8.6	4710	630
92	"	.00172	17.9	18	.242	8.6	4650	690
93	"	.00172	17.9	18	.322	3.4	4820	520
94	"	.00172	17.9	18	.392	8.6	4900	440
367	1 in.	.00172	17.9	36	.0247	16.0	3390	1950
368	"	.00172	17.9	36	.0412	11.7	3750	1590
369	"	.00172	17.9	36	.0722	7.7	4100	1240
370	"	.00172	17.9	36	.0925	9.2	4200	1140
371	"	.00172	17.9	36	.0833	8.2	4040	1300
372	"	.00172	17.9	36	.151	13.15	3950	1390
373	"	.00172	17.9	36	.198	11.85	4190	1150
374	"	.00172	17.9	36	.333	9.05	4530	810
375	"	.00172	17.9	36	.584	8.75	4890	450
377	"	.00172	17.9	36	.153	13.15	4000	1340
378	"	.00172	17.9	36	.277	9.55	4440	900
379	"	.00172	17.9	36	.368	8.45	4600	740
95	1 in.	.0050	51.9	18	.0107	25.6	2600	2740
96	"	.0050	51.9	18	.0164	19.9	3170	2170
97	"	.0050	51.9	18	.0240	15.8	3540	1800
98	"	.0050	51.9	18	.0343	13.5	3760	1580
99	"	.0050	51.9	18	.0439	13.3	3850	1490
100	"	.0050	51.9	18	.0536	13.7	3980	1360
101	"	.0050	51.9	18	.0610	14.3	3970	1370
102	"	.0050	51.9	18	.0649	14.2	3630	1710

TABLE VII (Continued)

103	1 in.	.0050	51.9	18	.0739	14.7	4020	1320
104	"	.0050	51.9	18	.0610	13.7	3760	1580
105	"	.0050	51.9	18	.0771	14.9	3930	1410
106	"	.0050	51.9	18	.0974	16.0	3980	1360
107	"	.0050	51.9	18	.113	15.8	4030	1310
108	"	.0050	51.9	18	.136	15.8	4020	1320
109	"	.0050	51.9	18	.176	15.3	4190	1150
110	"	.0050	51.9	18	.162	15.1	4200	1140
111	"	.0050	51.9	18	.215	14.5	4330	1010
112	"	.0050	51.9	18	.262	14.7	4420	920
113	"	.0050	51.9	18	.248	14.7	4420	920
114	"	.0050	51.9	18	.363	16.5	4570	770
380	1 in.	.0050	51.9	36	.155	16.0	3740	1600
381	"	.0050	51.9	36	.293	14.9	4190	1150
382	"	.0050	51.9	36	.396	15.1	4340	1000
383	"	.0050	51.9	36	.331	15.2	4300	1040
386	"	.0050	51.9	36	.0802	13.2	3800	1540
387	"	.0050	51.9	36	.149	17.0	3700	1640
388	"	.0050	51.9	36	.205	16.55	3940	1400
389	"	.0050	51.9	36	.0400	17.8	3450	1890
390	"	.0050	51.9	36	.0723	14.0	3710	1630
391	"	.0050	51.9	36	.0970	12.9	3910	1430
392	"	.0050	51.9	36	.0204	25.6	2570	2770

TABLE VIII. EXPERIMENTAL DATA - EFFECT OF LIQUID PHASE SURFACE TENSION* (1-INCH TUBE)

Constant Water Rate
= 0.00040 ft^3/sec.
= 4.15 lbs./ft^2 sec.

Constant Mid-Point Pressure = 18 p.s.i.a.

1	2	3
Test No.	Air Rate ft^3/sec. at 14.4 p.s.i.a. and 60°F.	Measured Pressure Drop cm. Hg under air
417	.0557	7.0
419	.0376	6.6
421	.0231	7.3
424	.166	6.5
426	.220	4.6

---

* A detergant (Tergitol Penetrant No. 4) added to the water such that its concentration is 1:10,000. The surface tension of the resulting liquid phase is 0.80 compared to water equal to 1.

APPENDIX C

CALCULATED DATA

TABLE IX. SINGLE-PHASE WATER FLOW CALCULATED RESULTS (1/2-INCH TUBE)

1	2	3	4	5
Test No.	Water Velocity V ft./sec.	Pressure Drop F ft. of H_2O	Reynolds* numbers	Friction** Factor
1	1.31	.416	6280	.00916
2	1.65	.608	8000	.00843
3	1.88	.763	9200	.00814
4	1.48	.516	7160	.00888
5	2.15	.983	10100	.00801
6	2.62	1.40	12000	.00772
7	2.82	1.63	12800	.00772
8	2.98	1.67	16200	.00710
9	3.72	2.56	18900	.00697
10	4.26	3.15	21200	.00654
11	5.33	5.07	25800	.00674
12	7.48	9.22	35300	.00622
13	9.95	15.3	46500	.00583
14	11.8	20.8	55200	.00563
15	14.2	29.0	66400	.00542

* $\frac{DV\rho}{\mu}$

** $\frac{\beta FD}{2V^2N}$

[illegible]

[illegible]	[illegible]	[illegible]	[illegible]
[illegible]	[illegible]	[illegible]	[illegible]
[illegible]	[illegible]	[illegible]	[illegible]
[illegible]	[illegible]	[illegible]	[illegible]
[illegible]	[illegible]	[illegible]	[illegible]
[illegible]	[illegible]	[illegible]	[illegible]
[illegible]	[illegible]	[illegible]	[illegible]
[illegible]	[illegible]	[illegible]	[illegible]
[illegible]	[illegible]	[illegible]	[illegible]
[illegible]	[illegible]	[illegible]	[illegible]
[illegible]	[illegible]	[illegible]	[illegible]
[illegible]	[illegible]	[illegible]	[illegible]
[illegible]	[illegible]	[illegible]	[illegible]
[illegible]	[illegible]	[illegible]	[illegible]
[illegible]	[illegible]	[illegible]	[illegible]
[illegible]	[illegible]	[illegible]	[illegible]

[illegible]

TABLE X. SINGLE-PHASE AIR FLOW CALCULATED RESULTS

1	2	3	4	5	6	7	8
Test No.	Test Section	Mid-Point Pressure p.s.i.a.	Air-Rate ft^3/sec. at flowing P & T	Air Velocity V ft./sec.	Pressure Drop ft. of air	Reynolds Number	Friction Factor
307	1/2 in.	36	.0517	23.2	97.2	19,500	.00681
308	"	36	.0619	27.7	145	23,200	.00712
309	"	36	.0755	33.8	186	28,400	.00614
310	"	36	.0893	40.0	249	33,500	.00587
311	"	36	.134	60.2	508	55,000	.00528
312	"	36	.195	87.4	964	73,200	.00476
313	"	36	.242	108	1400	90,900	.00449
314	"	36	.315	141	2160	119,000	.00408
315	"	36	.372	167	2840	140,000	.00386
316	"	36	.0633	28.4	131	23,800	.00617
317	"	36	.0874	39.2	243	32,900	.00596
318	"	36	.111	49.6	351	41,600	.00538
319	"	36	.141	63.4	503	53,100	.00472
320	"	36	.165	74.1	657	62,100	.00452
327	"	18	.0712	31.9	194	13,400	.00719
328	"	18	.0920	41.3	304	17,300	.00674
329	"	18	.115	51.5	414	21,500	.00590
330	"	18	.140	62.9	536	26,400	.00512
332	"	18	.0876	39.3	308	16,600	.00752
332	1/2 in.	18	.132	58.9	571	25,000	.00621
333	"	18	.177	79.2	887	33,500	.00533
334	"	18	.227	102	1300	43,200	.00473
335	"	18	.265	119	1650	50,400	.00440
336	"	18	.197	88.2	1160	37,400	.00562
337	"	18	.291	130	2220	54,700	.00492
338	"	18	.415	186	4070	78,000	.00444
343	1 in.	36	.298	49.6	185	67,300	.00462
344	"	36	.254	42.3	143	56,600	.00492
345	"	18	.216	36.1	101	48,300	.00473
412	"	18	.386	64.3	317	43,700	.00471
413	"	18	.525	87.5	523	59,400	.00420

TABLE XI. TWO-PHASE FLOW CALCULATED RESULTS

1	2	3	4	5	6	7	8
		Water Rate					
Test No.	Test Section	ft^3/sec.	lbs./ft^2 sec.	Mid-Point Pressure p.s.i.a.	Discharge Air-Water Ratio ft^3 s.c./ft^3	Measured Pressure Drop psi/100 ft.	Test Section Air-Water Ratio
157	1/2 in.	.000149	4.17	18	32.9	8.75	2.71
158	"	.000149	4.17	18.	51.5	5.75	3.64
159	"	.000149	4.17	18	127	6.5	4.34
160	"	.000149	4.17	18	70.7	5.1	4.20
161	"	.000149	4.17	18	84.1	5.25	4.42
162	"	.000149	4.17	18	99.1	5.4	4.49
163	"	.000149	4.17	18	115	5.9	4.13
164	"	.000149	4.17	18	192	7.2	4.34
165	"	.000149	4.18	18	284	6.8	5.39
166	"	.000149	4.18	18	233	6.95	4.82
167	"	.000149	4.18	18	337	5.9	6.80
168	"	.000149	4.18	18	390	4.9	7.48
169	"	.000149	4.17	18	465	4.2	9.26
170	"	.000149	4.17	18	543	4.0	12.9
171	"	.000149	4.17	18	403	6.0	6.50
172	"	.000149	4.17	18	592	4.3	11.6
173	"	.000149	4.17	18	735	3.8	15.3
174	"	.000149	4.17	18	905	4.0	17.6
175	"	.000149	4.17	18	1070	4.3	20.7
176	"	.000149	4.17	18	1210	4.9	25.0
177	"	.000149	4.17	18	708	4.0	16.7
178	"	.000149	4.17	18	1140	5.0	31.5
179	"	.000149	4.17	18	1440	6.7	34.5
180	"	.000149	4.17	18	1730	7.6	38.0
181	"	.000149	4.17	18	2000	9.2	64.0
182	"	.000149	4.17	18	2240	11.1	47.8
183	"	.000149	4.17	18	1730	8.05	64.0

TABLE XI -(Continued)

207	1/2 in.	.000149	4.17	36	177	5.4	4.34
208	"	.000149	4.17	36	254	7.9	3.43
209	"	.000149	4.17	36	314	8.45	3.59
210	"	.000149	4.17	36	386	7.9	4.13
211	"	.000149	4.17	36	491	7.1	5.29
212	"	.000149	4.17	36	585	5.8	5.96
213	"	.000149	4.17	36	685	4.9	7.67
214	"	.000149	4.17	36	547	6.55	5.50
215	"	.000149	4.17	36	816	4.6	9.83
216	"	.000149	4.17	36	1020	4.1	14.0
217	"	.000149	4.17	36	1230	4.0	14.6
218	"	.000149	4.17	36	1470	4.35	20.7
219	"	.000149	4.17	36	997	3.9	12.9
220	"	.000149	4.17	36	1430	4.5	20.7
221	"	.000149	4.17	36	1820	5.4	31.5
224	"	.000149	4.17	36	2130	6.7	31.5
229	"	.000149	4.17	36	68.7	7.9	2.24
230	"	.000149	4.17	36	95.3	6.0	3.64
231	"	.000149	4.17	36	127	5.24	4.27
232	"	.000149	4.17	36	160	5.07	4.13
185	1/2 in.	.000290	8.10	18	17.2	9.45	2.28
186	"	.000290	8.10	18	26.0	7.0	3.53
187	"	.000290	8.10	18	36.8	5.6	3.88
188	"	.000290	8.10	18	45.8	5.8	4.00
189	"	.000290	8.10	18	55.6	5.6	4.13
190	"	.000290	8.10	18	58.7	5.75	3.88
191	"	.000290	8.10	18	100	8.8	3.88
192	"	.000290	8.10	18	151	7.9	4.27
193	"	.000290	8.10	18	195	7.2	5.39
194	"	.000290	8.10	18	172	7.6	4.82
195	"	.000290	8.10	18	247	6.4	6.36
196	"	.000290	8.10	18	295	6.1	8.07
197	"	.000290	8.10	18	211	6.4	6.65
198	"	.000290	8.10	18	310	5.1	10.5
199	"	.000290	8.10	18	394	5.3	12.9

TABLE XI - (Continued)

200	1/2 in.	.000290	8.10	18	505	6.8	16.0
201	"	.000290	8.10	18	629	8.4	15.3
202	"	.000290	8.10	18	406	6.1	12.9
203	"	.000290	8.10	18	581	5.75	16.7
204	"	.000290	8.10	18	777	8.4	26.9
205	"	.000290	8.10	18	927	11.6	29.0
206	"	.000290	8.10	18	1280	16.0	38.0
233	1/2 in.	.000290	8.10	36	35.2	8.8	2.51
234	"	.000290	8.10	36	52.4	6.85	3.48
235	"	.000290	8.10	36	66.5	5.9	3.81
236	"	.000290	8.10	36	76.2	5.4	4.0
237	"	.000290	8.10	36	135	7.9	3.70
238	"	.000290	8.10	36	200	8.8	3.64
239	"	.000290	8.10	36	249	8.1	4.13
240	"	.000290	8.10	36	298	7.5	4.91
241	"	.000290	8.10	36	360	6.3	6.09
242	"	.000290	8.10	36	279	7.5	5.09
243	"	.000290	8.10	36	402	6.05	8.07
244	"	.000290	8.10	36	513	5.7	11.2
245	"	.000290	8.10	36	632	6.0	15.3
246	"	.000290	8.10	36	754	6.2	16.7
247	"	.000290	8.10	36	549	5.7	10.5
248	"	.000290	8.10	36	735	6.4	15.3
249	"	.000290	8.10	36	1020	9.0	23.3
250	"	.000290	8.10	36	1210	10.6	31.5
251	"	.000290	8.10	36	1460	12.8	38.0
252	"	.000290	8.10	36	1140	10.6	26.9
115	1/2 in.	.00063	17.6	18	7.52	12.4	1.91
116	"	.00063	17.6	18	12.1	9.2	2.9
117	"	.00063	17.6	18	15.8	7.45	3.24
118	"	.00063	17.6	18	20.9	6.8	3.53
119	"	.00063	17.6	18	25.4	7.0	3.70
120	"	.00063	17.6	18	30.9	7.5	3.76
121	"	.00063	17.6	18	34.4	8.55	3.70

TABLE XI - (Continued)

122	1/2 in.	.00063	17.6	18	44.8	10.1	3.76
123	"	.00063	17.6	18	69.3	9.5	4.00
124	"	.00063	17.6	18	86.3	9.2	4.57
125	"	.00063	17.6	18	111	8.6	5.50
126	"	.00063	17.6	18	142	8.2	6.96
127	"	.00063	17.6	18	76.3	10.2	3.94
128	"	.00063	17.6	18	94.8	8.7	5.00
129	"	.00063	17.6	18	150	8.5	8.07
130	"	.00063	17.6	18	175	8.6	9.00
131	"	.00063	17.6	18	222	9.8	10.50
132	"	.00063	17.6	18	255	10.5	14.0
133	"	.00063	17.6	18	280	11.9	12.90
134	"	.00063	17.6	18	327	13.4	16.7
135	"	.00063	17.6	18	176	8.9	9.54
136	"	.00063	17.6	18	278	12.6	14.6
137	"	.00063	17.6	18	355	16.0	16.7
257	1/2 in.	.00063	17.6	18	63.5	9.15	3.38
258	"	.00063	17.6	18	90.1	10.9	3.02
259	"	.00063	17.6	18	114	10.9	3.59
260	"	.00063	17.6	18	141	9.7	4.06
261	"	.00063	17.6	18	173	9.27	4.74
262	"	.00063	17.6	18	135	9.44	4.42
263	"	.00063	17.6	18	188	9.06	5.96
264	"	.00063	17.6	18	257	9.48	8.51
265	"	.00063	17.6	18	298	9.9	9.26
266	"	.00063	17.6	18	351	11.6	11.2
267	"	.00063	17.6	18	246	9.22	8.29
268	"	.00063	17.6	18	368	11.6	12.9
140	1/2 in.	.00183	51.0	18	5.41	13.6	2.02
141	"	.00183	51.0	18	6.46	13.0	2.28
142	"	.00183	51.0	18	7.85	12.4	2.68
143	"	.00183	18.0	18	8.77	12.3	2.68
144	"	.00183	51.0	18	10.5	12.3	2.79
145	"	.00183	51.0	18	4.38	14.8	1.77
146	"	.00183	51.0	18	14.8	13.9	2.94

TABLE XI - (Continued)

147	1/2 in.	.00183	51.0	18	24.0	15.2	3.48
148	"	.00183	51.0	18	30.7	15.6	3.76
149	"	.00183	51.0	18	36.2	16.0	4.00
150	"	.00183	51.0	18	42.6	16.8	4.27
151	"	.00183	51.0	18	75.5	22.0	7.13
152	"	.00183	51.0	18	66.0	20.1	5.61
153	"	.00183	51.0	18	33.7	16.1	3.59
154	"	.00183	51.0	18	50.7	17.8	4.57
155	"	.00183	51.0	18	70.9	20.8	6.36
280	1/2 in.	.00183	51.0	36	6.16	17.9	1.29
281	"	.00183	51.0	36	8.32	15.1	1.73
282	"	.00183	51.0	36	12.0	13.0	2.12
283	"	.00183	51.0	36	22.2	13.0	2.71
284	"	.00183	51.0	36	32.5	14.3	2.79
285	"	.00183	51.0	36	39.6	15.6	2.71
286	"	.00183	51.0	36	47.3	16.1	3.02
287	"	.00183	51.0	36	57.5	16.3	3.33
288	"	.00183	51.0	36	45.4	16.1	2.71
289	"	.00183	51.0	36	66.2	16.8	4.49
290	"	.00183	51.0	36	85.2	18.4	4.91
296	"	.00183	51.0	36	87.4	18.5	4.74
27	1 in.	.00040	4.15	18	23.2	13.6	1.67
28	"	.00040	4.15	18	61.6	6.3	3.38
29	"	.00040	41.5	18	55.2	6.8	3.56
30	"	.00040	92.	18	92.2	5.7	3.99
31	"	.00040	41.5	18	118	7.15	3.94
32	"	.00040	41.5	18	110	6.5	3.68
33	"	.00040	41.5	18	145	8.7	3.38
34	"	.00040	41.5	18	132	8.25	3.24
35	"	.00040	41.5	18	170	8.5	3.60
36	"	.00040	41.5	18	213	8.4	3.90
37	"	.00040	41.5	18	271	8.0	4.24
38	"	.00040	41.5	18	322	7.3	4.74
39	"	.00040	41.5	18	405	6.5	5.36
40	"	.00040	41.5	18	420	55.5	6.32

TABLE XI - (Continued)

41	1 in.	.00040	4.15	18	258	7.4	4.24
42	"	.00040	4.15	18	515	4.55	8.21
43	"	.00040	4.15	18	617	3.7	10.9
44	"	.00040	4.15	18	617	4.0	10.6
45	"	.00040	4.15	18	805	3.1	14.3
46	"	.00040	4.15	18	333	7.3	4.74
47	"	.00040	4.15	18	145	8.25	3.56
48	"	.00040	4.15	18	427	9.7	2.81
395	1 in.	.00040	4.15	36	49.5	12.7	1.73
396	"	.00040	4.15	36	95.4	8.7	3.11
397	"	.00040	4.15	36	180	7.6	3.30
398	"	.00040	4.15	36	251	8.4	3.45
399	"	.00040	4.15	36	218	7.8	3.41
400	"	.00040	4.15	36	385	8.6	3.81
401	"	.00040	4.15	36	503	7.5	4.74
402	"	.00040	4.15	36	841	4.7	9.47
405	"	.00040	4.15	36	406	8.7	3.86
406	"	.00040	4.15	36	699	6.0	7.10
51	1 in.	.00077	8.00	18	14.5	14.2	1.43
52	"	.00077	8.00	18	19.1	11.4	1.97
53	"	.00077	8.00	18	25.4	9.0	2.63
54	"	.00077	8.00	18	37.5	6.9	3.24
55	"	.00077	8.00	18	53.1	6.3	3.49
56	"	.00077	8.00	18	68.3	7.2	3.31
57	"	.00077	8.00	18	81.8	8.1	3.14
58	"	.00077	8.00	18	97.0	8.5	3.85
59	"	.00077	8.00	18	108	9.1	3.53
60	"	.00077	8.00	18	80.0	8.6	3.53
61	"	.00077	8.00	18	113	9.0	3.60
62	"	.00077	8.00	18	144	8.5	4.09
63	"	.00077	8.00	18	171	7.75	4.18
64	"	.00077	8.00	18	199	7.1	4.74
65	"	.00077	8.00	18	225	6.65	5.51
66	"	.00077	8.00	18	145	8.25	4.09

TABLE XI - (Continued)

67	1 in	.00077	8.00	18	210	6.5	5.68
68	"	.00077	8.00	18	266	5.5	7.34
69	"	.00077	8.00	18	351	4.55	10.1
70	"	.00077	8.00	18	312	4.7	8.54
71	"	.00077	8.00	18	390	4.55	11.4
72	"	.00077	8.00	18	500	4.55	15.2
351	1 in.	.00077	8.00	36	212	9.0	3.56
352	"	.00077	8.00	36	356	6.14	5.76
353	"	.00077	8.00	36	491	4.8	8.71
354	"	.00077	8.00	36	410	5.4	7.10
355	"	.00077	8.00	36	763	4.75	15.7
357	"	.00077	8.00	36	102	6.9	3.56
359	"	.00077	8.00	36	355	8.5	4.00
360	"	.00077	8.00	36	192	9.4	3.38
361	"	.00077	8.00	36	53.6	7.8	2.90
362	"	.00077	8.00	36	91.2	6.2	3.95
363	"	.00077	8.00	36	120	6.9	3.14
365	"	.00077	8.00	36	31.3	12.0	2.07
74	1 in.	.00172	17.9	18	5.05	17.8	1.22
75	"	.00172	17.9	18	6.8	15.1	1.54
76	"	.00172	17.9	18	10.7	10.1	2.54
77	"	.00172	17.9	18	16.4	8.5	2.99
78	"	.00172	17.9	18	26.8	7.75	3.38
79	"	.00172	17.9	18	33.4	9.9	3.45
80	"	.00172	17.9	18	38.5	10.4	3.02
81	"	.00172	17.9	18	47.0	10.6	3.17
82	"	.00172	17.9	18	34.6	8.7	3.17
83	"	.00172	17.9	18	51.5	10.3	3.27
84	"	.00172	17.9	18	64.0	10.1	3.56
85	"	.00172	17.9	18	78.5	9.5	3.73
86	"	.00172	17.9	18	88.9	8.8	4.13
87	"	.00172	17.9	18	102	8.5	4.51
88	"	.00172	17.9	18	64.0	9.7	3.64
89	"	.00172	17.9	18	95.7	8.5	4.74
90	"	.00172	17.9	18	120	7.5	5.68

TABLE XI - (Continued)

91	1 in.	.00172.	17.9	18	158	7.2	7.48
92	"	.00172	17.9	18	141	7.2	6.74
93	"	.00172	17.9	18	187	7.1	9.27
94	"	.00172	17.9	18	228	7.2	11.1
367	1 in.	.00172	17.9	36	14.4	13.5	1.74
368	"	.00172	17.9	36	23.9	9.85	2.36
369	"	.00172	17.9	36	42.0	6.5	3.30
370	"	.00172	17.9	36	53.7	7.7	3.68
371	"	.00172	17.9	36	48.4	6.9	3.11
372	"	.00172	17.9	36	88.0	11.1	2.84
373	"	.00172	17.9	36	115	10.0	3.65
374	"	.00172	17.9	36	193	7.6	5.60
375	"	.00172	17.9	36	340	7.4	10.9
377	"	.00172	17.9	36	88.7	11.1	2.98
378	"	.00172	17.9	36	161	8.0	4.93
379	"	.00172	17.9	36	214	7.1	6.22
95	1 in.	.0050	51.9	18	2.14	21.6	0.95
96	"	.0050	51.9	18	3.28	16.7	1.46
97	"	.0050	51.9	18	4.80	13.3	1.97
98	"	.0050	51.9	18	6.87	11.4	2.38
99	"	.0050	51.9	18	8.78	11.2	2.58
100	"	.0050	51.9	18	10.7	11.5	2.93
101	"	.0050	51.9	18	12.2	12.0	2.90
102	"	.0050	51.9	18	13.0	11.9	2.12
103	"	.0050	51.9	18	14.8	12.4	3.05
104	"	.0050	51.9	18	12.2	11.5	2.38
105	"	.0050	51.9	18	15.4	12.5	2.79
106	"	.0050	51.9	18	19.5	13.5	2.93
107	"	.0050	51.9	18	22.6	13.3	3.08
108	"	.0050	51.9	18	27.2	13.3	3.05
109	"	.0050	51.9	18	35.2	12.9	3.64
110	"	.0050	51.9	18	32.4	12.7	3.68
111	"	.0050	51.9	18	43.0	12.2	4.29
112	"	.0050	51.9	18	52.4	12.4	4.80
113	"	.0050	51.9	18	49.6	12.4	4.80

TABLE XI - (Continued)

114	1 in.	.0050	51.9	18	72.7	13.9	5.94
380	1 in.	.0050	51.9	36	31	13.5	2.32
381	"	.0050	51.9	36	58.5	12.5	3.65
382	"	.0050	51.9	36	79.2	12.7	4.34
383	"	.0050	51.9	36	66.1	12.8	4.13
386	"	.0050	51.9	36	16.0	11.1	2.47
387	"	.0050	51.9	36	29.8	14.3	2.26
388	"	.0050	51.9	36	4.09	13.9	2.81
389	"	.0050	51.9	36	8.0	15.0	1.83
390	"	.0050	51.9	36	14.5	11.8	2.28
391	"	.0050	51.9	36	19.4	10.9	2.74
392	"	.0050	51.9	36	4.1	21.6	0.93

TABLE XII. VARIATION OF MAXIMUM AND MINIMUM POINTS WITH WATER RATE

1	2	3	4	5	6	7	8	9
			First Minimum		Maximum		Second Minimum	
Test Section	Mid-Point Pressure p.s.i.a.	Water Rate lbs/ft^2 sec.	Pressure Drop psi/100 ft.	Air-Water Discharge Ratio ft^3 s.c./ft^3	Pressure Drop psi/100 ft.	Air-Water Discharge Ratio ft^3 s.c./ft^3	Pressure Drop psi/100 ft.	Air-Water Discharge Ratio. ft^3 s.c./ft^3
1 inch	18	4.15	5.7	88	8.8	170	---	---
"	18	8.00	6.3	55	9.1	110	4.5	420
"	18	17.9	7.7	26	10.6	48	7.1	168
"	18	51.9	11.2	9	13.5	21	12.2	45
"	36	4.15	6.5	150	9.5	300	---	---
"	36	8.00	6.2	90	9.4	180	4.6	620
"	36	17.9	6.5	42	11.1	82	6.9	260
"	36	51.0	10.8	19	14.2	35	12.4	63
1/2 in.	18	4.17	5.1	85	7.2	200	3.9	750
"	18	8.10	5.6	50	8.8	100	5.5	340
"	18	17.6	6.8	23	10.1	50	8.25	140
"	18	51.0	12.3	10	---	---	----	---
"	36	4.17	5.1	150	8.5	315	3.9	1075
" "	36	8.10	5.4	90	8.8	190	5.65	510
"	36	17.6	7.65	42	10.9	95	8.95	205
"	36	51.0	12.6	16	---	---	----	---

TABLE XIII. CALCULATED RESULTS - EFFECT OF LIQUID PHASE SURFACE TENSION* (1-INCH TUBE)

Constant Water Rate
0.00040 $ft^3/sec.$
= 4.15 $lbs./ft^2$ sec.

Constant Mid-Point
Pressure - 18 p.s.i.a.

1	2	3
Test No.	Discharge Air - H_2O Ratio ft^3 s.c./ft^3	Measured Pressure Drop psi/100 ft.
417	139	5.90
419	94.0	5.54
421	57.8	6.10
424	415	5.50
426	550	3.90

* A detergent (Tergitol Penetrant No. 4) added to the water such that its concentration is 1:10,000.

TABLE XIV. HYDROSTATIC HEAD AND IRREVERSIBILITY COMPONENTS OF PRESSURE DROP

1	2	3	4
Discharge Air-Water Ratio ft^3 s.c./ft^3	Measured Pressure Drop p.s.i./100 ft.	Hydrostatic Head Component p.s.i./100 ft.	Irreversibility Component p.s.i./100 ft.
30	11.7	1.76	9.9
60	6.55	.94	5.6
85	5.7	.67	5.0
120	7.3	.50	6.8
170	8.75	.37	8.4
240	8.2	.29	7.9
480	5.1	.17	4.9
805	3.1	.13	3.0

TABLE XV. FRICTION FACTOR - REYNOLDS NUMBER RESULTS

1	2	3	4	5	6	7	8	9	10
Test Section	Water Rate lbs./ft^3 sec.	Mid-Point Pressure PSIA	Pressure Drop PSI/100ft.	Discharge Air-Water Ratio Ft^3 S.C./Ft^3	Saturated Gas Rate G lbs./sec.	ΣF_L	ΣF_G	f_G	Re_G
1/2 in.	4.17	18	5.75	52	.000584	466	7420	8.05	1155
"	4.17	18	5.1	85	.000956	714	6950	2.81	1890
"	4.17	18	6.5	127	.00143	1440	9400	1.70	2830
"	4.17	18	7.2	200	.00225	2590	10700	.779	4450
"	4.17	18	5.2	400	.00450	3760	7770	.142	8900
"	4.17	18	3.9	800	.00900	5650	5840	.0266	17800
"	4.17	18	7.0	1600	.0180	20700	10700	.0121	35600
"	4.17	18	9.3	2000	.0225	34400	14200	.0104	44500
1/2 in.	8.10	18	9.0	20	.000438	255	10500	20.2	867
"	8.10	18	5.7	40	.000876	335	6920	3.37	1730
"	8.10	18	5.65	48	.00105	414	7140	2.40	2080
"	8.10	18	6.8	70	.00153	798	9430	1.48	3030
"	8.10	18	8.0	80	.00175	1110	11500	1.38	3460
"	8.10	18	8.8	100	.00219	1560	12900	.993	4430
"	8.10	18	7.8	160	.00350	2240	11600	.350	6930
"	8.10	18	5.5	320	.00700	3170	8200	.0616	13900
"	8.10	18	5.45	350	.00766	3450	8150	.0513	15200
"	8.10	18	7.9	640	.0140	9300	12900	.0241	27700
"	8.10	18	16.0	1280	.0281	38300	24700	.0116	55600
1/2 in.	17.6	18	10.7	10	.000475	124	10200	16.6	940
"	17.6	18	6.85	20	.000950	170	7020	2.87	1880
"	17.6	18	6.8	23	.00109	207	7420	2.29	2160
"	17.6	18	7.5	31	.00147	358	9520	1.62	2920
"	17.6	18	9.9	40	.00190	661	13600	1.39	2760
"	17.6	18	10.1	48	.00228	827	14200	1.01	4520
"	17.6	18	9.15	80	.00380	1280	13200	.338	7520
"	17.6	18	8.35	135	.00642	2020	12300	.110	12700
"	17.6	18	8.45	160	.00761	2440	12600	.0801	15100
"	17.6	18	13.8	320	.0152	8190	21100	.0335	30200

TABLE XV -(Continued)

1/2 in.	51.0	18	13.95	5	.000691	62.6	10300	7.97	1370
"	51.0	18	12.3	9.5	.00131	137	12450	2.68	2590
"	51.0	18	13.9	15	.00209	324	17700	1.49	4140
"	51.0	18	14.7	20	.00276	486	19900	.963	5460
"	51.0	18	16.5	40	.00553	1170	24100	.290	11000
"	51.0	18	22.5	80	.0111	3330	34300	.103	21900
1/2 in.	4.17	36	7.3	75	.000840	417	4620	9.68	1660
"	4.17	36	5.1	150	.00168	607	3360	1.76	3330
"	4.17	36	6.0	100	.00112	460	3820	4.51	2220
"	4.17	36	7.1	225	.00252	1380	5080	1.18	4980
"	4.17	36	8.45	314	.00352	2360	6240	.743	6970
"	4.17	36	5.7	600	.00672	3130	4330	.143	13300
"	4.17	36	3.85	1100	.0123	3720	2800	.0272	24400
"	4.17	36	3.9	1200	.0134	4120	2850	.0232	26600
"	4.17	36	5.4	1800	.0202	8760	4040	.0146	40000
1/2 in.	8.10	36	8.2	40	.000872	220	4560	8.86	1730
"	8.10	36	5.3	85	.00185	322	3140	1.35	3670
"	8.10	36	7.6	130	.00283	821	5250	.970	5600
"	8.10	36	8.7	160	.00349	1200	6220	.755	6910
"	8.10	36	8.8	190	.00414	1460	6360	.548	8200
"	8.10	36	6.8	320	.00697	1900	4930	.150	13800
"	8.10	36	5.65	510	.0111	2540	4130	.0494	22000
"	8.10	36	5.9	640	.0140	3380	4370	.0330	27700
"	8.10	36	11.45	1280	.0279	13400	8710	.0165	55200
1/2 in.	17.6	36	10.0	20	.000946	108	4470	7.38	1870
"	17.6	36	7.6	42	.00199	211	4150	1.55	3940
"	17.6	36	9.15	64	.00303	468	6060	.975	6000
"	17.6	36	10.6	80	.00379	707	7320	.754	7500
"	17.6	36	10.9	95	.00449	878	7660	.561	8900
"	17.6	36	9.3	160	.00757	1290	6670	.172	15000
"	17.6	36	9.0	210	.00993	1660	6550	.0982	19700
"	17.6	36	10.6	320	.0152	3070	7930	.0512	30000

TABLE XV - (Continued)

1/2 in.	51.0	36	16.7	7	.000963	47.0	5560	8.86	1910
"	51.0	36	12.6	14	.00193	95.0	5610	2.23	3810
"	51.0	36	12.6	16	.00220	116	5980	1.83	4350
"	51.0	36	13.0	22.5	.00309	200	7370	1.14	6120
"	51.0	36	18.5	87	.0120	1430	13600	.142	23700
"	51.0	36	13.8	28	.00386	289	8520	.846	7640
"	51.0	36	16.3	56	.00770	782	11600	.288	15200
1 in.	4.15	18	11.7	30	.000905	582	16000	85.6	1090
"	4.15	18	6.55	60	.00181	644	8870	11.9	2180
"	4.15	18	5.7	85	.00256	809	7860	5.26	3080
"	4.15	18	7.3	120	.00362	1550	10700	3.56	4360
"	4.15	18	8.75	170	.00513	2690	13100	2.18	6170
"	4.15	18	8.2	240	.00724	3580	12300	1.03	8720
"	4.15	18	5.1	480	.0145	4520	7760	.162	17400
"	4.15	18	3.1	805	.0243	4500	4610	.0342	29200
1 in.	8.00	18	11.0	20	.00116	338	14000	45.1	1400
"	8.00	18	6.8	40	.00232	418	8650	7.06	2800
"	8.00	18	6.3	54	.00314	546	8350	3.70	3780
"	8.00	18	8.1	80	.00465	1110	11500	2.33	5600
"	8.00	18	9.1	108	.00628	1755	13400	1.49	7560
"	8.00	18	8.0	160	.00930	2300	11900	.600	11200
"	8.00	18	4.75	320	.0186	2720	7010	.0885	22400
"	8.00	18	4.55	500	.0291	4120	6800	.0351	35000
1 in.	17.9	18	14.4	6	.000779	95.1	13100	94.2	940
"	17.9	18	9.6	12	.00155	136	9350	17.1	1870
"	17.9	18	7.75	24	.00312	265	9070	4.08	3760
"	17.9	18	7.75	26	.00337	292	9300	3.59	4060
"	17.9	18	10.6	48	.00623	874	15000	1.69	7510
"	17.9	18	8.55	96	.0125	1450	12400	.382	14400
"	17.9	18	7.1	192	.0249	2450	10600	.0745	30000
"	17.9	18	7.2	228	.0296	2970	10800	.0537	35700

TABLE XV (Continued)

1 in.	51.9	18	17.7	3	.00113	39.5	10900	37.4	1360
"	51.9	18	11.9	6	.00226	60.0	8280	7.10	2720
"	51.9	18	11.2	9	.00339	113	10400	3.96	3960
"	51.9	18	11.7	12	.00452	188	13000	2.79	5450
"	51.9	18	13.5	21	.00792	459	18100	1.26	9540
"	51.9	18	13.4	24	.00905	530	18300	.980	10900
"	51.9	18	12.2	45	.0170	952	17500	.265	20500
"	51.9	18	12.85	60	.0226	1360	18800	.161	27200
"	51.9	18	13.7	70	.0264	1720	20400	.128	31800
1 in.	4.15	36	12.7	50	.00150	515	8550	66.6	1810
"	4.15	36	8.4	100	.00300	689	5720	11.2	3620
"	4.15	36	7.7	200	.00601	1330	5520	2.68	7250
"	4.15	36	8.65	400	.0120	3100	6430	.782	14500
"	4.15	36	5.0	800	.0240	3550	3680	.112	28900
1 in.	8.00	36	8.3	50	.00289	296	4920	10.4	3480
"	8.00	36	6.25	100	.00578	484	4020	2.10	6960
"	8.00	36	8.3	200	.0116	1440	5970	.794	13900
"	8.00	36	5.5	400	.0231	1990	4130	.136	27800
"	8.00	36	4.9	800	.0462	2520	2620	.0216	55600
1 in.	17.9	36	10.8	20	.00258	124	5150	13.5	3110
"	17.9	36	6.55	40	.00516	155	3220	2.12	6220
"	17.9	36	11.1	80	.0103	746	7720	1.26	12500
"	17.9	36	8.25	160	.0207	1140	5860	.240	25000
"	17.9	36	7.15	320	.0414	2020	5200	.0532	49800
1 in.	51.9	36	19.7	5	.00188	36.7	6100	30.3	2270
"	51.9	36	12.6	10	.00376	45.2	3750	4.64	4530
"	51.9	36	10.9	20	.00751	126	5230	1.62	9050
"	51.9	36	13.95	40	.0150	448	9280	.720	18100
"	51.9	36	13.0	80	.0300	887	9220	.179	36200

TABLE XVI. FRICTION FACTORS AT CERTAIN REYNOLDS NUMBERS

1	2	3	4	5	6	7	8
Test Section	Mid-Point Pressure p.s.i.a.	Water Rate lbs/ft^2 sec.	$\frac{\rho_G}{\rho_L}$	Reynolds Numbers			
				2000	6000	10000	20000
1/2 inch	18	4.17	.00149	2.56	.38	.100	.022
"	18	8.10	.00149	2.56	.50	.135	.035
"	18	17.6	.00149	2.56	.57	.185	.052
"	18	51.0	.00149	4.00	.80	.34	.117
"	36	4.17	.00298	5.7	.94	.35	.042
"	36	8.10	.00298	5.9	.90	.35	.062
"	36	17.6	.00298	6.3	.98	.44	.096
"	36	51.0	.00298	7.9	1.16	.55	.186
1-inch	18	4.15	.00149	15.5	2.33	.74	.107
"	18	8.00	.00149	----	2.14	.80	.120
"	18	17.9	.00149	-----	2.30	.92	.175
"	18	51.9	.00149	----	2.48	1.15	.28
"	36	4.15	.00298	50	3.7	1.62	.31
"	36	8.00	.00298	---	3.1	1.35	.31
"	36	17.9	.00298	----	2.3	1.5	.41
"	36	51.9	.00298	----	2.6	1.5	.60

[illegible]

[illegible]	[illegible]	[illegible]	[illegible]	[illegible]	[illegible]	[illegible]	[illegible]
[illegible]	[illegible]	[illegible]	[illegible]	[illegible]	[illegible]	[illegible]	[illegible]
[illegible]	[illegible]	[illegible]	[illegible]	[illegible]	[illegible]	[illegible]	"
[illegible]	[illegible]	[illegible]	[illegible]	[illegible]	[illegible]	[illegible]	"
[illegible]	[illegible]	[illegible]	[illegible]	[illegible]	[illegible]	[illegible]	"
[illegible]	[illegible]	[illegible]	[illegible]	[illegible]	[illegible]	[illegible]	"
[illegible]	[illegible]	[illegible]	[illegible]	[illegible]	[illegible]	[illegible]	"
[illegible]	[illegible]	[illegible]	[illegible]	[illegible]	[illegible]	[illegible]	
[illegible]	[illegible]	[illegible]	[illegible]	[illegible]	[illegible]	[illegible]	"
[illegible]	[illegible]	[illegible]	[illegible]	[illegible]	[illegible]	[illegible]	[illegible]
[illegible]	[illegible]	[illegible]		[illegible]	[illegible]	[illegible]	"
[illegible]	[illegible]	[illegible]	[illegible]	[illegible]	[illegible]	[illegible]	"
[illegible]	[illegible]	[illegible]		[illegible]	[illegible]	[illegible]	"
[illegible]	[illegible]	[illegible]	[illegible]	[illegible]	[illegible]	[illegible]	"
[illegible]	[illegible]	[illegible]	[illegible]	[illegible]	[illegible]	[illegible]	"
[illegible]	[illegible]	[illegible]	[illegible]	[illegible]	[illegible]	[illegible]	"
[illegible]	[illegible]	[illegible]	[illegible]	[illegible]	[illegible]	[illegible]	"

NOMENCLATURE

A = cross-section of tube, ft.^{2}

C = critical flow constant

D = diameter of pipe, ft.

F = friction loss (single-phase flow), ft. of flowing fluid

ΣF_L = summation of all friction and other irreversibility losses, lbs_f ft/lb_m of flowing liquid

ΣF_G = summation of all friction and other irreversibility losses, lbs_f ft/lbs_m of flowing gas

f_G = superficial friction factor based on flowing gas phase (see text)

G = saturated air-rate, lbs_m/sec.

g = acceleration due to gravity, ft/sec^2

h_f = differential manometer reading, inches mercury under air

K = air orifice constant

L = water rate, lbs_m/sec.

N = length of tube, ft.

P_1 = downstream pressure, lbs_f/ft^2

P_2 = upstream pressure, lbs_f/ft^2

ΔP = measured pressure drop, p.s.i./100 ft.

P_c = pressure upstream of critical flow orifice, p.s.i.a.

P_f = pressure upstream of air orifice, p.s.i.a.

Q_c = rate of gas flow, 1000 ft^3/24 hrs. at 14.4 p.s.i.a. and 60°F.

Re_G = superficial Reynolds number based on flowing gas (see text)

S = specific gravity of the gas (= 1 for air)

T = absolute temperature °R.

NOMENCLATURE - (Continued)

V = fluid velocity, ft/sec.

V_G = gas phase velocity based on the empty cross-section of the tube, ft/sec.

v_G = specific volume of saturated air at flowing conditions, ft^3/lb_m

v_L = specific volume of water ft^3/lb_m

X_1 = downstream pressure tap position above datum, ft.

X_2 = upstream pressure tap position above datum, ft.

β = proportionality constant, lbs_m ft/lb_f sec^2

μ_G = viscosity of air at flowing conditions, $lbs._m$/sec. ft.

ρ_G = specific weight of air at flowing conditions, $lbs._m/ft^3$

ρ_L = specific weight of water, $lbs._m/ft^3$

BIBLIOGRAPHY

1. Binder, R.C. "Fluid Mechanics", 2nd Edition, p.96. Prentice-Hall, Inc., New York, 1949.
2. Carpenter, F.G. Ph.D. Thesis, University of Delaware, 1949.
3. Cromer, S. and Huntington, R.L. Trans. A.I.M.E., 136, 79, 1940.
4. Gazley, C. Jr. Ph.D. Thesis, University of Delaware, 1949.
5. Gosline, J.E. Trans. A.I.M.E., 118, 56, 1936.
6. Jenkins, R.M. Ch.E. Thesis, University of Delaware, 1947.
7. Lockhart, R.W. and Martinelli, R.C. Chem. Eng. Prog., 45, 1, 45, 1949.
8. Martinelli, R.C., Boelter, L.M.K., Thomsen, E.G., Taylor, T.H.M. and Morrin, E.H. Trans. A.S.M.E., 66, 2, 139, 1944.
9. Martinelli, R.C., Putnam, J.A. and Lockhart, R.W. Trans. A.I. Ch.E., 42, 4, 681, 1946.
10. McElwee, F.D. M.S. Thesis, University of California, 1947.
11. Moore, T.V. and Wilde, H.D. Jr. Trans. A.I.M.E., 92, 296, 1931.
12. Moore, T.V. and Schilthuis, R.J. Trans. A.I.M.E., 103, 170, 1933.
13. Nowels, K.B. Trans. A.I.M.E., 98, 401, 1932.
14. Radford, B.A. M.Sc. Thesis, University of Alberta, 1949.
15. Shaw, S.F. Trans. A.I.M.E., 86, 220, 1930.
16. Shaw, S.F. Canadian Oil and Gas Industries, 3, 2, 1950.
17. Shaw, S.F. "Flow Characteristics of Gas Lift in Oil Production", Bulletin #13, A. & M. College of Texas, July, 1949.
18. Uren, L.C. et al. Trans. A.I.M.E., 86, 209, 1930.
19. Van Wingen, N. World Oil, 122, #7, 156, 1949.
20. Versluys, J. Trans. A.I.M.E., 86, 209, 1930.
21. Versluys, J. Trans. A.I.M.E., 92, 293, 1931.
22. Versluys, J. Journal Inst. Pet. Tech., 19, 687, 1933.
23. Versluys, J. Journal Inst. Pet. Tech., 19, 694, 1933.

This abridged version may be used for
circulation purposes for Interlibrary
Loans.

THE UPWARDS VERTICAL FLOW
OF AIR-WATER MIXTURES

I. EFFECT OF AIR AND WATER RATES ON FLOW PATTERN, HOLDUP AND PRESSURE DROP

UNIVERSITY OF ALBERTA
MAR 27 1957
LIBRARY

by

G. W. Govier, B. A. Radford, J. S. C. Dunn

Department of Chemical and Petroleum Engineering

University of Alberta

January 25, 1957

THE UPWARDS VERTICAL FLOW
OF AIR-WATER MIXTURES

I. EFFECT OF AIR AND WATER RATES ON FLOW PATTERN, HOLDUP AND PRESSURE DROP

G. W. Govier, B. A. Radford*, J. S. C. Dunn**

Department of Chemical and Petroleum Engineering
University of Alberta

ABSTRACT

The elementary thermodynamics and the flow pattern terminology of the upwards vertical flow of gas-liquid mixtures is reviewed and new terminology is proposed.

Data on the upwards vertical flow of air-water mixtures in a smooth bore 1.025 inch I.D. tube are presented for a range of nine water rates from 0.00040 to 0.0421 cu. ft. per sec. and for air-water volume ratios under flow conditions from 0 to 348. The properties of the gas and liquid phases were held constant through the maintenance of constant average flowing pressure and temperature at 36.0 psia and 70°F.

A correlation of the data based upon the thermodynamic analysis is presented. The correlation enables the prediction of flow pattern, pressure drop and holdup ratio for gas and liquid rates within the range tested but is restricted as to tube diameter and liquid and gas phase properties.

INTRODUCTION

The general problem of the vertical flow of gas-liquid mixtures has received attention by a number of workers from the early days of the invention of the airlift pump to the present time. The application of gas lift principles to oil well production in the late 1920's stimulated further interest in two phase vertical flow and resulted in a number of mathematical and experimental studies. These investigations have shown that the vertical flow of two phase mixtures differs materially from that of single phase systems in two important respects:

---

* Plastics Division, Canadian Industries Limited, Box 10, Montreal
** Standard Oil Company of British Columbia, Burnaby, B.C.

(1) The flow pattern cannot be described simply (as for single phase systems) as laminar, transitional or turbulent. In the complex flow pattern of two phase systems the relative amounts of the phases, their dispersion one in the other, and their individual motions are all important.

(2) The two phase mixture actually in motion in a vertical tube is never of the same overall composition as that admitted or released from the tube even under conditions of steady state. This difference in relative quantities of the two phases has been referred to under the headings of "slip" and "holdup". In general the fluid of lower density tends to slip past that of higher density so that, in the case of a gas-liquid system, the gas-liquid ratio in the flow tube is reduced over that of the entering or leaving mixtures.

The complexity of the flow pattern and the existence of holdup make it obvious that the relationships between pressure drop and the pertinent variables will also be much more complex than is the case in the flow of single phase fluids. Moreover the differences in terminology used, the many variables involved, and the lack of or differences in the control of certain of the variables has made the interpretation and correlation of experimental data difficult. While considerable progress has been made in the overall and qualitative understanding of the problem much remains to be done from a quantitative viewpoint.

The work to be reported in the series of papers of which this is the first was undertaken with the pruposes of

(1) clarifying the terminology and descriptions of the flow patterns encountered,

(2) obtaining data, under controlled conditions, on the influence of the pertinent variables on flow patterh, holdup and pressure drop,

and (3) obtaining a general correlation which would enable the predicti of flow pattern, holdup and pressure drop for any gas-liquid system in upwards vertical flow.

This paper includes a thermodynamic analysis of the problem and deals specifically with the upwards vertical flow of air-water mixtures. Experimental data and certain correlations are presented on the effect of air-water volume ratio, at various water rates, on the flow pattern, the holdup, and the pressure drop.

VARIABLES INVOLVED

The primary variables involved in the upwards vertical flow of gas-liquid mixtures are the following:

Liquid Properties

Density, ρ_L, or specific volume, v_L

Viscosity, μ_L

Surface tension (to gas), σ

Gas Properties

Density, ρ_G, or specific volume, v_G

Viscosity, μ_G

Geometrical Properties

Tube diameter, D

Tube roughness, $\frac{\delta}{D}$

Tube height, X

Flow Rates

Mass flow of liquid phase, L

Mass flow of Gas phase, G

Certain of these basic properties are dependent upon other variables. For example the gas phase density will depend upon the nature of the gas, the extent of vaporization into it of the liquid, the pressure and the temperature. Similarily the liquid density, viscosity and surface tension will depend upon the nature of the liquid, the temperature, and the solubility in it of the gas - this latter depending again on pressure and temperature. Despite the complex interrelationship of properties with pressure, temp-

erature and solubility it seems clear that the effects of pressure, temperature and solubility need not be considered as separate from those of the basic properties listed above. One may, therefore, expect that the pressure drop per unit height, the flow pattern, and the slip or holdup would all be functions of the primary variables. i.e.

$$\frac{dP}{dX} = \phi' \left(v_L, \mu_L, \sigma, v_G, \mu_G, L, G, D, \frac{\delta}{D}\right) \qquad (1)$$

$$\text{Flow Pattern} = \phi'' \left(v_L, \mu_L, \sigma, v_G, \mu_G, L, G, D, \frac{\delta}{D}\right) \qquad (2)$$

$$\text{Holdup} = \phi''' \left(v_L, \mu_L, \sigma, v_G, \mu_G, L, G, D, \frac{\delta}{D}\right) \qquad (3)$$

These relationships point out a difficulty which has not always been appreciated by other workers. It is this: to the extent that the specific volume of the gas phase (in particular) influences flow pattern, holdup and pressure drop, this variable should be controlled in any experimental study of the effect of the other variables. The most practical approach to this seems to be through the conduct of tests at constant average temperature and at constant average pressure. Another point clarified by the above equations is that, in principle, one should be able to correlate the pressure drop with the pertinent variables indicated without separately including flow pattern or holdup. Certainly, however, a pressure drop correlation would be expected to reflect the basically different flow patterns.

While it seems reasonable the surface tension and liquid and gas viscosities would be variables, work of Gosline(1) and Poettmann and Carpenter(2) in particular suggests that the effect of surface tension is small and that, in regions of turbulent motion, gas phase viscosity may not be important.

THERMODYNAMIC ANALYSIS

Consider a differential height, dX, of a smooth vertical tube of diameter, D, to which is admitted a liquid and a gas phase at rates L and G. Assume the phases are saturated with respect to one another upon admittance. Thus for the time interval $d\mathcal{T}$ the well known mechanical energy

balance may be written for each phase

$$LdT\left(v_L dP + dX + \frac{V_L' \, dV_L'}{g_c} + dF_L\right) = 0 \tag{4}$$

$$GdT\left(v_G dP + dX + \frac{V_G' \, dV_G'}{g_c} + dF_G\right) = 0 \tag{5}$$

where

L = rate of supply of liquid, lbs/hr

G = rate of supply of gas, lbs/hr

v_L = specific volume of liquid, ft^3/lb

v_G = specific volume of gas, ft^3/lb

dX = differential height, ft

P = pressure, lbs/ft^2 absolute

V_L' = actual linear velocity of liquid, ft/sec

V_G' = actual linear velocity of gas, ft/sec

dF_L = irreversibility effect attributable to liquid in height dX, ft. liquid

dF_G = irreversibility effect attributable to gas in height dX, ft. gas

dT = differential element of time, hrs.

(These equations neglect any energy associated with interfacial surface.)

Adding these relations yields

$$v_L dP + dX = \frac{V_L' \, dV_L'}{g_c} + dF_L + \frac{G}{L} v_G dP + \frac{G}{L} dX + \frac{G V_G' \, dV_G'}{L \, g_c} + \frac{G}{L} dF_G = 0 \tag{6}$$

If the kinetic energy effects are neglected, or considered to be included within the terms dF_L and dF_G, then

$$dP\left(v_L + \frac{G}{L} v_G\right) + dX\left(1 + \frac{G}{L}\right) + (dF)_L = 0 \tag{7}$$

where

$$(dF)_L = dF_L + \frac{G}{L} dF_G \tag{8}$$

Rearranging, one obtains

$$-v_L \frac{dP}{dX} = \frac{1 + R_M}{1 + R_V} + \frac{1}{1 + R_V} \left(\frac{dF}{dX}\right)_L$$

where

$$R_M = \text{gas-liquid mass ratio, } \frac{G}{L}$$

$$R_V = \text{gas-liquid volume ratio, } \frac{Gv_G}{Lv_L} \qquad (9)$$

This equation indicates that the total unit pressure drop, measured in terms of feet of the flowing liquid phase per foot of height, $-v_L \frac{dP}{dX}$, is equal to the sum of two components

$\frac{1 + R_M}{1 + R_V}$, the hydrostatic head component, ft of liquid per ft of height, and

$\frac{1}{1 + R_V} \left(\frac{dF}{dX}\right)_L$ the irreversibility component, ft. of liquid per ft. of height.

Equation (9) may be applied to a system of finite height only if the fractional variations in R_M and R_V are small enough to justify the use of average values based upon an average system pressure and temperature. Under these conditions

$$-v_L \frac{\Delta P}{\Delta X} = \frac{1 + R_M}{1 + R_V} + \frac{1}{1 + R_V} \left(\frac{\Delta F}{\Delta X}\right)_L \qquad (10)$$

(It is of interest to note that the expression $-v_L \frac{\Delta P}{\Delta X}$ is exactly equivalent to the "submergence ratio" referred to in works on air lift pumps.)

In the limiting condition when $R_M = R_V = 0$, or a single phase liquid is flowing, the equation reduces to

$$-v_L \frac{\Delta P}{\Delta X} = 1 + \frac{\Delta F_L}{\Delta X} \qquad (11)$$

where

$$\frac{\Delta F_L}{\Delta X} = \frac{2f_L V_L^2}{g_c D} \qquad (12)$$

and f_L is the common friction factor dependent upon $\frac{DV_L}{\mu_L v_L}$ and $\frac{\delta}{D}$

In the general case a two phase friction factor f_L' may be defined through the relation

$$\left(\frac{\Delta F}{\Delta X}\right)_L = \frac{2f_L' V_L^2}{g_c D} \qquad (13)$$

where V_L is the superficial liquid phase velocity based upon the total tube cross section. This two phase friction factor might be expected to depend upon $\frac{DV_L}{v_L \mu_L}$, $\frac{\delta}{D}$ and either the mass or the volume ratio of the two phases.

An alternate rearrangement of equations (4) and (5) yields

$$dP\left(\frac{L}{G} v_L + v_G\right) + dX\left(\frac{L}{G} + 1\right) + (dF)_G = 0 \qquad (14)$$

where

$$(dF)_G = \frac{L}{G}\, dF_L + dF_G$$

Under conditions where average values of R_M and R_V may be used this leads to

$$-v_G \frac{\Delta P}{\Delta X} = \frac{1 + \frac{1}{R_M}}{1 + \frac{1}{R_V}} + \frac{1}{1 + \frac{1}{R_V}} \left(\frac{\Delta F}{\Delta X}\right)_G \qquad (16)$$

relating the total unit pressure drop measured in terms of feet of the flowing gas phase per foot of height, $-v_G \frac{\Delta P}{\Delta X}$, to corresponding by hdyrostatic and irreversibility components.

In limiting condition of the flow of a single gas phase $\frac{1}{R_M} = \frac{1}{R_V} = 0$ and the equation reduces to

$$-v_G \frac{\Delta P}{\Delta X} = 1 + \frac{\Delta F_G}{\Delta X} \qquad (17)$$

where

$$\frac{\Delta F_G}{\Delta X} = \frac{2f_G V_G^2}{g_c D} \qquad (18)$$

and f_G is the common friction factor dependent upon $\frac{DV_G}{\mu_G v_G}$ and $\frac{\delta}{D}$

Again, in the general case, a two phase friction factor f'_G might be defined by the relation

$$\left(\frac{\Delta F}{\Delta X}\right)_G = \frac{2f'_G V_G^2}{g_c D} \qquad (19)$$

where V_G is the superficial gas velocity based upon the total tube cross section. The choice between equations (10) and (13) in terms of ft. of liquid, and equations (16) and (19) in terms of ft. of gas would appear arbitrary as the two are mathematically equivalent.

These basic relationships suggest that pressure drop data for the vertical flow of two phase systems might best be understood

(1) by separating the unit irreversibility component from the total pressure drop,

(2) by calculating a two phase friction factor (either f'_L or f'_G from equation (13) or (19))

and (3) by seeking a correlation of the friction factor with a superficial Reynolds number, a relative roughness term and a mass or volume ratio of the phases.

The fact that even a very small amount of liquid in a gas stream greatly increases pressure drop indicates further that the presence of the liquid phase may well outshadow the effect of roughness (3) and also that at high velocities (fully developed turbulence) viscosity effects may be very small. In this work, where tube diameter and gas and liquid properties are held constant, the pressure drop data are correlated as functions of superficial liquid velocity (proportional to liquid Reynolds number) and the volume ratio of the phases.

Poettmann and Carpenter (2) have also applied the mechanical energy balance to the vertical two phase flow problem but in an approximate manner. Their assumption that a two (or three) phase mixture could be treated as a pseudo homogeneous phase of constant equivalent specific volume has led to a useful practical correlation but is not too sound fundamentally.

HOLDUP and SLIP

As has been mentioned one of the distinguishing characteristics of two phase vertical flow is the development, within the flow section, of a

concentration of the denser phase greater than that in the supply mixture. The term "holdup ratio" is used in this paper as a quantitative measure of this liquid accumulation. Holdup ratio is here defined as the ratio of (a) the gas-liquid volume ratio in the supply mixture to (b) the gas-liquid volume ratio in the flow section. Both volume ratios are expressed in cu. ft. per cu. ft. at average flow pressure and temperature. Galegar, Stovall and Huntington(4) have reported quantities equivalent to the individual ratios (a) and (b) and Calvert and Williams(5) have made a mathematical analysis of holdup in the film or annular flow region. Other workers (1, 4, 6, 7) have referred to the "slip velocity" of the gas phase. Slip velocity has been defined as the difference in the average lineal velocities of the gas and the liquid phases both measured at average flow pressure and temperature.

The two quantities, holdup ratio and slip velocity are two measures of the same phenomenon and are simply interrelated as follows:

Let the volume fraction of the flow section occupied by the gas phase be defined as q. Then 1-q represents the volume fraction occupied by the liquid phase.

$$\text{Holdup Ratio, } H_R = \frac{Gv_G\ (1 - q)}{Lv_L\ (q)} = \frac{R_v\ (1 - q)}{q}$$

Let A be the cross sectional area of the empty flow section. Then the average lineal velocities are

$$V_G' = \frac{Gv_G}{Aq}$$

$$V_L' = \frac{Lv_L}{A\ (1 - q)}$$

$$\text{and the slip velocity} = \frac{1}{A}\left(\frac{Gv_G}{q} - \frac{Lv_L}{1 - q}\right)$$

or

$$V_G' - V_L' = \frac{Lv_L}{A(1-q)}\ (H_R - 1) = V_L'\ (H_R - 1)$$

or

$$H_R = \frac{V_G' - V_L'}{V_L'} + 1$$

FLOW PATTERN TERMINOLOGY

The flow pattern for the upwards vertical flow of gas-liquid mixtures has been variously described by Gosline(1), Bergelin(3), Stovall and Huntington(4), Calvert and Williams(5), Cromer and Huntington(8), Radford(9), Dunn(10), Martinelli, R. C. et al(11) and others. The descriptions of most of these workers were based either upon visual and qualitative studies or upon "efficiency" or liquid "yield" considerations. Radford and Dunn and, later, Calvert and Williams correlated their flow pattern descriptions with pressure drop observations. This method, which has the advantage of greater precision of definition, is used here.

A typical pressure drop vs gas-liquid volume ratio curve at constant low liquid rate and at constant average pressure and temperature for air-water flow in a smooth tube of 1.025 inch i.d. is shown in Figure 1. (At higher liquid rates the curve changes its shape and shifts upwards as will be discussed later.) On the basis of this relationship it seems reasonable to divide the curve as indicated into four pressure drop regimes I, II, III, IV characterized respectively by a decreasing, an increasing, a decreasing and an increasing unit pressure drop with increasing gas-liquid volume ratio at constant liquid rate. This basic division may then be subdivided, and given qualitative description by reference to visual observations. The terminology used by previous investigators has been reviewed and compared on this basis. Figure 2 shows the interrelationship of the terminology as nearly as this can be determined from the published work. While the importance of flow pattern as determined visually is recognized, the primary subdivision on the basis of pressure drop regime is considered more precise and to offer greater possibilities as an air to correlation. The flow patterns encountered in the four pressure drop regimes are illustrated by diagrams and photographs in Figure 3.

LOW LIQUID RATES

Regime I

As the gas rate, at any constant liquid rate, is increased from zero to low values (gas-liquid volume ratios up to 1 - 5) the gas is dispersed as discrete bubbles which increase steadily in number and size. This is the bubble flow pattern and it extends only a short way into

Regime I. With a further increase in gas flow some of the bubbles coalesce to form larger bullet shaped slugs. These slugs grow in length and diameter and their upward velocity increases as the gas rate is further increased. This slug flow pattern is characterized by alternating slugs of gas which are surrounded by a thin liquid annulus and interspersed with regions of bubble flow. As a slug passes any given tube section some of the liquid falls downward into the bubble filled region beneath it. Slug flow continues to the end of Regime I and well into Regime II.

Regime II

As the gas-liquid volume ratio is still further increased the tendency of the liquid phase to fall downwards beneath the slugs decreases and finally stops. At this latter point the slugs seem to merge and degenerate into a froth. Froth flow would seem to appear first at a point roughly mid-way in Regime II. This pattern is highly turbulent with coarse agitation of the liquid phase being its most predominant characteristic. It extends through the second half of Regime II into Regime III.

Regime III

The flow pattern in Regime III is primarily froth. As the gas-liquid volume ratio is increased the amount of relative motion between phases seems to decrease. This phenomenon continues with increasing gas rate until a region of ripple flow is entered. Ripple flow is characterized by an upwards moving wavy or ripply layer of liquid on the tube wall. The zone of ripple flow is rather narrow and actually forms a transition region between Regimes III and IV.

Regime IV

The ripple flow pattern continues a short way into Regime IV and then develops into film flow. In this flow pattern the liquid flows as an annular film and the gas flows at a higher velocity through the inner core. This flow pattern results from the smoothing of the waves or ripples of ripple flow by the attrition of the higher gas rates. Calvert and Williams(5) have analyzed the film flow pattern from the viewpoint of the actual shearing forces involved. Eventually, at some sufficiently high gas rate, a sufficient number of water droplets will be captured from the

liquid interface to remove the liquid layer and to result in a region of mist flow. The occurrence of this zone is obvious but has not been directly observed in this work.

HIGH LIQUID RATES

The above description of flow patterns does not apply in its entirety to higher water rates. It will be shown that as the water rate is increased Regimes II and III become progressively narrower and finally disappear. At these higher water rates the flow pattern of the liquid phase seems much the same as at the lower rates but the gas phase pattern changes markedly. Atthe close of Regime I the gas phase, as before, is characterized by an agitated pattern which extends the entire length of the tube with fast moving slugs travelling intermittently through the system. As the gas rate increases these slugs become faster moving and more frequent in occurrence. No froth flow pattern is observed. The amount of turbulence present in the liquid phase decreases with increasing gas rates and develops directly into a pattern similar to ripple flow. Ripple flow gives way to film flow as at the lower water rates.

EXPERIMENTAL EQUIPMENT

The experimental equipment is illustrated schematically in Figure 4. It consisted of an air supply and metering system, a water supply and metering system, the two-phase test section and a manometer system for measuring pressure drop.

Air was supplied at approximately 100 psi from a central compressor, passed through a reducing valve to maintain a nearly constant downstream pressure of about 75 psi and then through an orifice metering station to the base of the test equipment. Control was effected manually by a suitable valve in the main one inch line and by a needle valve in a quarter inch by-pass line. Water was supplied through a 70 gallon per minute capacity centrifugal pump having a maximum head of about 110 psi. The water was admitted to the base of the equipment through one of four rotameters connected in parallel. These rotameters had maximum capacities of .000272, .00247, .0211 and .0219 cu. ft. per sec. thus permitting relatively accurate metering of the water over the full range from .0004 to .0421 cu. ft. per sec.

Preliminary tests were conducted with different designs of mixing sections at the base of the two-phase flow column. It was found however that the design of the mixing section affected the flow pattern only for a very short distance above it and that with an adequate calming section no special mixing device was required. Accordingly the air and water were combined in a simple tee at the base of the test section.

The test section itself consisted of a transparent section of cellulose acetate-butyrate plastic tubing approximately 30 ft long and of 1 inch nominal diameter. The lower end of the plastic tube was connected to the mixing tee with a two foot section of 1 inch galvanized iron pipe containing a full flow plug valve. The upper end of the plastic pipe was similarly connected to the discharge piping of the system through another full flow plug valve. These plug valves operated with a 90° turn of the handle. The handles of the two were linked together with a length of 1 inch aluminum angle iron. This permitted the two plug valves to be opened or closed simultaneously. Three pressure taps were made in the plastic tube. The lower or upstream tap was approximately 8 ft above the mixing chamber and the upper or downstream tap 22.88 ft above it. The third pressure tap was located midway between the upstream and downstream ones. All pressure taps were made in blocks of lucite, machined to fit around the tube and sealed to it with chloroform. The block and tube were then bored with a 3/16 hole which was carefully reamed and the block was counter-bored and tapped for 1/8 inch standard pipe fittings. Connected to the discharge end of the test section were an air-water separator which permitted the water to be discharged to sewer and a pneumatic control valve (installed in the air discharge line from the separator).

Two 30 inch Meriam manometers, one filled with water, the other with mercury, were provided for measuring the pressure drop across the air metering orificies. A 60 inch mercury manometer and a 0 to 50 psig recording Brown pressure controller were connected in parallel to the mid-point pressure tap of the test section. This connection was made through a small plastic separator directly connected to the mid-point pressure tap. This separator enabled the operator to keep the pressure lead line to the manometer and the Brown instrument clear of water by periodic draining from its base. The pressure controller actuated the pneumatic valve in the air discharge line from the main separator at the outlet end of the

test section. Two 60 inch Meriam manometers were provided for the measurement of the pressure drop between the upstream and the downstream pressure taps. One of these manometers was filled with water, the other with mercury. They were connected in parallel through plastic separators directly connected to the pressure taps.

Thermometers were provided for measuring the inlet temperatures of the water and the air and the outlet temperature of the two-phase mixture. The orifice plates used for measuring the air rates, were each calibrated with the aid of a critical flow prover. The calibrations were checked one against another for consistency between plates. The four rotameters used for measuring water flow were calibrated by a direct weighing technique.

EXPERIMENTAL PROCEDURE

The tests reported here were all carried out at the same mid-point test section pressure of 36 psia. This pressure was controlled to within 0.1 or 0.2 psia by the Brown pressure controller. Extensive tests were made at each of the nine water rates. The test procedure was essentially the same in each case.

A test was started by opening the two plug valves on the test section, closing all pressure tap connections and introducing water at a desired rate through the appropriate rotameter to the base of the test section. With this rate set a small flow of air was started through an appropriate sized orifice to the base of the column. The mid-point pressure tap was the opened. The two-phase mixture discharging from the top of the test section was separated in the separator with pressure control on the entire system being maintained by the Brown instrument and the pneumatic valve handling the air discharge from the separator. With steady state conditions reached the upstream and downstream pressure taps were opened, the small separators flushed to give an indication of the pressure drop on one of the two 60 inch manometers. After conditions appeared completely stabilized, readings were taken of the water flow rate, the air flow rate and the pressure drop. A check reading of the mid-point pressure was taken on the Meriam manometer in parallel with the Brown instrument. Following this the upstream and downstream pressure taps were closed and the connecting link joining the two plug valves was operated rapidly to close both valves simultaneously and trap the flowing mixture in the test section. Some time

was allowed for the mixture to settle out and then the relative volumes of water and air confined between the two plug valves were observed with the aid of a calibrated scale. Following this conditions were adjusted to successively higher air rates at the constant water rate. Careful visual observations were made of the flow pattern for each test and several series of photographs were taken.

EXPERIMENTAL RESULTS

The basic experimental data are tabulated in Table 1 (Partial) for the lowest, the highest and one of the intermediate water rates. (The complete tabular data including those of the other six water rates is given in Table 1 of material deposited as Document No. ______ with the American Documentation Institute Photo Duplication Service, Library of Congress, Washington 25, D.C.).

Referring to Table 1, Column 2 gives the water rate in cubic feet per second of liquid saturated gas-phase at the mid-point temperature given by Column 4 and the constant mid-point pressure of 36.0 psia. These rates were calculated from the actual measured air rates to correct for the saturation of the air with water which took place in the calming section. Column 5 presents the ratio of the air to water rates, both on a volume and on a mass basis. Column 6 gives the ratio of air to water trapped in the test section at the completion of each test. Column 7 gives the specific volume of the saturated gas-phase at mid-point test section conditions. Column 8 presents the holdup ratio, being the ratio of the discharge air-water volume ratio to the test section air-water volume ratio i.e. of Column 5 to Column 6. Column 9 is the total pressure drop between the upstream and downstream pressure measuring stations, expressed in terms of feet of water per foot of height. Column 10 presents the ratio of the specific volumes of the liquid-phase to the saturated gas-phase at average test section pressure and temperature. Column 11 identifies the pressure drop regime and Column 12 the flow pattern.

The basic data are summarized for each of the constant water rates in Figure 5 through 13. These figures show by separate curves (a) the relationship between unit pressure drop and the air-water volume ratio at test conditions and (b) the relationship between holdup ratio and air-water

volume ratio at test conditions. The different constant water rates for each of the figures is represented by the superficial water velocity, V_L. The existence of the four pressure drop regimes and the two minima points in the pressure drop curves is clearly indicated in Figures 5 through 9 covering superficial water velocities from 0.0698 to 2.06 feet per second and at least perceptible at the rate of Figure 10. The data for the higher water rates shown in Figures 11 to 13 indicate a mergence of the maximum point in the pressure drop curve with the second minimum point. This mergence is reflected by the inflection point of Figure 11 and results in the disappearance of pressure drop regimes II and III at a superficial water velocity of about 3.5 feet per second.

The interrelationship between the holdup curves and the pressure drop curves is to be noted. In each instance the holdup curve exhibits a region of inflection about in the middle of pressure drop regime I and a very abrupt change of slope at about the end of pressure drop regime II. It is also to be noted that the holdup curve is nearly linear from about the middle of regime I to the end of regime II. At low water rates the holdup curve has a slight negative slope through pressure drop regime III. This slope gradually increases until, at a superficial lineal velocity of near 0.6 feet per second, the slope becomes zero. With increasing water rates the slope of the holdup curves in regime III increases further in a positive sense.

The loci of the two minima and the maximum points in the pressure drop curves of Figures 5 - 13 are plotted in Figures 14 and 15. Figure 14 shows the loci as functions of the unit pressure drop and the superficial water velocity. The convergence of the loci corresponding with the maximum and the second minimum at a superficial water velocity of about 3.5 feet per second is again evident. Figure 15 which shows the loci as functions of superficial water velocity and air-water volume ratio (under flow conditions) is perhaps more revealing and certainly more useful from the viewpoint of delineating the various pressure drop regimes and flow patterns. The locus of the first pressure drop minimum, which is the boundary between regimes I and II, is seen to be a straight line on logarithmic paper of slope equal to -1.17. The locus of the maximum point is more or less parallel to this and displaced toward higher air-water volume ratios. The

locus of the second minimum point is again not too far from being parallel to that of the first minimum and the maximum points but is displaced further toward higher air-water volume ratios. The maximum locus begins to approach that of the second minimum at superficial water velocities above about 1 feet per second and merges with it at the velocity of about 3.5 feet per second. Thus above a water rate of 3.5 ft. per sec. regime III does not exist and regime II becomes continuous with regime IV.

The loci of the points of inflection on the holdup curves and of the points of abrupt change of slope are seen also to be roughly parallel to the pressure drop minima and maximum loci. The approximate boundaries between bubble and slug flow and between slug and froth flow, froth and wave entrainment flow and wave entrainment and annular flow are shown as dashed lines. These lines have been located on the basis of visual observations during the tests.

INTERPRETATION OF RESULTS

A considerable amount of time has been devoted to an interpretation of the pressure drop results. In the light of the fluid flow thermodynamics presented earlier the total pressure drop was, by calculation, separated into its two components - the hydrostatic head and the irreversibility component. The relationship between these two components and the total pressure drop, all in feet of water per foot, is indicated in Figure 16 for the superficial water velocity corresponding with Figure 10, namely 0.873 feet per second. The components bare a similar relationship to the total at the other water flow rates. Both the friction factors, f'_L and f'_G, were calculated for all of the test data and plots of these were made vs the air-water volume ratios at each of the nine constant water rates. Both sets of plots yielded surprisingly smooth curves. (Complete numerical values of the components and the two friction factors are given in Table 2 of the material deposited as Document No. _____ with the American Documentation Institute Photo Duplication Service, Library of Congress, Washington 25, D.C.)

Typical curves of f'_L versus the air-water volume ratio at the lowest, the highest and an intermediate water velocity are given for illustrative purposes in Figure 17. Figure 18 was prepared from the set of

these curves representing all nine water rates. This is a logarithmic plot of f_L' versus the superficial water velocity showing lines of constant air-water volume ratio. For reference purposes the conventional friction factor is also plotted against water velocity for single phase water flow. The friction factor lines representing the two-phase flow condition are seen to lie well above and to the right of the single-phase lines. At the lowest gas-liquid ratios the two-phase lines appear to be approaching the single-phase line but at the highest water velocities fall below the single-phase line representing turbulent water flow. Clearly more data are required at lower R_V ratios to determine the manner in which the two-phase lines blend into the single-phase lines.

The loci of the pressure drop minima and maximum points are also plotted in Figure 18, the points on each R_V curve being taken from Figure 15. The smooth curve loci resulting in Figure 18 attest the the consistency of the data for the derived f_L' values are sensitive to minor errors in the total measured pressure drop.

Figure 19 showing the holdup ratio as functions of air-water volume ratio and superficial water velocity was prepared from the holdup curves of Figures 5 to 13 inclusive. Again the minima and maximum pressure drop loci are superimposed. The relationship between these loci and the minima and maxima in the family of holdup curves is apparent.

CONCLUSIONS

The correlation of Equations 10 and 13 and Figures 15, 18 and 19 enable the prediction of the flow pattern, the pressure drop and the holdup as functions of the air and water rates for the upwards vertical flow of air-water mixtures at an average pressure of 36.0 psia in smooth tubes of approximately 1 inch diameter.

These correlations apply only to a system in which the average pressure is 36.0 psia and over which the fractional change in specific volume of the water saturated air is small enough to justify the use of an average value. Experimental work now nearly completed and to be reported shortly has been undertaken to extend the application of the correlation to other diameters and other average pressures (or average gas phase densities). With the effect of gas phase density known, integration or

step-wise use of the correlation will permit its application to systems wherein there is a large change in gas phase specific volume.

LITERATURE CITED

1. Gosline, J. E., Trans. A.I.M.E., (Pet. Dev. and Tech.), 118, 56 1936

2. Poettmann, F. H., Carpenter, P. G., Drilling and Production Practice A.P.I., p257, (1952)

3. Bergelin, O. P., Che. Eng. 56, 104, (1949)

4. Galegar, W. C., Stovall, W. B., Huntington, R. L., Pipeline Industry, Feb. 1956

5. Calvert, S. and Williams, B., A.I.Ch.E. J. 1, 78, (1955)

6. Moore, T. V. and Wilde, H. C., Trans. A.I.M.E. (Pet. Dev. and Tech.), 92, 296, (1931)

7. Stein, N., Elfrink, E.B., Wiener, L. D., Sandberg, C. R., Petrol. Trans. A.I.M.E., 195, 233 (1952)

8. Cromer, S., Huntington, R. L., Trans. A.I.M.E., 136, 79 (1940)

9. Radford, B. A., M. Sc. Thesis in Chem. Eng., Univ. of Alberta, (1949)

10. Dunn, J. S. C., M.Sc. Thesis in Chem. Eng., Univ. of Alberta, (1952)

11. Martinelli, R. C., Boelter, L. M. K., Taylor, T. H. M., Thomsen, E. G. and Morrin, E. H. , Trans. A.S.M.E., 66, 139, (1944)

ACKNOWLEDGMENT

The authors gratefully acknowledge the interest and financial assistance of Imperial Oil Limited and the hard work of Mr. W. L. Short, Graduate Student in the Department of Chemical and Petroleum Engineering in checking and extending the experimental data and carrying out the bulk of the calculations.

LIST OF FIGURES

1. Typical Pressure Drop Relationship at Low Liquid Rate
2. Interrelationship of Flow Pattern Terminology
3. Flow Patterns and Pressure Drop Regimes
4. Schematic Flow Diagram of Equipment
5. Pressure Drop and Holdup Relationship, V_L = 0.0698 ft/sec
6. Pressure Drop and Holdup Relationship, V_L = 0.135 ft/sec
7. Pressure Drop and Holdup Relationship, V_L = 0.298 ft/sec
8. Pressure Drop and Holdup Relationship, V_L = 0.627 ft/sec
9. Pressure Drop and Holdup Relationship, V_L = 0.873 ft/sec
10. Pressure Drop and Holdup Relationship, V_L = 2.06 ft/sec
11. Pressure Drop and Holdup Relationship, V_L = 2.51 ft/sec
12. Pressure Drop and Holdup Relationship, V_L = 3.47 ft/sec
13. Pressure Drop and Holdup Relationship, V_L = 7.35 ft/sec
14. Minima and Maximum Pressure Drop Loci (vs V_L)
15. Minima and Maximum Pressure Drop Loci (vs R_V)
16. Pressure Drop Components
17. Typical f_L' Relationships
18. Two Phase Friction Factor, f_L', Correlation
19. Holdup Ratio Correlation

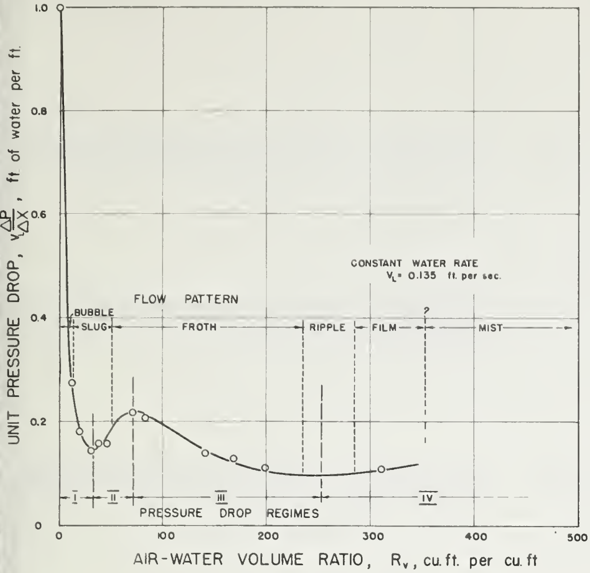

Figure 1. Typical Pressure Drop Relationship at Low Liquid Rate

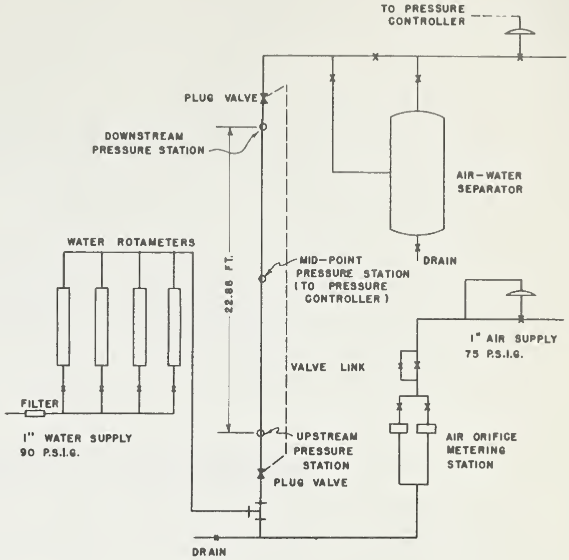
TO PRESSURE CONTROLLER
PLUG VALVE
DOWNSTREAM PRESSURE STATION
AIR-WATER SEPARATOR
WATER ROTAMETERS
DRAIN
MID-POINT PRESSURE STATION (TO PRESSURE CONTROLLER)
22.88 FT.
1" AIR SUPPLY 75 P.S.I.G.
VALVE LINK
FILTER
1" WATER SUPPLY 90 P.S.I.G.
UPSTREAM PRESSURE STATION
PLUG VALVE
AIR ORIFICE METERING STATION
DRAIN

Figure 4. Schematic Flow Diagram of Equipment

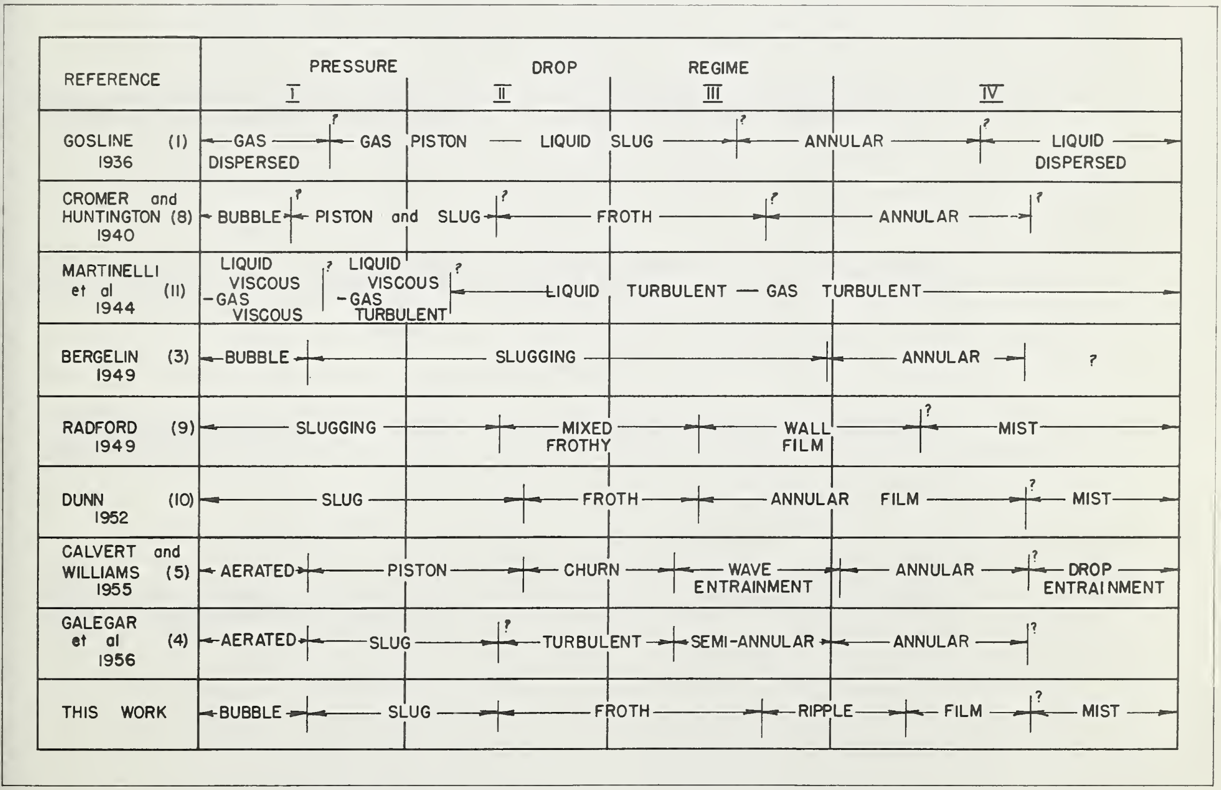

REFERENCE	PRESSURE DROP REGIME I	II	III	IV
GOSLINE (1) 1936	GAS DISPERSED ? GAS	PISTON — LIQUID	SLUG ? ANNULAR	? LIQUID DISPERSED
CROMER and HUNTINGTON (8) 1940	BUBBLE ? PISTON and	SLUG ?	FROTH ?	ANNULAR ?
MARTINELLI et al (11) 1944	LIQUID VISCOUS -GAS VISCOUS ? LIQUID VISCOUS -GAS TURBULENT ?	LIQUID	TURBULENT — GAS	TURBULENT
BERGELIN (3) 1949	BUBBLE	SLUGGING		ANNULAR ?
RADFORD (9) 1949	SLUGGING	MIXED FROTHY	WALL FILM	? MIST
DUNN (10) 1952	SLUG	FROTH	ANNULAR	FILM ? MIST
CALVERT and WILLIAMS (5) 1955	AERATED	PISTON CHURN	WAVE ENTRAINMENT	ANNULAR ? DROP ENTRAINMENT
GALEGAR et al (4) 1956	AERATED SLUG	? TURBULENT	SEMI-ANNULAR	ANNULAR ?
THIS WORK	BUBBLE SLUG		FROTH RIPPLE	FILM ? MIST

Figure 2. Interrelationship of Flow Pattern Terminology

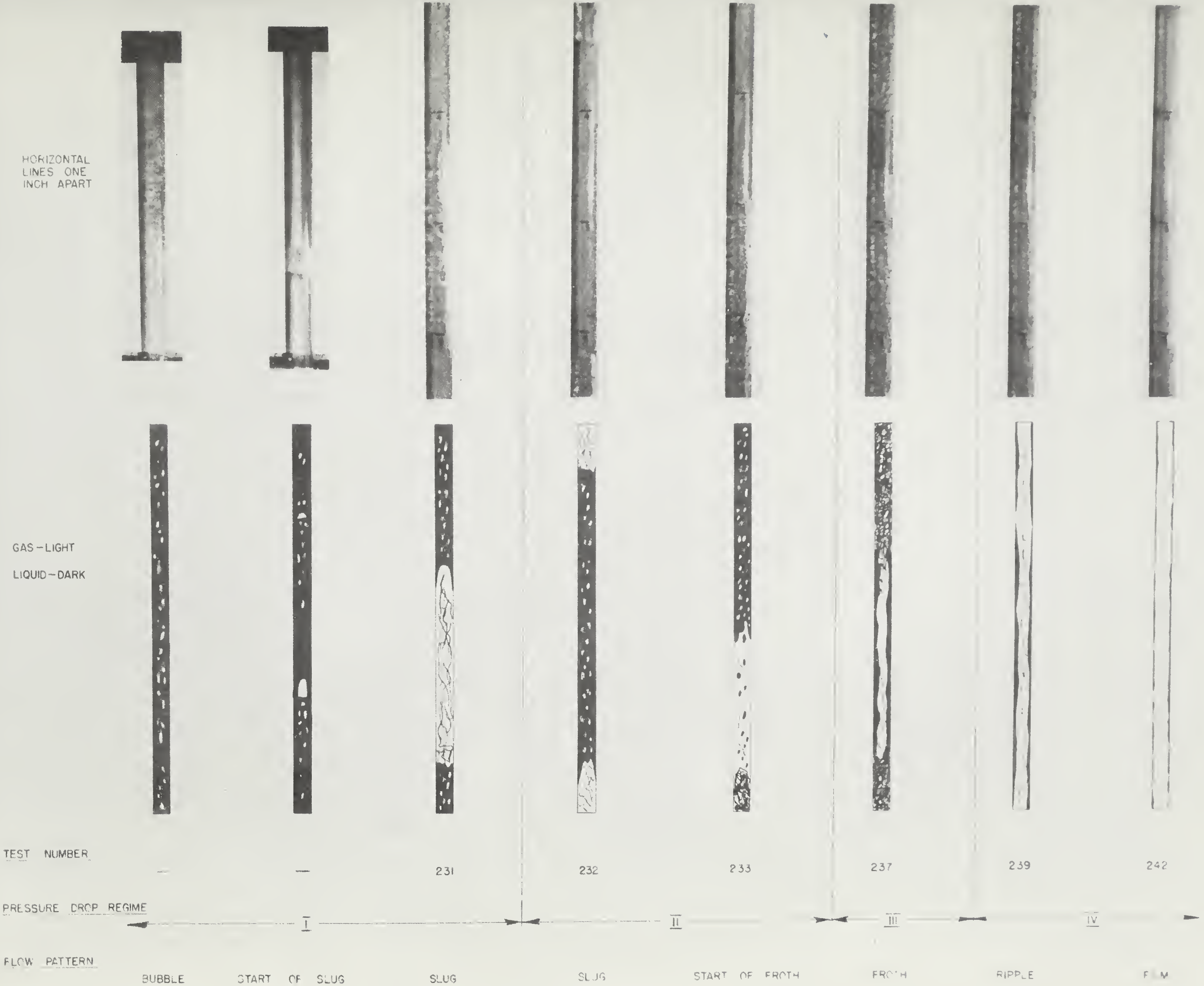
HORIZONTAL LINES ONE INCH APART
GAS-LIGHT
LIQUID-DARK
TEST NUMBER
—
—
231
232
233
237
239
242
PRESSURE DROP REGIME
I
II
III
IV
FLOW PATTERN
BUBBLE
START OF SLUG
SLUG
SLUG
START OF FROTH
FROTH
RIPPLE
FILM

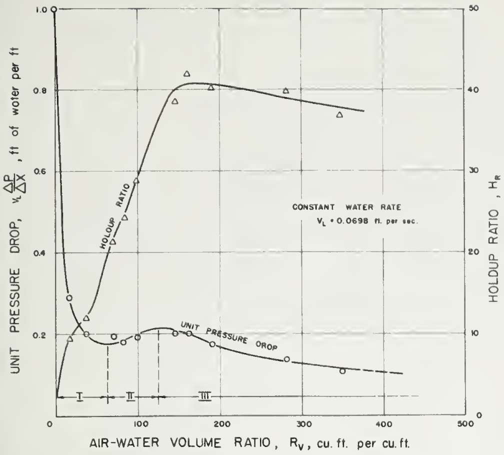

Figure 5.

ressure Drop and Holdup Relationship, $V_L = 0.0698$ ft/sec.

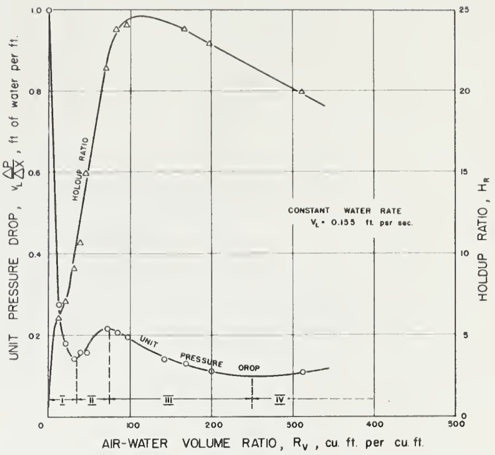

Figure 6.

Pressure Drop and Holdup Relationship, $V_L = 0.135$ ft/sec.

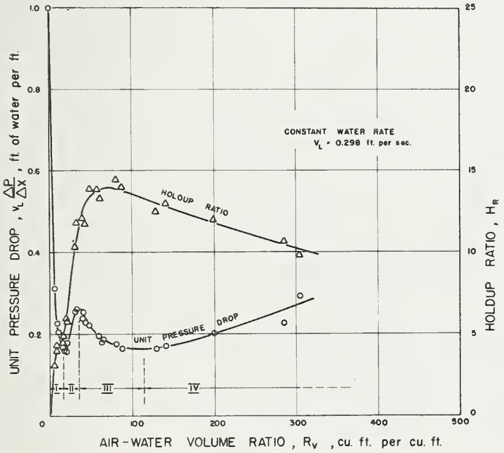

Figure 7.

Pressure Drop and Holdup Relationship, $V_L = 0.298$ ft/sec.

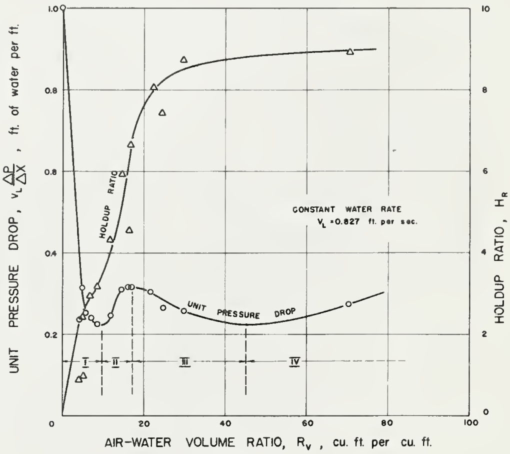

Figure 8.

Pressure Drop and Holdup Relationship, $V_L = 0.627$ ft/sec.

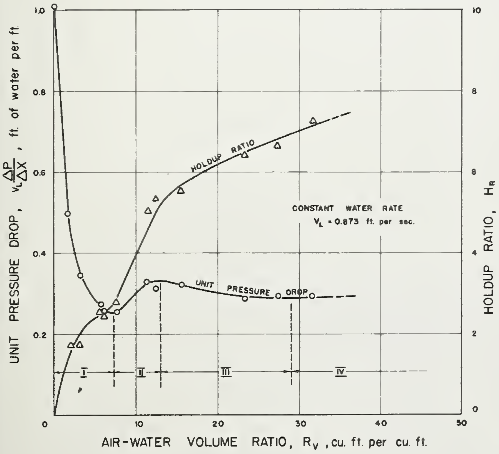

Figure 9.

Pressure Drop and Holdup Relationship, $V_L = 0.873$ ft/sec.

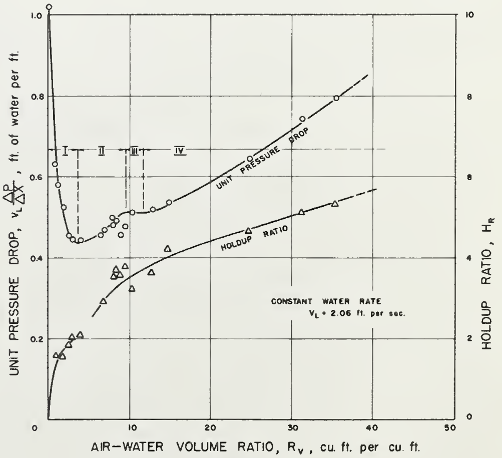

Figure 10.

Pressure Drop and Holdup Relationship, $V_L = 2.06$ ft/sec.

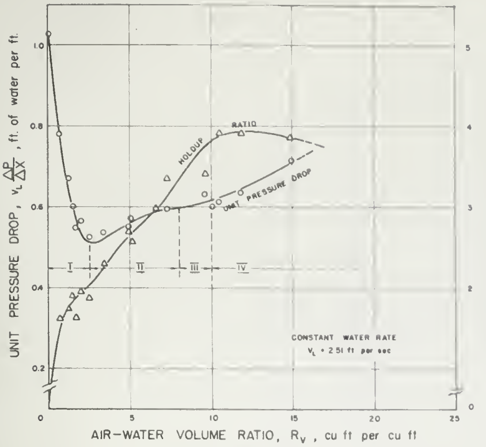

Figure 11.

Pressure Drop and Holdup Relationship, $V_L = 2.51$ ft/sec.

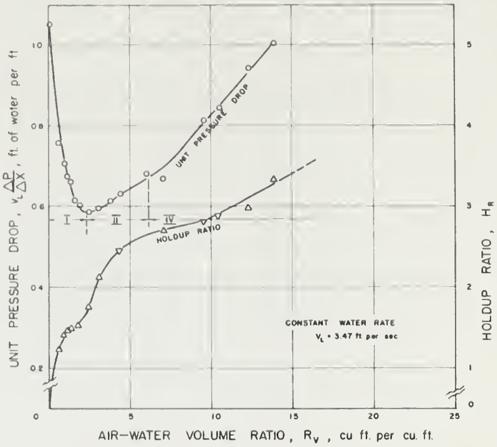

Figure 12.

Pressure Drop and Holdup Relationship, $V_L = 3.47$ ft/sec.

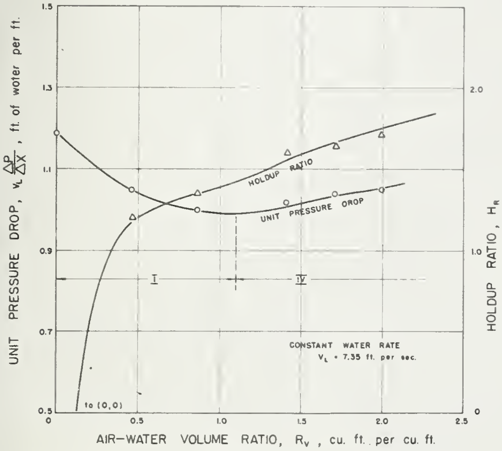

Figure 13.

Pressure Drop and Holdup Relationship, $V_L = 7.35$ ft/sec.

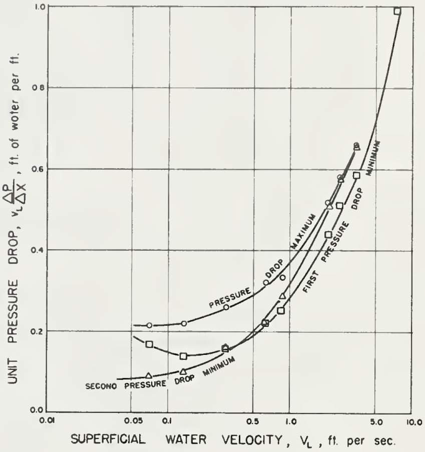

Figure 14.

Minima and Maximum Pressure Drop Loci (vs V_L)

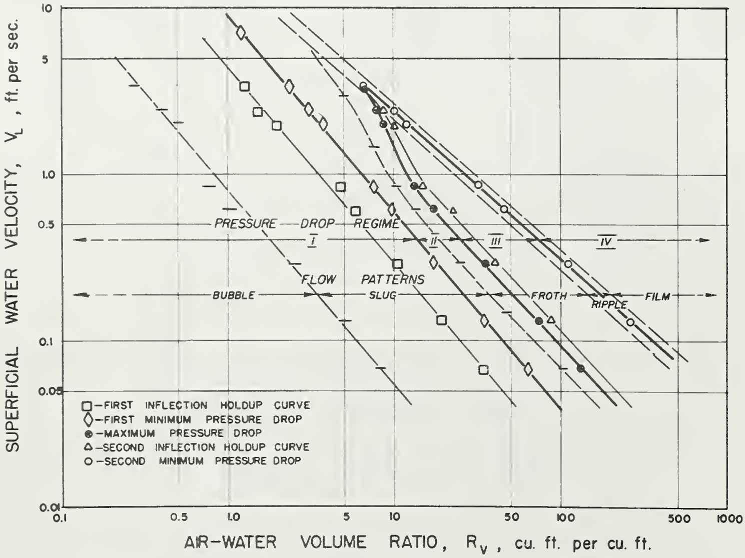

Figure 15. Minima and Maximum Pressure Drop Loci (vs R_V)

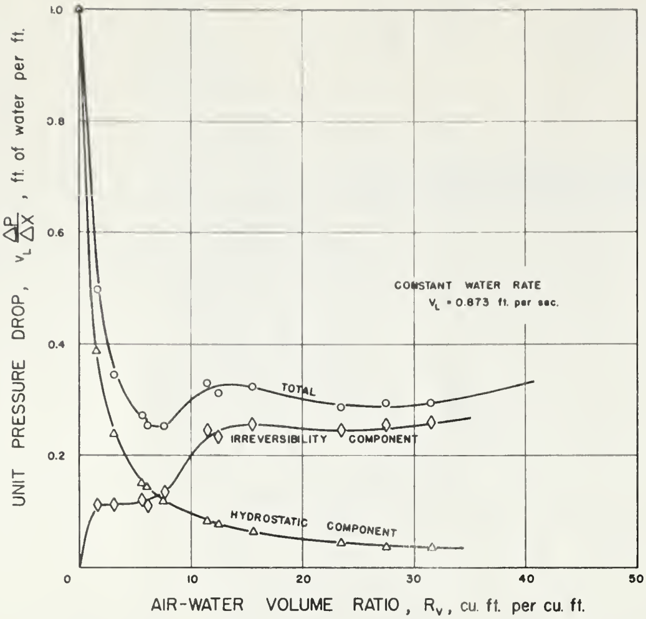

Figure 16. Pressure Drop Components

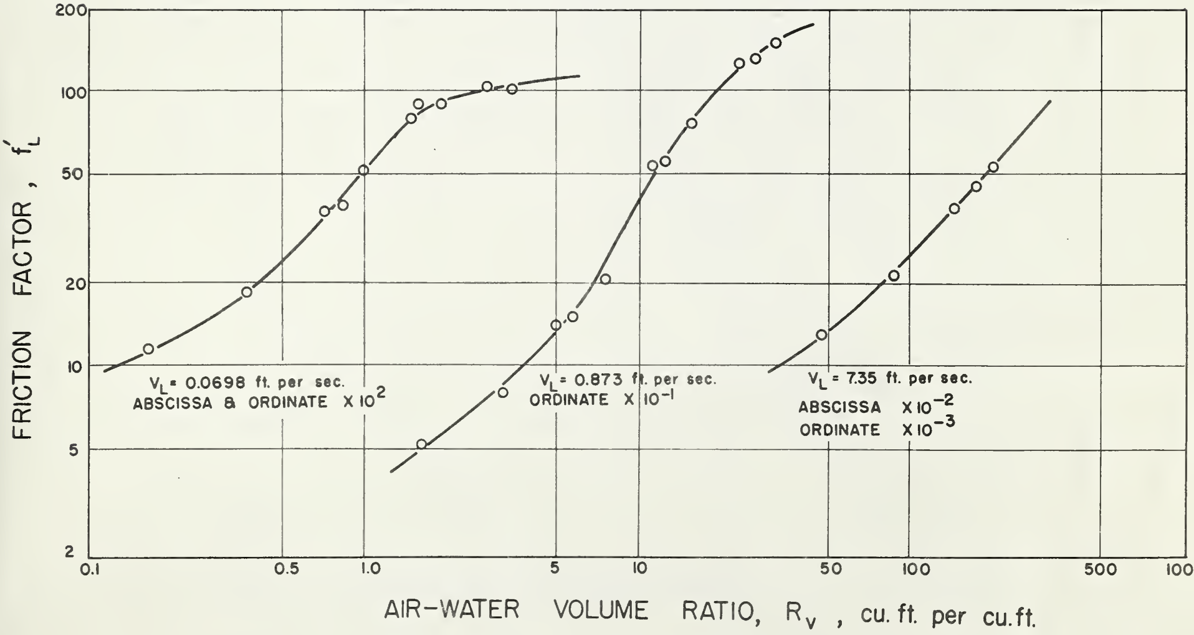

Figure 17. Typical f'_L Relationships

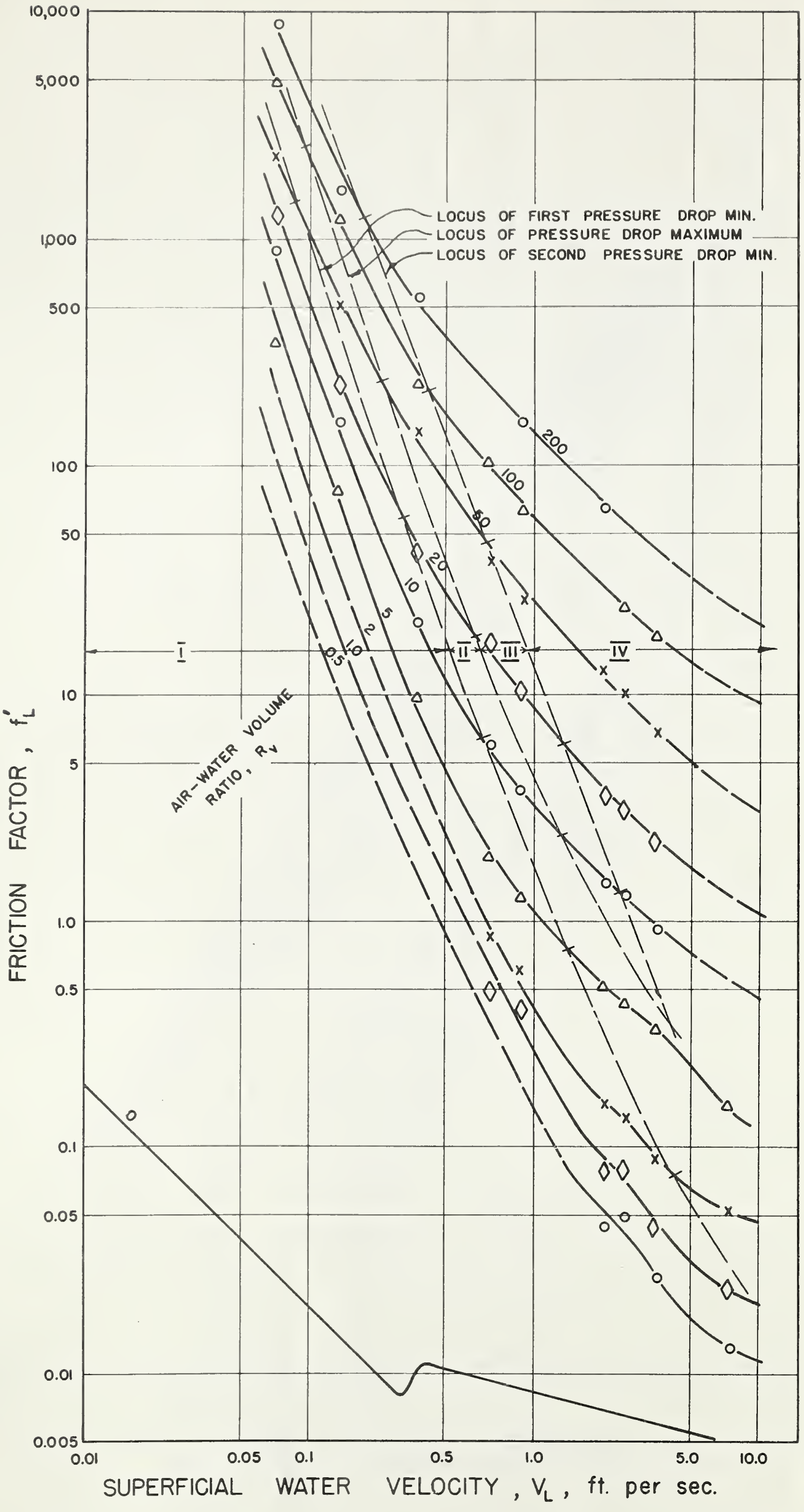

Figure 18. Two Phase Friction Factor, f'_L, Correlation

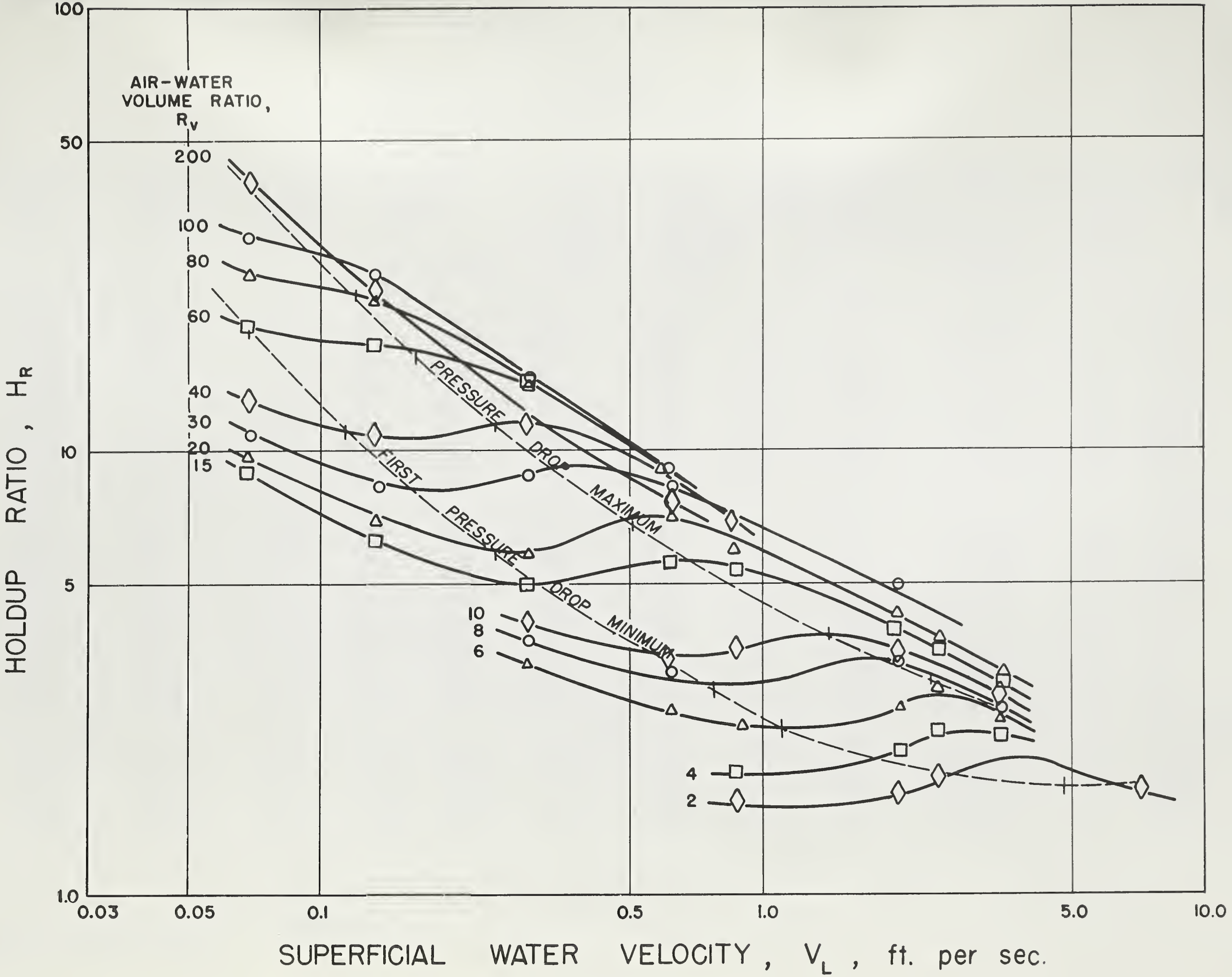

Figure 19. Holdup Ratio Correlation

TABLE I (PARTIAL)

EXPERIMENTAL DATA

TUBE DIAMETER 1.025 INCHES I.D.
TEST SECTION LENGTH 22.88 FT.
TEST SECTION MID POINT PRESSURE 36.0 PSIA.
TEST SECTION MID POINT TEMPERATURE AS INDICATED.
SPECIFIC VOLUME OF LIQUID PHASE = .01603 FT^3/LB.
SPECIFIC VOLUME OF SATURATED GAS PHASE AS INDICATED.

(1) TEST NUMBER	(2) WATER RATE $FT^3/SEC.$	(3) SATURATED AIR RATE FT^3/SEC*	(4) MID POINT TEMPERATURE ^oF	(5) DISCHARGE AIR WATER RATIO ** (a) FT^3/FT^3.	(5) (b) LB/LB.	(6) TEST SECTION AIR WATER RATIO FT^3/FT^3.	(7) SPECIFIC VOLUME SATURATED GAS PHASE FT^3/LB	(8) HOLDUP RATIO***	(9) PRESSURE DROP Ft. H_2O/FT.	(10) SPECIFIC VOLUME RATIO v_L/v_G at P_{av}, T_{av}.	(11) PRESSURE DROP REGIME	(12) FLOW PATTERN
-	.00040	0.	70	0.	0.	0.	-	-	1.00011	-	I	SINGLE PHASE
395D	.00040	.00660	70	16.5	.0483	1.73	5.47	9.54	0.293	29.3×10^{-4}	I	SLUG
396D	.00040	.0149	72	37.3	.109	3.11	5.49	12.0	0.201	29.2×10^{-4}	I	SLUG
397D	.00040	.0283	72	70.7	.206	3.30	5.49	21.4	0.195	29.2×10^{-4}	II	SLUG
398D	.00040	.0397	72	99.2	.290	3.45	5.49	28.8	0.194	29.2×10^{-4}	II	FROTH
399D	.00040	.0331	72	82.7	.241	3.41	5.49	24.3	0.180	29.2×10^{-4}	II	SLUG
400D	.00040	.0587	72	147.	.429	3.81	5.49	38.6	0.198	29.2×10^{-4}	III	FROTH
401D	.00040	.0765	72	191.	.557	4.74	5.49	40.3	0.173	29.2×10^{-4}	III	FROTH
402D	.00040	.139	71	348.	1.02	9.47	5.48	36.7	0.108	29.25×10^{-4}	III	FROTH
405D	.00040	.0652	70	163.	.477	3.86	5.47	42.2	0.201	29.3×10^{-4}	III	FROTH
406D	.00040	.113	70	283.	.829	7.10	5.47	39.9	0.138	29.3×10^{-4}	III	FROTH
-	.0050	0.	70	0.	0.	0.	-	-	1.0047	-	I	SINGLE PHASE
380D	.0050	.0620	69	12.4	.0365	2.32	5.45	5.35	.312	29.4×10^{-4}	II	FROTH
381D	.0050	.117	69	23.4	.0688	3.65	5.45	6.41	.288	29.4×10^{-4}	III	FROTH
382D	.0050	.158	70	31.6	.0926	4.34	5.47	7.28	.293	29.3×10^{-4}	IV	RIPPLE
383D	.0050	.137	75	27.4	.0795	4.13	5.53	6.63	.295	29.0×10^{-4}	III	RIPPLE
386D	.0050	.0303	73	6.06	.0176	2.47	5.51	2.45	.256	29.1×10^{-4}	I	SLUG
387D	.0050	.0568	74	11.4	.0332	2.26	5.51	5.04	.330	29.1×10^{-4}	II	FROTH
388D	.0050	.0775	72	15.5	.0451	2.81	5.51	5.52	.321	29.1×10^{-4}	III	FROTH
389D	.0050	.0157	73	3.2	.00931	1.83	5.51	1.75	.346	29.1×10^{-4}	I	SLUG
390D	.0050	.0285	72	5.8	.0169	2.28	5.51	2.54	.272	29.1×10^{-4}	I	SLUG
391D	.0050	.0383	72	7.6	.0221	2.74	5.51	2.77	.252	29.1×10^{-4}	I	SLUG
392D	.0050	.00788	70	1.6	.00469	0.93	5.47	1.72	.498	29.3×10^{-4}	I	SLUG
-	.0421	0.	70	0.	0.	0.	-	-	1.19	-	I	SINGLE PHASE
308S	.0421	.0720	69	1.71	.00502	1.06	5.45	1.64	1.04	29.4×10^{-4}	IV	ANNULAR
309S	.0421	.0360	67	.855	.00252	.628	5.44	1.36	1.00	29.5×10^{-4}	I	SLUG
310S	.0421	.0598	67	1.42	.00419	.879	5.44	1.61	1.02	29.5×10^{-4}	IV	ANNULAR
311S	.0421	.0791	67	1.99	.00587	1.16	5.44	1.72	1.05	29.5×10^{-4}	IV	ANNULAR
312S	.0421	.0194	72	.461	.00136	.318	5.49	1.45	1.05	29.2×10^{-4}	I	SLUG

* AT TEST SECTION TEMPERATURE AND AVERAGE PRESSURE
** COLUMN 3 DIVIDED BY COLUMN 2
*** COLUMN 5 (a) DIVIDED BY COLUMN 6